

**OPTICAL AND ELECTRICAL PROPERTIES OF
PLASMA POLYMERIZED CEDAR WOOD OIL THIN
FILMS**

Happy Dey

Roll No. 100714002 F

Session: October, 2007



DEPARTMENT OF PHYSICS
BANGLADESH UNIVERSITY OF ENGINEERING AND TECHNOLOGY (BUET)
DHAKA- 1000, BANGLADESH.

February, 2012

OPTICAL AND ELECTRICAL PROPERTIES OF PLASMA POLYMERIZED CEDAR WOOD OIL THIN FILMS

*A Thesis Submitted to the Department of Physics, Bangladesh University of
Engineering and Technology (BUET) in Partial Fulfillment of the Requirement for
the Degree of MASTER OF PHILOSOPHY (M. Phil.) in PHYSICS*

By

Happy Dey

Student No. 100714002 F

Session: October, 2007



**DEPARTMENT OF PHYSICS
BANGLADESH UNIVERSITY OF ENGINEERING AND TECHNOLOGY (BUET)
DHAKA- 1000, BANGLADESH.**

February, 2012



BANGLADESH UNIVERSITY OF ENGINEERING AND TECHNOLOGY (BUET)

Candidate's Declaration

It is hereby declared that this thesis or any part of it has not been submitted elsewhere for the award of any degree or diploma.

Signature of the Candidate

(Happy Dey)

Student no. 100714002 F

Session : October, 2007.

Dedicated

To

My Parents

Acknowledgements

Regarding the outcome of this thesis, I express my deepest sense of gratitude, indebtedness and deep appreciation to my respected supervisor Professor Dr. Md. Abu Hashan Bhuiyan, Department of Physics, Bangladesh University of Engineering & Technology (BUET), Dhaka, for his continuous personal care, close supervision, constant inspiration, helpful attitude, effective suggestions throughout the long period of my research work and also for acquainting me with the advanced world of research.

I am grateful to the Head, Prof. Dr. Md. Mostak Hossain, Department of Physics, BUET for providing necessary facilities, also for his inspiration, affection and constructive suggestions throughout the long road of research. I am thankful to my respected teachers Prof. Dr. Nazma Zaman, Prof. Dr. Md. Feroz Alam Khan, Professor Dr. Jiban Podder, Prof. Dr. A. K. M. Akther Hossain, Ms. Fahima Khanam, Dr. Afia Begum, Dr. Md. Forhad Mina, and all the other teachers of the Department of Physics, BUET. The encouragement and cooperation I received from Mr. Rama Bijoy Sarker, and Dr. Sunirmal Majumder are greatly acknowledged. I would like to extend my thanks to all other Ph. D and M. Phil students of the Department for scientific discussions and making this Department a pleasant and friendly working place.

I would like to thank all the staff members of this Department specially Mr. Md. Idris Munshi, Mr. Md. Liakat Ali and Mr. Swapan Kumar Das for their sincere help to do this research work. Thanks are directed to all my friends who showed an interest in my work. Finally, I would like to express my heartfelt gratitude to my parents, brothers, sister and all other family members for their multifaceted support.

I acknowledge the financial support offered by the authority of BUET and the National Science, Information and Communication Technology fellowship granted by The Ministry of Science, Information and Communication Technology, Government of The People's Republic of Bangladesh.

Happy Dey

25th February, 2012.

Abstract

Plasma polymerized organic thin films have recently attained considerable attention due to their widespread applications in the fields of electronics, optics, etc. The aims of the thesis are to study the optical and electrical properties of plasma polymerized Cedar Wood Oil (PPCWO) thin film. The uniform and pinhole-free PPCWO thin films were deposited at room temperature onto glass substrates by a parallel plate capacitively coupled glow discharge reactor. The thicknesses of the films were measured by a Multiple Beam Interferometric method.

The thermal behavior has been investigated by thermogravimetric analysis (TGA) and differential thermal analysis (DTA). The TGA/DTA measurements indicate that the materials exhibit single-stage weight loss and thermal stability up to 505 K. The FTIR analysis reveals that the heat treated sample of PPCWO thin film does not have the chemical structure to that of the CWO monomer and the presence of carbon double bond group is detected.

Ultraviolet-visible spectroscopic studies have been carried out on the as deposited and heat treated PPCWO thin films of different thicknesses. The effect of heat treatment on the optical properties of PPCWO thin films is significant. It is seen that the absorbance increases with the increase of the thickness and heat treatment temperature. An increasing trend is observed in the values of band gap. Thus it can be attributed that the band gap of the PPCWO thin films is dependent of thickness. The direct band gap of the PPCWO thin film decreases gradually with increasing heat treatment temperature used.

The alternating current (AC) capacitance and conductance of PPCWO thin films in Al/PPCWO/Al sandwich structure were measured as functions of frequency ($10^3 < f < 10^6$ Hz) and of temperature ($300 < T < 400$ K). The AC conductivity, σ_{ac} , increases as frequency increases with a lower slope in the high frequency (above 1×10^5 Hz) region at all temperatures. The σ_{ac} is more dependent on temperature in the low frequency region than that in the high frequency region. The dielectric constant, ϵ' , decreases slowly with increasing frequency up to 20 kHz and then decreases very sharply in the high frequency region. The variation of ϵ' and dielectric loss tangent with frequency which is related with multicomponent contribution of polarizability of the polar materials, as more or less all thin polymer films deposited by plasma polymerization technique.

CHAPTER 1 INTRODUCTION

1.1	Introduction	2
1.2	Evaluation of Earlier Research Work	2
1.3	Aim of the Present Study	8
1.4	The Thesis –at a Glance	9
	References	10

CHAPTER 2 FUNDAMENTAL ASPECTS OF PLASMA, POLYMER, AND PLASMA POLYMERIZATION

2.1	Introduction	14
2.2	Polymers	14
2.2.1	Classification based upon different factors related to polymers	15
2.2.2	Description of the different types of polymers	15
2.2.2.1	Depending on their origin polymers	15
2.2.2.2	Depending on its ultimate form and use	16
2.2.2.3	Depending on reaction mode of polymerization	17
2.2.2.4	Depending upon Tacticity	17
2.2.2.5	Depending on the biggest differences in polymer properties	18
2.2.2.6	Depending on physical property related to heating	18
2.2.3	Crystalline and amorphous states of polymer	19
2.3	Plasma and Plasma Polymerization	20
2.3.1	Plasma: The fourth State of Matter	20
2.3.2	An summary of gas discharge plasma	23
2.3.3	Direct current glow discharge	25
2.3.4	Alternating current (ac) glow discharge	26
2.3.5	Advantages of plasma polymerization	27
2.3.6	Details of Plasma polymerization	28
2.4	Different Types of Glow Discharge Reactors	29
2.4.1	Capacitively coupled (cc) radio-frequency discharge	31
2.4.2	Inductively coupled glow discharges	32
2.5	Overall reactions and growth mechanism in plasma polymerization	32
2.6	Advantages and Disadvantages of Plasma Polymers	35
2.7	Applications of Plasma-polymerized Organic Thin Films	36
	References	36

CHAPTER 3 EXPERIMENTAL DETAILS

3.1.	Introduction	40
3.2.	The Monomer	40
3.3.	Substrate Material and its Cleaning Process	42
3.4.	Capacitively Coupled Plasma Polymerization Set-up	42
3.5	Deposition of Plasma Polymerized Thin Film	45
3.6	Contact Electrodes for Electrical Measurements	46
3.7	Measurement of Thickness of the Thin Films	47
	References	49

CHAPTER 4 THERMAL AND STRUCTURAL ANALYSES OF PPCWO

4.1	Introduction	51
4.2	Thermal Analysis	51
4.2.1	Differential thermal analysis	51
4.2.2	Thermogravimetric analysis	52
4.2.3	Applications of DTA/TGA	53
4.2.4	Experimental procedure	54
4.2.5	Results and discussion	55
4.3	Theory of Infrared Spectroscopy	56
4.3.1	Introduction	56
4.3.2	Importance of FTIR	58
4.3.3	Infrared frequency range and spectrum presentation	59
4.3.4	Infrared absorption	60
4.3.5	Molecular Vibrations	61
4.3.6	Infrared Activity	63
4.3.7	Interpretation of FTIR Spectra	64
4.3.8	The Fingerprint region	64
4.3.9	Sample Preparation	65
4.3.10	Results and Discussion	65
	References	68

CHAPTER 5	UV-Vis SPECTROSCOPY OF PPCWO	
5.1	Introduction	70
5.2	Theory of UV-vis Spectroscopy	70
5.2.1	Different types of Electronic transitions	71
5.2.2	Absorbing species containing π , σ , and n electrons	72
5.2.3	Direct and Indirect optical transitions	73
5.2.4	Beer –Lambert Law: The law of Absorption	74
5.3	Experimental Procedure	76
5.4	Results and Discussion	76
5.4.1	Ultraviolet-visible spectroscopic analysis	76
	References	82
CHAPTER 6	AC ELECTRICAL PROPERTIES OF PPCWO	
6.1	Introduction	84
6.2	Brief Description of dielectrics	85
6.2.1	Plasma Polymers as Dielectrics	85
6.2.1.1	Polarization and its classification	85
6.2.1.2	Dielectric constant	87
6.2.1.3	Dielectric Losses	88
6.2.2	The Debye theory of dielectric	89
6.2.2.1	The Cole-Cole function	91
6.3	Measurement of dielectric properties by an Impedance Analyzer	92
6.4	Results and Discussion	93
6.4.1	Frequency and temperature dependence of ac electrical conductivity	93
6.4.2	Frequency and temperature dependence of the dielectric constant	95
6.4.3	Frequency and temperature dependence of dielectric loss tangent	96
6.4.4	Cole- Cole plot	99
	References	100
CHAPTER 7	CONCLUSIONS	
7.1	Conclusions	103
7.2	Suggestions for further research	104

List of Figures

2.1	The types of polymer depending on tacticity	18
2.2	Different types of copolymers	19
2.3	Different states of Polymers	20
2.4	Schematic overview of the basic processes in a glow discharge	24
2.5	Normal glow discharge; (a) the shaded areas are luminous, (b) distribution of potential among luminous zones	25
2.6	A schematic plasma polymerization configuration	28
2.7	Different types of reactor configuration used for plasma polymerization (a) schematic of a bell jar reactor, (b) parallel plate internal electrode reactor, (c) electrode less microwave reactor.	30
2.8	Schematic representation of bicycle step growth mechanism of plasma polymerization	34
3.1	Chemical Structure of Cedar Wood Oil	41
3.2	Schematic diagram of the plasma polymerization set-up	43
3.3	Glow discharge plasma during deposition	45
3.4	Schematic diagram of sandwich Al/PPCWO/Al film	46
3.5	The Edward vacuum coating unit E306A.	47
3.6	Multiple Beam Interferometric set-up in laboratory	48
3.7	Interferometer arrangement for producing reflection Fizeau fringes of equal thickness.	49
4.1	Schematic illustration of a DTA cell	52
4.2	A pictorial set-up for TGA measurements	54
4.3	The DTA/TGA traces of Cedar Wood Oil	55
4.4	The DTA/TGA traces of as deposited PPCWO	55
4.5	Stretching vibrations	62
4.6	Bending vibrations	63
4.7	The FTIR spectra of different samples: CWO, spectrum a; as deposited PPCWO, spectrum b; PPCWO heat treated at 473 K, spectrum c; PPCWO, heat treated at 673 K, spectrum d.	66
5.1	Light Spectrum	71
5.2	Vibrational and rotational energy levels of absorbing materials	71
5.3	Summary of electronic energy levels	72
5.4	Schematic band diagrams for the photoluminescence processes in a	74

	direct gap material (left) and an indirect gap material (right)	
5.5	Wavelength versus absorbance plot for different PPCWO thin films	77
5.6	Photon energy versus absorption coefficient (α) plot for PPCWO of different thicknesses	78
5.7	$(\alpha \cdot h\nu)^2$ vs. $h\nu$ curves for as deposited PPCWO thin films of different thicknesses	79
5.8	Absorbance versus wavelength plot at different temperature of PPCWO films with thickness 310nm	79
5.9	Variation of absorbance with wavelength for PPCWO thin film heat treated at different temperatures (Thickness: 310 nm)	80
5.10	$(\alpha \cdot h\nu)^2$ vs. $h\nu$ curves for PPCWO thin film heat treated at different temperatures (Thickness: 310 nm)	80
5.11	Absorbance versus wavelength plot at different temperature of PPCWO films with thickness 220nm.	81
5.12	Variation of absorbance with wavelength for PPCWO thin film heat treated at different temperatures (Thickness: 220 nm)	81
5.13	$(\alpha \cdot h\nu)^2$ vs. $h\nu$ curves for PPCWO thin film heat treated at different temperatures (Thickness: 220 nm)	81
6.1	Dispersion of molar polarization in a dielectric (schematic)	87
6.2	AC losses in a dielectric : (a) circuit diagram, (b) simplified diagram of current-voltage relationship	89
6.3	Debye dielectric dispersion curves	90
6.4	A Cole-Cole circular arc plot constructed from the ϵ' and ϵ'' data	92
6.5	Photographs of the the ac electrical measurement set-up	92
6.6	Dependence of ac conductivity, σ_{ac} , on frequency at different temperatures for PPCWO thin films of thicknesses 300 nm	93
6.7	Dependence of ac conductivity, σ_{ac} , on temperature at different frequencies for PPCWO thin films of thicknesses 300 nm	93
6.8	Variation of dielectric constant with frequency at different temperatures for PPCWO thin films of thicknesses 300 nm	96
6.9	Dependence of loss tangent, $\tan\delta$, on frequency at different temperatures for PPCWO thin films of thicknesses 300 nm	97
6.10	Dependence of ac conductivity, σ_{ac} , on frequency at different temperatures for	97

	PPCW thin films of thicknesses 215 nm	
6.11	Dependence of ac conductivity, σ_{ac} , on temperature at different frequencies for PPCWO thin films of thicknesses 215 nm.	98
6.12	Variation of dielectric constant with frequency at different temperatures for PPCWO thin films of thicknesses 215 nm	98
6.13	Dependence of loss tangent, $\tan\delta$, on frequency at different temperatures for PPCWO thin films of thicknesses 215 nm	99
6.14	Cole-Cole plot between ϵ' and ϵ'' for a PPCWO thin film of thickness 300 nm	100

List of Tables

2.1	Classification of polymer	15
3.1	General properties of Cedar Wood Oil	41
4.1	Common subdivisions of the Infrared regions	60
4.2	Assignments of IR absorption bands for CWO and PPCWO	67
5.1	Values of direct band gap energy	78
5.2	Direct band gap of PPCWO thin film heat treated at different temperatures (Thickness: 300 nm)	80

Glossary

ABS	Absorbance
ac	Alternating Current
Al	Aluminum
Cr-Al	Chromel-Alumel
CC	Capacitively Coupled
IC	Inductively Coupled
CRT	Cathode-ray Tube
d	Sample Thickness
PPCWO	Plasma Polymerized Cedar Wood Oil
$E_{g(d)}$	Direct transition energy gap,
FTIR	Fourier Transform Infrared
I	Intensity of Radiation
IR	Infrared
k	Boltzmann Constant
K	Extinction Co-efficient
MHz	MegaHertz

PPBMI	Plasma Polymerized 1-Benzyl-2-Methylimidazole
PECVD	Plasma Enhanced Chemical Vapor Deposition
LA	Lavandula Angustifolia
PPDP	Plasma-polymerized Diphenyl
PPPA	Plasma-Polymerized Polyaniline
PFETS	Polymer field-effect transistors
PPTMA	Plasma-Polymerized N,N,3,5-Tetramethylaniline
PPPy	Plasma-Polymerized polymer film from Pyrrole
PPCPD	Plasma-Polymerized 4-Cyanopyridine
PEMOCVD	Plasma Enhanced Metal-organic Chemical Vapor Deposition
rf	Radio Frequency
TGA	Thermogravimetric Analysis
DTA	Differential Thermal Analysis
UV-Vis	Ultraviolet-Visible
•	Absorption Coefficient
ϕ	Columbic barrier height of the electrode polymer interface
ϕ_c	Ionization potential of the PF centers
λ	Wavelength
ΔE	Activation Energy
σ	Electrical Conductivity
ε	Dielectric Constant
ε_0	Permittivity of Free Space
μ	Mobility of Charge Carrier

CHAPTER 1
INTRODUCTION

- 1.1. Introduction
- 1.2. Evaluation of Earlier Research Work
- 1.3. Objectives of the Present Study
- 1.4. Thesis Layout
- References

1.1 Introduction

In this day and age, material preparation and processing have become one of the most active areas of research in the development of science and technology. Since 1960s the formation of undesired by-products in plasma has been recognized as a means of synthesizing polymers and the related process referred to as plasma polymerization or glow discharge polymerization. The process has drawn the attention of scientist and technologist as an exotic method of polymerization. Numerous potential applications and the uniqueness of the polymer formation process revealed in the modern technology. Two important characteristics of the by-products are (i) excellent adhesion to substrate materials and (ii) strong resistance to most chemicals. The most recognized concept of polymerization is based on the molecular processes where the size of the molecules increases. During the organic synthesis of monomer the arrangement of the atoms that constitute the molecules of a monomer is accomplished. In polymerization of a monomer rearrangement of atoms within the molecule seldom occurs. Thus polymer formation in plasma has been recognized as an atomic process. In this respect, plasma polymerization is one of the unique methods to prepare pinhole free, highly resistive, chemically inert polymer thin films of varying thickness on various substrates from almost any organic vapor. Organic thin films have received a great deal of interest due to their interesting applications in the fields of mechanics, electronics and optics; such as chemical, physical and biological sensors, microelectronic devices, nonlinear optical device, molecular devices, coatings for chemical fibers and films, passivation of metals, surface hardening of tool, spaceship components, etc.[1-4]. Therefore, it is of interest to develop polymer thin films of high quality for a variety of industrial applications. As a consequence, the study of the electronic, electrical and optical properties of organic polymers received special attention of the scientist as potential materials. Recently, there has been increasing interest in the study of the optical and electrical properties of plasma deposited organic thin films.

1.2 Evaluation of Earlier Research Work

Sarker, Bhuiyan, et al. [5] shows that chemical composition of plasma polymerized 1-Benzyl-2-Methylimidazole (PPBMI) is different from that of the 1-Benzyl-2-

Methylimidazole (BMI). From the Ultraviolet-Visible (UV-Vis) spectra, the direct transition energy gap was determined to be between 3.10 and 3.35 eV. The indirect transition energy gap was found between 1.80 and 1.95 eV for PPBMI thin films of different thicknesses. Both direct and indirect transition energy gaps increased with increasing thickness and decreased upon heat treatment .

The ageing and thermal degradation of polymer thin films prepared at various RF powers from oil of *Lavandula angustifolia* (LA) were investigated by Spectroscopic ellipsometry and Fourier Transform Infrared (FTIR) spectroscopy to monitor the optical parameters, thickness and chemical structure, over a period of 1400 h. The degradation under ambient conditions was found to occur within the first 100 h after fabrication. An increase in thermal stability was found for films fabricated at increased radio Frequency (RF) power levels. Between 200 and 300 °C, the properties indicate that a phase change occurs in the poly (LA) [6].

The optical properties, thickness and roughness of non- synthetic Terpinen-4-ol were studied in the wavelength range 200 to 1000 nm using ellipsometry. The polymer thin films of thickness from 100 to 1000 nm were fabricated and the films exhibited smooth and defect-free surfaces. At 500 nm wavelength, the refractive index and extinction coefficient were found to be 1.55 and 0.0007 respectively [7]. It has been shown that the ac conductivity of plasma polymerized diphenyl (PPDP) thin films is more dependent on temperature in the low frequency region than in the high frequency region. Dielectric constant of as deposited PPDP is dependent on frequency above 303 K and that of heat treated PPDP is dependent on frequency above 343 K [8]. Plasma polymerized 1-cyanoicoquinoline thin films were prepared by plasma polymerization under different glow discharge conditions and their dielectric properties were investigated [9]. It has been shown that the dielectric constant of N,N,3,5 tetramethylaniline (TMA) decreases with the increase of frequency and that decreases with the increase of temperature but dielectric loss increases with increasing frequency with a minimum in the low frequency region [10].

The physicochemical characteristics of the cedar wood oil (CWO) were determined, such as refractive index, numbers: acidic, peroxide, iodine, saponification, colour and mass fraction of non-lipid admixtures. Fractional and fatty acid compositions of the oil was investigated [11].

Marinov et al. [12] reported that the performance of polymer thin film transistors, made of different semiconducting polymers, depends mostly on the type of polymer and its deposition conditions. For these reason, in polymer field-effect transistors (PFETs), the current transport is limited by the carrier injection from the source electrode into the polymer.

Mitu et al. [13] reported on the deposition of parylene like films by plasma polymerization, starting from the sublimation of the di-paraxylene precursor. The good charge stability of the plasma deposited parylene like films make them interesting for electrostatic applications. Venkatesh and Raghavan [14] discussed the various methods of measurement (and principles) of dielectric properties and their applicability for agri-food and biological materials.

The development of scientific interest in application of materials of organic compound produced through plasma polymerization technique has drawn much attention of the scientists to investigate the various properties of the polymers such as structural, physical, chemical, optical and electrical properties. The attention in plasma-polymerized thin films as a possible optical and dielectric material has triggered academic interest in the polymerization process [15].

The structural behavior of plasma polymerized thin films is different than that of the conventionally prepared polymer thin films. Fourier Transform Infrared (FTIR) spectroscopic analysis provide information about the chemical structure of the plasma polymers. UV-Vis spectroscopic analyses of organic or inorganic materials can provide the information about electronic structure and can be ascertained the existence of optical transition mechanisms: allowed direct and indirect transitions.

Chowdhury and Bhuiyan [16] investigated the optical properties and chemical structure of plasma polymerized diphenyl (PPDP) thin films. The IR spectroscopic analyses have revealed that the structure of PPDP thin films grown by glow discharge polymerization is not structurally the same as that of the monomer diphenyl and cyclization / aggregation by conjugation occurs in the PPDP structure on heat treatment which is partially relieved on aging. They have concluded that the band gap is not affected appreciably by heat treatment whereas it is modified on aging. The values of E_{opt} (3.59 eV)

for unaged PPDP films are less in comparison to E_{opt} (4.08 eV) for aged PPDP films. The values of E_{qd} and E_{qi} are also changed due to heat treatment and aging.

Plasma polymerized N, N, 3, 5 Tetramethylaniline (PPTMA) thin films were deposited on to glass substrates at room temperature by a capacitatively coupled parallel plate reactor by Akther and Bhuiyan [17]. The structural analyses have revealed that PPTMA thin films are formed with certain amount of conjugation, which modifies on heat treatment. From the UV-Vis absorption spectra, allowed direct transition (E_{qd}) and indirect transition (E_{qi}) energy gaps are determined to be 2.80 and 1.56 eV respectively, while E_{qd} increases a little, E_{qi} decreases, on heat treatment of PPTMA. The calculated values of Tauc parameter B for all the samples indicate an increase in structural order/conjugation in PPTMA thin films improved by heat treatment. The allowed direct and indirect transition energy gaps are also modified when the samples are heat treated.

Akther and Bhuiyan [18] reported on electrical and optical properties of PPTMA thin films deposited onto glass substrates at room temperature. The EA, IR and UV-Vis spectroscopy revealed that there are conjugations in the matrix of the PPTMA thin films. From UV-Vis spectroscopy they found that indirect energy gap varies from 1.49 to 1.86 eV with film thickness.

Saravanan et al. [19] investigated low dielectric constant k , ($k < 3.9$) thin films based on radio frequency plasma polymerized aniline. The FTIR studies have revealed that the aromatic ring is retained in the polyaniline, thereby increasing the thermal stability. They measured dielectric constant and ac conductivity in the frequency range 100 Hz – 1 MHz and the temperature range 300 – 373 K. The dielectric permittivity in the high frequency range is considerably low.

Sakthi Kumar and Yoshida [20] reported that plasma polymerized polymer film from pyrrole (PPPy) was produced by rf plasma polymerization. Their dielectric properties were studied in the frequency range from 1 kHz to 1 MHz at various temperatures from 303 to 423 K. The large increase in the capacitance towards the low frequency region indicates the possibility of an interfacial polarization mechanism prevailing in that region. They have concluded that to consider a material to be a good dielectric material it should have high dielectric constant with small variations against frequency and temperature, low dielectric losses, chemical inertness and also stability against environment. As the

experimental results of plasma polymerized pyrrole films satisfy all the above mentioned quality so it is an ideal material to consider as a good dielectric material.

The dielectric properties from a set of molybdenum (Mo) containing diamond like carbon films deposited using electron cyclotron resonance chemical vapor deposition were investigated by Huang et al.[21]. It is shown that the film permittivity can be greatly increased by the introduction of Mo. There is a drastic reduction in the permittivity at frequencies of up to 10 kHz, followed by a slight decrease. The ac conductivity exhibits three characteristic regions in the frequency range investigated: constant, linear and super linear regions. The high ϵ'' and $\tan\delta$ at low frequencies resulted from the high dc conductivity of the films. The relaxation polarizations in the film are responsible for the peaks of ϵ'' and $\tan\delta$ which are approximately 0.8 and 4 kHz, respectively, for the film with Mo content of 3%. For the film with high Mo content, the permittivity is frequency dependent at low temperature. However, for the high frequency of 1 MHz, the film permittivity is weakly Mo dependent at the temperature below 145 K. The relaxation time decreases with increasing Mo content in the films at room temperature. The effect of voltage on the permittivity of the films is insignificant at frequencies above 10 kHz. They have concluded that the films have a potential application in microwave devices.

Moon Gyu Han and Seung Soon Im [22] reported that dielectric responses of polyaniline (PANI) salt films, made from two different methods, were compared to investigate the effect of a dopant and film formation methods on the dielectric properties. One of the film formation methods for emeraldine salt was the film doping method, and the other, the solution doping method. The conductivity, relaxation and dielectric properties were measured by a microdielectrometer at 293 K in the frequency range of 1 – 10^5 Hz. Dielectric spectra were a function of the dopant in the case of the film doping method, whereas it was a function of solvent dopant combinations as well as the dopants in the solution doping method. The dielectric responses of film doped samples had similar patterns irrespective of the dopants, while those of solution doped samples were varied, probably due to different conjugation conditions or/and the conduction mechanism. In the case of film doped samples, dielectric loss and permittivity values were increased with decreasing dopant sizes. The dielectric relaxation times were also varied depending on the

kind of dopants. The different solvent dopant combinations led to variation of the dielectric responses in the solution doped PANI due to an altered chain structure.

Sajeev et al. [23] investigated the pristine and iodine doped polyaniline thin films prepared by ac and rf plasma polymerization techniques separately for the comparison of their optical and electrical properties. The structural properties of these films were evaluated by FTIR spectroscopy and the optical band gap was estimated from UV-VIS-NIR measurements. They have found the optical band gap of polyaniline thin films prepared by rf and ac plasma polymerization techniques differ considerably and the band gap is further reduced by in situ doping of iodine.

Xiao Hu et al. [24] prepared a series of novel plasma-polymerized 4-cyanopyridine (PPCPD) thin films of desired thickness using plasma polymerization under different glow discharge conditions and investigated by FTIR, UV-Vis and XPS. They observed that PPCPD thin films were transparent, pinhole-free and uniform. They also observed a red shift in the maximum absorption wavelength (λ_{\max}) for all the plasma-deposited films as compared with the monomer absorption spectrum.

Kumar et al. [25] worked on PPPy in the presence and absence of iodine, and characterized its optical and electrical properties, IR and SEM result revealed that iodine was not bonded in any manner to the polymer chain of PPPy that it made the surface morphology of the PPPy film smoother. An analysis of the electronic spectra gave band gap energies of 13 and 0.8 eV for the undoped and doped PPPy films respectively. The current-voltage characteristics of the two types of polymer films revealed that the conductivity of the doped PPPy film was approximately two times greater than that of the undoped one. Thermally inactive compounds have sufficient stability so that such condensation reactions do not occur prior to complete volatilization. Copolymerization of diphenylamine (DPA) with N-methylaniline (NMA) were studied by Buvanewari et al. [26]. They characterized it by conductivity measurement, IR spectroscopy, UV-VIS spectroscopic techniques and TGA. They showed that the copolymer was synthesized through oxidative polymerization and the maximum decomposition occurs at 345°C and the complete decomposition of poly (DPA-co-NMA) occurs in the temperature range 375-495 °C. Thus it shows the higher thermal stability of the copolymer than PDPA.

Valaski et al. [27] reported their investigation of charge transport properties of thin electrodeposited PPPy films. The positive charge carrier mobility was estimated and demonstrated that its value was higher for thinner films. Dhar et al. [28] deposited organic film with plasma enhanced metal-organic chemical vapor deposition (PEMOCVD). The plasma polymerized organic film and the final heat-treated catalyst-loaded substrate surface have been characterized by SEM, impedance spectroscopy and energy dispersive spectroscopy (EDS). EDS was used to detect the presence of the catalyst on the substrate. Impedance spectroscopy applied to the precalcination organic film showed that relative electric permittivity was 2.49 and that conduction in the organic film involved charge carrier migration via a hopping conduction mechanism.

In our laboratory, work has been done on several plasma polymerized organic thin films. It is seen that the plasma polymerization emerges as a very important technique for thin film deposition and surface modification. So in the present research work, plasma polymerization technique has been used for the preparation of thin films. On reviewing the earlier works, it is found that CWO has been used in aromatic purpose only and ac and dielectric properties are not yet investigated. CWO is an organic compound. Their physical properties will be mentioned in experimental details. This type of materials is used as coatings, insulators, dielectrics, etc. That is why this material was chosen as a potential organic monomer for thin film preparation.

1.3 Aim of the Present Study

Polymers contain some polar groups and the dielectric behavior of plasma polymerized polymers is a function of time and temperature. Moreover, detailed studies of dielectric parameters such as the dielectric constant and the dielectric loss tangent ($\tan\delta$) over a wide range of frequencies and temperature can provide some significant information on structural, optical and ac electrical behavior about polymeric thin films.

The curiosity to find out the unknown is the eternal nature of human mind. There is no report on experimental studies of the above mentioned parameters on CWO thin films. So CWO was chosen as a potential organic monomer for thin film preparation and study of its structural, optical and ac electrical properties.

Plasma polymerized CWO (PPCWO) thin films are to be deposited by glow discharge of CWO gas. The chemical structure, absorption co-efficient, optical energy gaps and ac electrical conduction and dielectric relaxation processes are to be investigated.

(a) Structural and thermal properties:

The differential thermal property, Thermogravimetric property and the infrared spectroscopic property of as deposited and heat treated PPCWO thin films are to be investigated.

(b) Optical Properties :

The optical energy gaps, the allowed direct transitions, allowed indirect transitions and forbidden transitions of as deposited and heat treated PPCWO thin films are to be investigated.

(c) Electrical Properties :

The ac electrical conductivity, dielectric constant and loss tangent of PPCWO thin films are to be determined as a function of frequency at different constant temperature. Thickness dependence of these parameters is to be observed and analyzed with the existing theories to elucidate the relaxation behavior and dielectric loss mechanism involved in these materials. This will help to understand the relaxation and ac conduction behavior of the material. These findings will add new knowledge in the field of dielectric properties of plasma polymerized organic thin films, which may indicate some suitable application of this type of material in the electrical and electronic devices.

1.4 The Thesis –at a Glance

This research work has been configured into seven chapters.

Chapter 1 presents a general introduction. Some earlier and a number of literatures of recent works are reviewed to understand the scientific importance of those studies need for the present investigation and the objectives of the study.

Chapter 2 describes the details about polymers, plasma polymers, different polymerization processes, advantages and disadvantages of plasma polymers. Application of plasma polymerized organic thin films is presented at the end of this chapter.

Chapter 3 describes the experimental techniques are briefly explained in this chapter along with the description of the plasma polymerization set up, generation of glow

discharge, film thickness measurement, sample formation etc. The monomer, substrate materials and its cleaning process are also included here.

Chapter 4 concerns with differential thermal analysis, Thermogravimetric analysis and existing theories of IR spectroscopy, characterizes the data on the basis of theories to investigate the presence of different functional groups in PPCWO thin films.

Chapter 5 basically focuses on the UV-Vis spectroscopic analysis. The experimental details of UV-Vis absorption measurement and calculated values of direct transition energy gaps are discussed here.

Chapter 6 begins with a brief account of the ac properties such as ac conductivity, dielectric relaxation processes of as-deposited PPCWO thin films are discussed in this chapter. The variation of ac conductivity, dielectric constant and dielectric loss tangent, with thickness and temperature are presented.

Chapter 7 the conclusions of the work done and suggestions for future research on this material are included in this chapter.

References

- [1] Yasuda H., "Plasma Polymerization", Academic Press; New York (1985).
- [2] Chermisinoff N. P., "Handbook of Polymer Science and Technology ", Vol. 4 Marcel Dekker Inc., New York (1989).
- [3] Biederman H. and Osada Y., "Plasma Chemistry of Polymers", Advance in Polymer Sci., Berlin (1990).
- [4] Morita S. and Hattori S., " Applications of Plasma Polymers," in Plasma Deposition, Treatment, and Etching of Polymers; R d'Agostino, (Ed.), Academic Press, San Diego, CA,(1990).
- [5] Sarker R. B. and Bhuiyan, A. H., ' Structural and optical properties of plasma polymerized 1- Benzyl- 2- Methimidazole thin films', Int. J. Mod. Phys. B,(2010).
- [6] Easton, C. D., Jacob, M. V., 'Ageing and thermal degradation of plasma polymerized thin films derived from Lavandula angustifolia essential oil', Polym. Degrad. Stab. 94 (2009) 597.
- [7] Bazaka K., Jacob, M. V., 'Synthesis of radio frequency plasma polymerized non-synthetic Terpinen-4-ol thin films', Mater. Lett., 63 (2009) 1594.

- [8] Chowdhury F.-U.-Z., Bhuiyan, A.H., 'Dielectric properties of plasma- polymerized diphenyl thin films', *Thin Solid Films*, 370 (2000) 78.
- [9] Xiong-Yan Zhao, Ming-Zhu Wang, Zhi Wang, "Deposition of plasma-polymerized 1-Cyanoisoquinoline thin films and their dielectric properties", *Plasma Process. Polym.*, 4 (2007) 840.
- [10] Akther H., Bhuiyan, A. H., 'Dielectric properties of plasma polymerized N,N,3,5 Tetramethylaniline thin films', *Int. J. Mod. Phys. B.*, (2011).
- [11] Khanturgaev, A.G., Shiretorova, V.G., Radnaeva, L. D., Khanturgaeva, G. I., Averina, E. S., Bodoev, N. V., 'Investigation of the composition of Lipids of Siberian pine seeds', *Chemistry for Sustainable Development*, 11 (2003) 589 .
- [12] Ognian Marinov and Jamal Deen M., Jianfei Yu., George Vamrounis and Steven Holdcroft, William woods, "Variable current transport in polymer thin film transistors," *J. Vac. Sci. Technol. A* 22(3) (2004)360.
- [13] Mitu B., Bauer-Gogonea S., Leonharts Berger H., Linder M., Bauer S., Dinescu G., "Plasma deposited paraylene-like thin films: process and material properties," *Surf. Coat. Technol.* 174-175 (2003) 124.
- [14] Venkatesh M. S. and Raghavan G. S. V., "An overview of dielectric properties measuring techniques," *Canada Biosystems Engg.* 47(2005)715.
- [15] Biederman H. and Slavinska D., " Plasma polymer films and their future prospects" , *Surf. Coat. Technol.* 15 (2000) 31.
- [16] Chowdhury F-U-Z. and Bhuiyan A. H., "An investigation of the optical properties of the plasma polymerized diphenyl thin films" ,*This Solid Films* 360 (1-2) (2000) 69.
- [17] Akther H. and Bhuiyan A. H., "Infrared and ultraviolet-visible spectroscopic investigation of plasma polymerized N, N, 3, 5 – tetrametylaniline thin films", *Thin Solid Films* 474 (2005) 14.
- [18] Akther H. and Bhuiyan A. H., "Electrical and Optical properties of plasma polymerized N, N, 3, 5 tetramethylamiline thin films", *New J. Phys.* 7 (2005) 173.
- [19] Saravanan S., Joseph Mathai C., Venkatachalam S. and Anantharaman M. R., "Low k thin films based on rf plasma –polymerized aniline", *New J. Phys* 6 (2004) 64.

- [20] Sakthi Kumar D. and Yasuhika Yoshida, “ Dielectric properties of plasma polymerized pyrrole thin film capacitors”, *Surf. Coat. Technol.*, 169-170 (2003) 600.
- [21] Huang Q. F., Yoon S. F., Rusli, Zhang Q. and Ahn J., “Dielectric properties of molybdenum-containing diamond-like carbon films deposited using electron cyclotron resonance chemical vapor deposition.” *Thin Solid Films* 409 (2002) 211.
- [22] Moon Gyu Han, Seung Soon Im, “Dielectric spectroscopy of conductive polyaniline salt films”, *J. Appl. Polym. Sci.*, 82 (2001) 2760
- [23] Sajeev U. S., Joseph Mathai C., Saravanan S. S., Rajeev R. Ashokan, Venkatchalam S., Anantharaman M. R., “On the optical and electrical properties of rf and ac plasma polymerized aniline thin films,” *Bull. Mater. Sci.*, 29(2) (2006) 159.
- [24] Xiao H., Xiongyan Zhao, Uddin A. and Lee C. B., “Preparation, characterization and electronic and optical properties of plasma-polymerized nitrites”, *Thin Solid Films* 477 (2005) 51.
- [25] Kumar D. S., Nakamura K., Nishiyama S., Ishil S., Noguchi H., Kashiwagi K. and Yoshida Y., “Optical and electrical characterization of plasma polymerized pyrrole films”, *J. Appl. Phys.* 93(5) (2003) 2705.
- [26] Buvaneswari R., Gopalan A., Vasudevan T., Hsing-Lung Wang and Ten-Chin Wen, “Deposition, growth processes and characterization of poly (diphenylamine-co-N-methyl aniline)”, *Thin Solid Films* 458 (2004) 77.
- [27] Valaski R., Ayoub S., Micaroni L. and Hummelgen I. A., “Influence of film thickness on charge transport of electrodeposited polypyrrole thin films”, *Thin Solid Films* 415 (2002) 206.

CHAPTER 2
FUNDAMENTAL ASPECTS OF PLASMA, POLYMER, AND
PLASMA POLYMERIZATION

- 2.1 Introduction
 - 2.2 Polymers
 - 2.2.1 Classification based upon different factors related to polymers
 - 2.2.2 Description of the different types of polymers
 - 2.2.2.1 Depending on their origin polymers
 - 2.2.2.2 Depending on its ultimate form and use
 - 2.2.2.3 Depending on reaction mode of polymerization
 - 2.2.2.4 Depending upon Tacticity
 - 2.2.2.5 Depending on the biggest differences in polymer properties
 - 2.2.2.6 Depending on physical property related to heating
 - 2.2.3 Crystalline and amorphous states of polymer
 - 2.3 Plasma and Plasma Polymerization
 - 2.3.1 Plasma: The fourth State of Matter
 - 2.3.2 A summary of gas discharge plasma
 - 2.3.3 Direct current glow discharge
 - 2.3.4 Alternating current glow discharge
 - 2.3.5 Advantages of plasma polymerization
 - 2.3.6 Details of Plasma polymerization
 - 2.4 Different Types of Glow Discharge Reactors
 - 2.4.1 Capacitively coupled radio-frequency discharge
 - 2.4.2 Inductively coupled glow discharges
 - 2.5 Overall reactions and growth mechanism in plasma polymerization
 - 2.6 Advantages and Disadvantages of Plasma Polymers
 - 2.7 Applications of Plasma-polymerized Organic Thin Films
- References

2.1 Introduction

Polymeric materials are widely used in a great number of applications because of their many advantageous, general properties such as low density and cost, and processability. Not only has these but also included chemical, physical and biological sensors, microelectronic devices, nonlinear optical device and molecular devices. Polymer uses are being developed in such diverse areas such as: conduction and storage of electricity, molecular based information storage and processing, molecular composites, unique separation membranes, new forms of food processing and packaging, health, housing, and transportation. Indeed, polymers will play an increasingly important role in all aspects of everyday life. The large number of current and future applications of polymeric materials has created a great interest for scientists to carry out research and development in polymer science and engineering [1]. Therefore it is very important to take this research programme to gather more knowledge in this field.

This chapter represents a detail of polymers with polymers classifications, plasma, an overview of gas discharge plasma, plasma polymerization, different types of glow discharge reactors, plasma polymerization mechanism, advantages and disadvantages of plasma polymerized thin films and applications of plasma polymerized organic thin films.

2.2 Polymers

The term 'polymer' is derived from the Greek words: *polys* meaning *many*, and *meros* meaning *parts*. Polymers are long chain giant organic molecules assembled from many smaller molecules called monomers that can be linked together to form long chains, thus they are known as *macromolecules*. A typical polymer may include tens of thousands of monomers. Because of their large size, polymers are classified as macromolecules. A polymer is a substance composed of molecules with large molecular mass composed of repeating structural units, or monomers, connected by covalent chemical bonds.

Polymers have anomalous properties because they were so different from the properties of low molecular weight compounds. The presumably anomalous properties of polymers were shown to be normal for such materials, as the consequences of their size were included in the theoretical treatments of their properties. Primary chemical bonds along polymer chains are entirely satisfied. The only forces between molecules are secondary bond forces of attraction, which are weak relative to primary bond forces. The

high molecular weight of polymers allows these forces to build up enough to impart excellent strength, dimensional stability and other mechanical properties to the substances. Polymers are thought to be colloidal substances i.e. glue-like materials. From chemical point of view, the colloidal substances are in fact large molecules and their behavior could be explained in terms of the size of the individual molecules. Polymers having molecular weight roughly in the range of 1000-20,000 are called low polymers and those having molecular weight higher than 20,000 as high polymers. [2,3]

2.2.1 Classification based upon different factors related to polymers

There exist many polymers or macro-molecules, which contain hundreds or thousands of atoms. Some of these are naturally occurring and some of these are man made, Both of these cover a wide range of polymers.

Table 2.1 Classification of polymer

Basic Classification	Polymer types
Source [origin]	Natural, Synthetic, Semi-synthetic polymers
Technological use	Adhesives, Fibers, Plastics, Elastomers, Paint & Coatings
Polymerization	Addition, Condensation
Microstructure	Crystalline, Semicrystalline, Amorphous
Tacticity	Isotactic, Syndiotactic, Atactic
Architecture	Linear, Branched, Cross-linked
Processing characteristics	Thermoplastic, Thermoset
Chemistry of composition	homo-polymer, co-polymer
Engineering performance	Commodity polymers, engineering polymers

2.2.2 Description of the different types of polymers

2.2.2.1 Depending on the origin of polymers

Depending on their origin polymers can be divided into three classes

(a) *Natural polymers*: The polymers which are obtained from nature (plants and animals) and very essential for life, are known as natural polymers. They are *Starch, Cellulose, Proteins, Nucleic acids*, etc.

(b) *Synthetic polymers*: The polymers which are prepared in the laboratories are called synthetic polymers. These types of polymers are synthesized from low molecular weight compounds. That's why, they are also known as man-made polymers. Polyethylene, PVC, nylon, teflon, bakelite, terylene, synthetic rubber etc. are such types of polymers.

(c) *Semisynthetic polymers*: These polymers are mostly derived from naturally occurring polymers by chemical modifications. For example, cellulose is a naturally occurring polymer, cellulose on acetylation with acetic anhydride in the presence of sulphuric acid forms cellulose diacetate polymers. It is used in making thread and materials like films, glasses etc. Vulcanized rubber is also an example of semisynthetic polymers used in making tyres etc. Gun cotton which is cellulose nitrate used in making explosive.

2.2.2.2 Depending on its ultimate form & use:

Depending on its ultimate form & use, there are three types of polymers, discussed below:

(a) *Rubbers*: In general, a rubber material is one which can be stretched to at least twice its original length and rapidly contract to its original length. Rubber must be a high polymer (polymers with very long chains) as rubber elasticity, from a molecular standpoint, is due to the coiling and uncoiling of very long chains.

(b) *Fibers*: *Fibers* are regarded by some as a separate class of polymers in spite of a considerable overlap with plastics. We can also say that fiber is that whose length is at least hundred times its diameter. While natural fibers (except silk) occur as staples, synthetic fibers can be produced as continuous filaments or cut to form staples.

If drawn into long filament-like materials, whose length is at least 100 times its diameter, polymers are said to have been converted into fibers, i.e. Nylon, Terylene. Like as:

- i) Fibers of natural origin: Cotton, Wool, Flax and Silk.
 - ii) Man-made or synthetic fibers made of nylon, polyesters, polypropylene and acrylics.
- (c) *Elastomers*: Elastomers are rubbery polymers that can be stretched easily to several times their unstretched length and which rapidly return to their original dimensions when the applied stress is released. In a simple word, it can be said that when vulcanized into rubbery products exhibiting good strength and elongation, polymers are used as elastomers. Elastomers are cross-linked, but have a low cross-link density. The polymer chains still

have some freedom to move, but are prevented from permanently moving relative to each other by the cross-links. Typically, about 1 in 100 molecules are cross-linked on average. When the average number of cross-links rises to about 1 in 30 the material becomes more rigid and brittle.

(d) *Plastics*: Plastics are polymers which, under appropriate conditions of temperature and pressure, can be molded or shaped (such as blowing to form a film). In contrast to elastomers, plastics have a greater stiffness and lack reversible elasticity. For example : Polystyrene, PVC(Fig:2.1) and polymethyl methacrylate. It is noted that All plastics are polymers but not all polymers are plastics.

2.2.2.3 Depending on reaction mode of polymerization:

Depending on reaction mode there are two types of polymerization. They are as follows

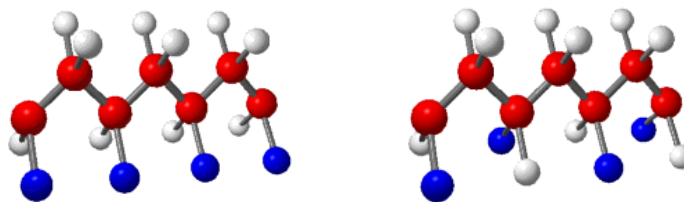
(a) Addition Polymers - the monomer molecules bond to each other without the loss of any other atoms. Alkene monomers are the biggest groups of polymers in this class.

(b) Condensation Polymers - usually two different monomers combine with the loss of a small molecule, usually water. Polyesters and polyamides (nylon) are in this class of polymers.

2.2.2.4 Depending upon tacticity:

Depending upon tacticity the types of polymer can be describes as follows-

Stereo regularity is the term used to describe the configuration of polymer chains. Three distinct structures can be obtained. *Biostatic* is an arrangement where all substituents are on the same side of the polymer chain. A *syndiotactic* polymer chain is composed of alternating groups and *atactic* is a random combination of the groups. The following figure 2.1 shows two of the three *stereo isomers* of polymer chain.



Isotactic

Syndiotactic

Fig. 2.1 The types of polymer depending on tacticity

2.2.2.5 Depending on the biggest differences in polymer properties

This classification result from how the atoms and chains are linked together in space.

(a) *Linear*: Linear polymers are most common. They can occur whenever two reacting chains join to make a chain. If the long-chains pack regularly, side-by-side, they tend to form crystalline polymers. If the long chain molecules are irregularly tangled, the polymer is amorphous since there is no long range order. Sometimes this type of polymer is called glassy.

(b) *Cross-Linking*: In addition to the bonds which hold monomers together in a polymer chain, many polymers form bonds between neighboring chains. These bonds can be formed directly between the neighboring chains, or two chains may bond to a third common molecule. Though not as strong or rigid as the bonds within the chain, these *cross-links* have an important effect on the polymer. Polymers with a high enough degree of cross-linking have "memory." When the polymer is stretched, the cross-links prevent the individual chains from sliding past each other. The chains may straighten out, but once the stress is removed they return to their original position and the object returns to its original shape.

2.2.2.6 Depending on physical property related to heating:

(a) *Thermoplastics* - plastics that soften when heated and become firm again when cooled. This is the most popular type of plastic because the heating and cooling may be repeated.

(b) *Thermosets* - plastics that soften when heated and can be molded, but harden permanently. They will decompose when reheated. An example is Bakelite, which is used in toasters, handles for pots and pans, dishes, electrical outlets and billiard balls.

Classification due to chemistry of composition:

(c) *Homopolymers* - consist of chains with identical bonding linkages to each monomer unit. This usually implies that the polymer is made from all identical monomer molecules. These may be represented as: - [A-A-A-A-A-A]-

(d) *Copolymers* - consist of chains with two or more linkages usually implying two or more different types of monomer units. These may be represented as: - [A-B-A-B-A-B]- Copolymers, in whose molecules long lengths (blocks), composed of monomer units of single type, alternate with blocks; with monomers units of another type, are called *block copolymers*. If in a branched polymer a long side branch consists of monomer units of a type different from those of the main chain, the material is called a *graft polymer*. Different types of copolymers are shown in figure 2.2.

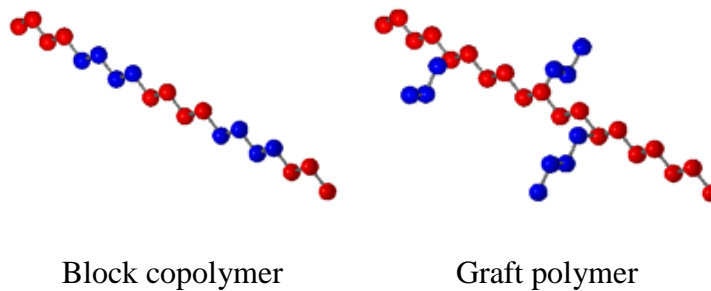


Fig. 2.2 Different types of copolymers.

(e) **Condensation Polymers**- Usually two different monomer combine with the loss of a small molecule, usually water. Polyesters and polyamides (nylon) are in this class of polymers.

2.2.3. Crystalline and amorphous states of polymer

Crystallinity in polymers: Molecular shape and the way molecules are arranged in a solid are important factors in determining the properties of polymers. The general concept of self-assembly enters into the organization of molecules on the micro and macroscopic scale as they aggregate into more ordered structures. The morphology of most polymers is semi-crystalline. That is, they form mixtures of small crystals and amorphous material and melt over a range of temperature instead of at a single melting point. The crystalline material shows a high degree of order formed by folding and stacking of the polymer chains. The amorphous or glass-like structure shows no long range order, and the chains are tangled as illustrated below in figure 2.3.

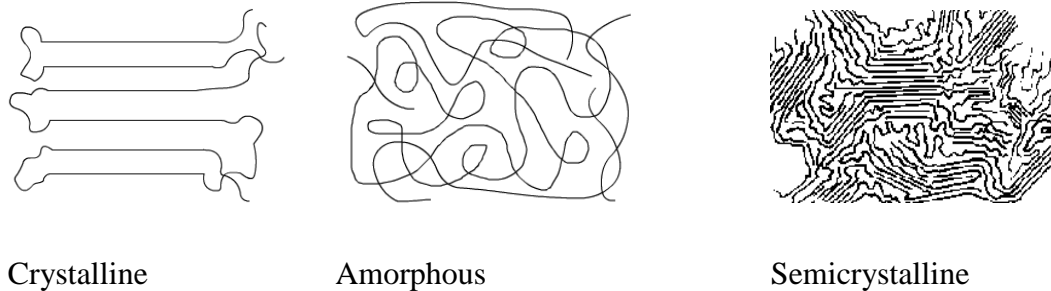


Fig. 2.3 Different states of Polymers

There are some polymers that are completely amorphous, but most are a combination with the tangled and disordered regions surrounding the crystalline areas. Such a combination is shown in the following diagram.

An *amorphous* solid is formed when the chains have little orientation throughout the bulk polymer. The *glass transition temperature* is the point at which the polymer hardens into an amorphous solid. This term is used because the amorphous solid has properties similar to glass.

2.3 Plasma and Plasma Polymerization

2.3.1 Plasma: The fourth state of materials

Plasma is ionized gases. Hence, they consist of positive and negative ions, electrons, as well as free radicals. The ionization degree can vary from 100% (fully ionized gases) to very low values (partially ionized gases). The plasma state is often referred to as the fourth state of matter. Much of the visible matter in the universe is in the plasma state. Stars, as well as visible interstellar matter, are in the plasma state. Besides the astroplasmas, which are omnipresent in the universe, there are two main groups of laboratory plasma, i.e., the high-temperature of fusion plasmas, and the so called low-temperature plasma or gas discharges. In general, a subdivision can be made between plasmas which are in the thermal equilibrium and those which are not in the thermal equilibrium. Thermal equilibrium implies that the temperature of all species (electrons, ions, neutral species) is the same. High temperature is required to form these equilibrium plasmas, typically

ranging from 4000 K to 20000 K. This is true for stars, as well as for fusion plasmas. On the other hand, interstellar plasma matter is typically not in thermal equilibrium [4].

Plasmas get used technically, i.e. in fluorescent tubes and, above all, in recent times in the surface technique. A current differentiation of plasmas is the division in hot (thermal) and cold (non-thermal) plasmas. In the case of thermal plasmas the pressure of the gases is relatively high, which raises the number of collisions between the particles (neutral, charges, excited, non-excited) and thereby encourages the conveyance of the energy between them. The result is plasma that finds itself in thermodynamic equilibrium, so that all the approximate particles show the same high energy, which we perceive as "hot". In comparison, non-thermal plasmas develop at reduced pressure (ca. $1\text{-}10^4\text{Pa}$). Macroscopically viewed, the system is placed at room temperature; but contains a known share of particles, namely electrons, that show very high energies (temperatures up to 10^5 °C). These high energy electrons and the high energy radiation from electron migration are qualified in the induction of chemical reactions on surfaces, or rather in near-surface ranges, where even the modification of very stable structures can occur. Simultaneously, no thermal strain of this surface occurs, due to the fact that the macroscopic plasma temperature is adapted to the surroundings.

Besides the astropasmas there are two main groups of laboratory plasmas, i.e. the high-temperature or fusion plasma and the so-called low temperature plasma or gas discharge. Generally subdivision can be made between plasmas, which are in thermal equilibrium, and those, which are not in thermal equilibrium [5,6]. Thermal equilibrium implies that the temperature of all species (electrons, ions, neutral species) is the same. Sometimes the term 'Local thermal equilibrium (LTE)' is used, which implies that the temperatures of all plasma species are the same in localized areas in the plasma. On the other hand, interstellar plasma matter is typically not in thermal equilibrium also called 'non-LTE'.

In recent years, the field of gas discharge plasma applications has rapidly expanded [7,8,9]. The wide variety of chemical non-equilibrium conditions is possible since parameters can easily be modified such as the chemical input pressure, electromagnetic field structure, discharge configuration, temporal behavior.

Four types of plasma i.e., the glow discharge (GD), capacitively coupled (CC), inductively coupled plasma (ICP), and the micro wave-inductively plasma (MIP), are commonly used in plasma spectrochemistry and are therefore familiar to most spectrochemists. However these plasmas, as well as related gas discharges, are more widely used in technological fields.

In general, plasma can be referred to as the fourth state of matter, composed of atomic, molecular and ionic species, radicals and photons, highly excited, with a neutral electrical charge in the macroscopic sense. It is typically obtained by exciting a gas or vapor into high energetic states by radiofrequency, microwave, ac or dc current glow discharges, or as well as by the electrons of a hot filament discharge. The high density of ionized and excited species in the plasma can change the surface of normally inert materials [4].

To generate the plasma, it is necessary to ionize atoms or molecules in the gas phase. When an atom or molecules gains enough energy from an external excitation source or through collisions with another molecule, ionization occurs [4]. This happens usually when the molecules are under specific conditions, like extreme heat, generating the so - called *hot plasmas*, or under electrical glow discharge, for the *cold plasmas* [10]. The plasmas loose energy to their surroundings through collision and radiation processes; as a result, energy must be supplied continuously to the system to maintain the plasma state. The easiest way to supply energy to a system in a continuous manner is with an electrical source. Therefore, electrical glow discharges are the most common plasmas [11].

In cold plasmas, a glow discharge can be generated by the transfer of power from an electric field to electrons. Different kinds of sources can be used, such as direct current or radiofrequency glow discharge, or electron cyclotron resonance, as an example, to generate uniform plasma in a relative big area with a controlled electronic density [4].

In an alternating current (ac) glow discharge, the mechanism depends on the frequency of the excitation. At low frequencies, the system can be looked upon as a DC glow discharge with alternating polarity. By increasing the frequency of the applied voltage, positive ions become immobile, because they can no longer follow the periodic changes in field polarity, and only respond to time - averaged fields. At frequencies above

500 kHz, the half - cycle is so short that all electrons and ions stay within the interelectrode volume. This reduces the loss of charged particles from the system significantly, and regeneration of electrons and ions occurs within the body of the plasma through collisions of electrons with gas molecules. In radiofrequency plasma (13.56 MHz) therefore, no contact between the electrodes and the plasma is required. The plasma can be initiated and sustained by external electrodes, at a much lower voltage than is required for maintaining a direct current glow discharge [11-13].

2.3.2 A summary of gas discharge plasma [7, 8]

Plasma polymerization take place in a low pressure (or low temperature) plasma that is provided by a glow discharge operated in an organic gas or vapor (monomer) at low pressure between two electrodes. When a sufficient high potential difference is applied between two electrodes placed in a gas, the latter will break down into positive ions and electrons, giving rise to a gas discharge. The mechanism of the gas breakdown can be explained as follows: a few electrons are emitted from the electrodes due to the omnipresent cosmic radiation.

However, when a potential difference is applied the electrons are accelerated by the electric field in front of the cathode and collide with the gas atoms. The most important collisions are the inelastic collisions leading to excitation and ionization. The excitation collisions create new electrons and ions. The ions are accelerated by the electric field toward the cathode, where they release new electrons by ion-induced secondary electron emission. The electrons give rise to new ionization collisions, creating new ions and electrons. These processes of electron emission at the cathode and ionization in the plasma make the glow discharge self-sustaining plasma.

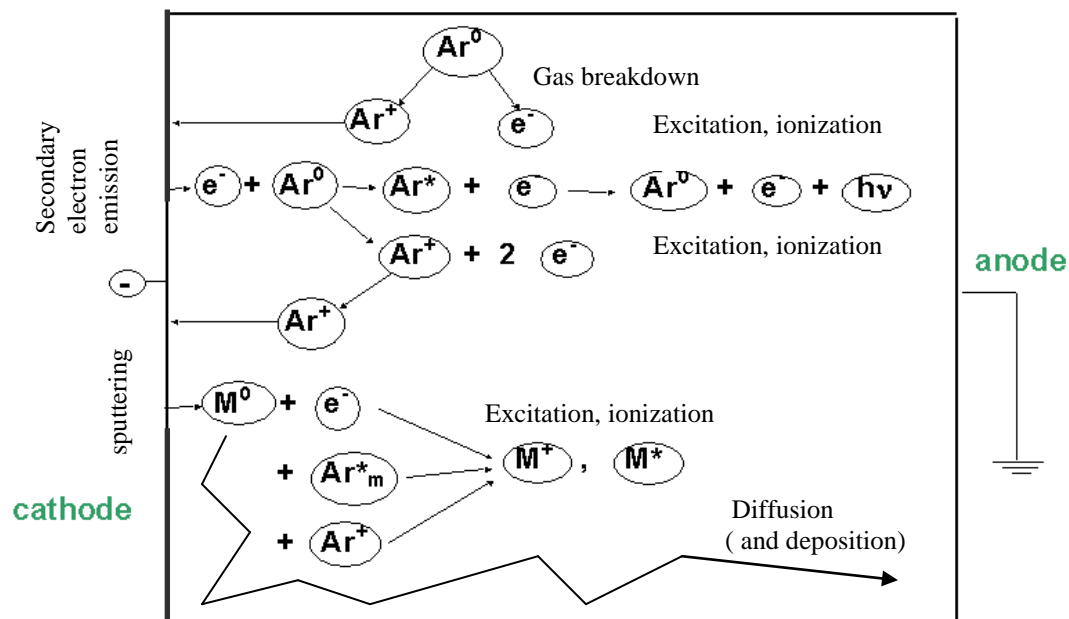


Fig.2.4 Schematic overview of the basic processes in a glow discharge.

Another important process in the glow discharge is the phenomenon of sputtering, which occurs at sufficiently high voltage. When the ions and fast atoms from the plasma bombard the cathode, they not only release secondary electrons, but also atoms of the cathode materials, which are called sputtering, shown in figure 2.4. This is the basis of the use of glow discharges for analytical spectrochemistry. The ions can be detected with a mass spectrometer and the excited atoms or ions emit characteristic photons, which can be measured with optical emission spectrometry. Alternatively, the sputtered atoms can also diffuse through the plasma and they can be deposited on a substrate, this technique used in materials technology e.g. for the deposition of thin films.

Glow discharge is characterized by the appearance of several luminous zones and by a constant potential difference between the electrodes independent of current. Basically the operation of the glow discharge depends critically on the role of the cathode dark space shown in figure 2.5. In order to have a steady state each electron emitted by the cathode must produce sufficient ionization and excitation to effect the release of a sufficient number of secondary electrons from the cathode upon impact of the ions. The role of the anode is to transform current from the glow discharge to the external circuit. When there is no positive column, the anode is usually in the Faraday dark space. In this case, the anode fall of potential can be very small, or even negative, because ions and electrons diffuse

together to the anode from the negative glow in such a way that the neutrality of charges is maintained.

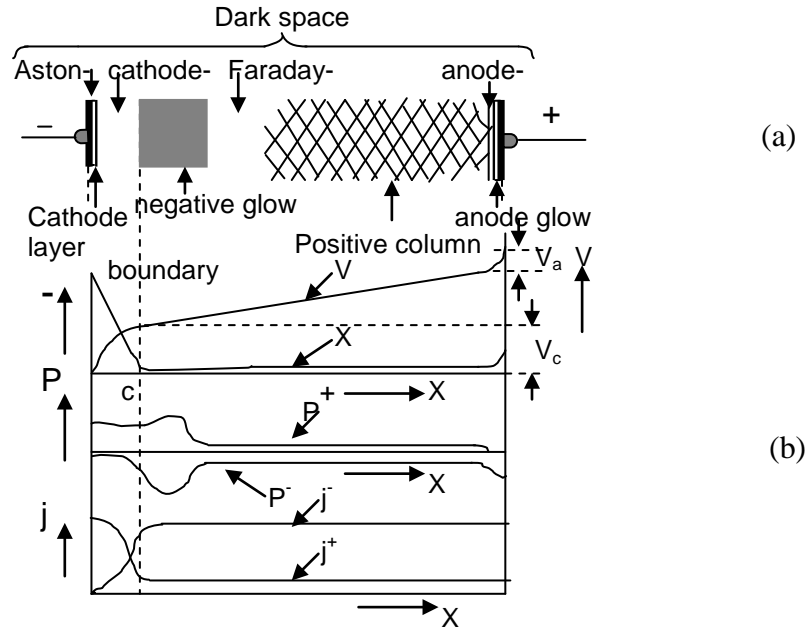


Fig.2.5 Normal glow discharge; (a) the shaded areas are luminous, (b) distribution of potential among luminous zones.

2.3.3 Direct Current (dc) glow discharge

Plasma polymerization process takes place usually in a low temperature generated by glow discharge. The space between the electrodes becomes visible when a glow discharge is established; the actual distribution of light in the glow discharge is significant and is dependent on the current-voltage characteristics of the discharge [15-17].

When a constant potential difference is applied between the cathode and anode, a continuous current will flow through the discharge; giving rise to a direct current (dc) glow discharge. In a dc glow discharge the electrodes play an essential role for sustaining the plasma by secondary electron emission. The potential difference applied between the two electrodes is generally not equally distributed between cathode and anode, but it drops almost completely in the first millimeters in front of the cathode. However, for most of the other applications of dc glow discharges (sputtering, deposition, chemical etching, analytical chemistry etc.), the distance between cathode and anode is generally short. So

normally a short anode zone is present beside cathode dark space and negative glow, where the slightly positive plasma potential returns back to zero at the anode.

A dc glow voltage can operate over a wide range of discharge conditions. The pressure can vary from below 1 Pa to atmospheric pressure. The product of pressure and distance between the electrodes (PD) is a better parameter to characterize the discharge. For instance, at lower pressure, the distance between cathode and anode should be longer to create a discharge with properties comparable to these of high pressure with small distance. The discharge can operate in a rare gas (most often argon or helium) or in a reactive gas (N_2 , O_2 , H_2 , CH_4 , SiH_4 , SiF_4 , etc.), as well as in a mixture of these gases.

Depending on the discharge conditions both ions and neutrals vary in their molecular weight arising from collisions with electrons. These electrons causes discharge typically and have average energy of 5-10 eV, which is more than sufficient to break the chemical bonds that are usually having binding energies within 3-9 eV. Generally free radicals are considered the most important species for plasma polymerization.

2.3.4 Alternating current (ac) glow discharge

The mechanism of glow discharge generation will basically depend on the frequency of the alternation. With increasing frequency, the motion of ions can no longer follow the periodic changes in the field. At low frequencies (60 Hz), the effect is simply to form dc glow discharges of alternating polarity. However the frequency is higher than 6GHz the motion of ions can no longer follow the periodic changes in field polarity. But above 500 kHz the electrode never maintains its polarity long enough to sweep all electrons or ions, originating at the opposite electrode, out of the inter-electrode volume. In this case the regeneration of electrons and ions that are lost to the walls and the electrodes takes place within the body of the plasma. The mechanism by which electrons pick up sufficient energy to cause bond dissociation or ionization involves random collisions of electrons with gas molecules, the electron picking up an increment of energy with each collision. A free electron in a vacuum under the action of an alternating electric field oscillates with its velocity 90° out of phase with the field, which obtains no energy, on the average, from the applied field. The electron can gain energy from the field only as a consequence of elastic collisions with the gas atoms, as the electric field converts the

electron's resulting random motion back to ordered oscillatory motion. Because of its interaction with the oscillating electric field, the electron gains energy on each collision until it acquires enough energy to be able to make an inelastic collision with a gas atom; In that case the process of these inelastic collisions is termed volume ionization.

Thus the transfer of energy from the electric field to electrons at high frequencies is generally accepted as that operative in microwave discharges. It has also been put forward as that applicable to the widely used rf of 13.56 MHz.

2.3.5 Advantages of plasma polymerization

The main advantage of plasma polymerization is that it can occur at moderate temperature compared to conventional chemical reaction. Plasma-based techniques offer the following advantages with consider to biomaterials engineering.

- i. The benefits of plasma processing take place from the good understanding of plasma physics and chemistry learned in other fields such as microelectronics, i.e, plasma homogeneity and effects of non-uniform plasma on the substrate surface [18].
- ii. Plasma engineering is usually reliable, reproducible, relatively inexpensive, and applicable to different sample geometries as well as different materials such as metals, polymers, ceramics, and composite [19].
- iii. Plasma treatment can result in changes of a variety of surface characteristics, for example, chemical, tribological, electrical, optical, biological, and mechanical. Proper applications yield dense and pinhole free coatings with excellent interfacial bonds due to the graded nature of the interface [20].
- vi. Plasma processing can provide hygienic surfaces and can be scaled up to industrial production relatively easily. On the opposing, the flexibility of non-plasma techniques for different substrate materials is smaller [21].
- v. Plasma techniques are compatible with masking techniques to enable surface patterning, a process that is commonly used in the microelectronics industry [22].

2.3.6 Details of Plasma polymerization

In the plasma polymerization process, a monomer gas is pumped into a vacuum chamber where it is polymerized by plasma to form a thin, clear coating. The monomer starts out as a liquid. It is converted to a gas in an evaporator and is pumped into the vacuum chamber. A glow discharge initiates polymerization. The excited electrons created in the glow discharge ionize the monomer molecules. The monomer molecules break apart (fractionate) to create free electrons, ions, excited molecules and radicals. The radicals adsorb, condense and polymerize on the substrate. The electrons and ions crosslink, or create a chemical bond, with the already deposited molecules, creating a harder, denser coating. A schematic plasma polymerization configuration is presented in the figure 2.6 below.

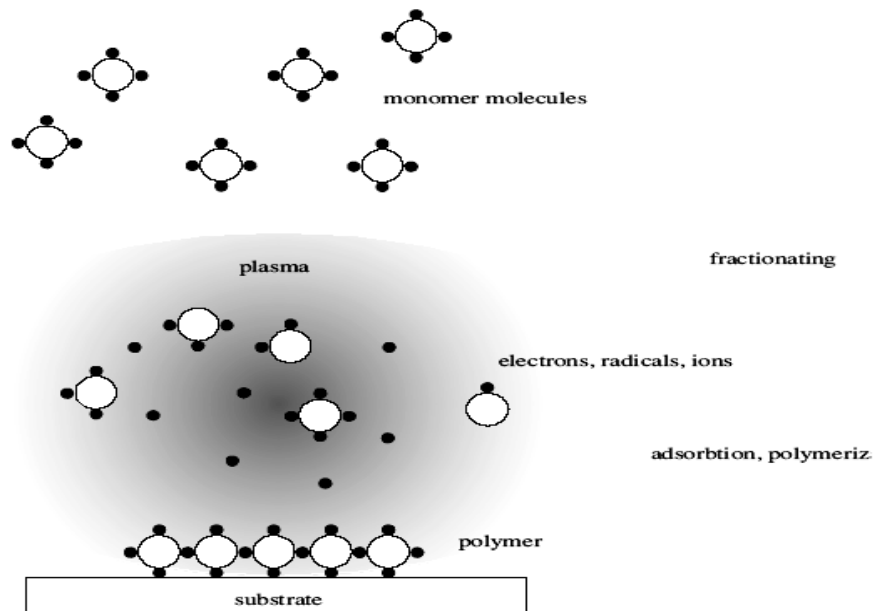


Fig.2.6 A schematic plasma polymerization configuration

The materials obtained by plasma polymerization are significantly different from conventional polymers and also different from most inorganic materials. Hence plasma polymerization should be considered as a method of forming new types of materials rather than a method of preparing conventional polymers. Thus plasma polymerization is a flexible technique for the deposition of films with functional properties suitable for a wide range of modern applications. Historically, it was known that electric discharge in a glass tube forms oily or polymer-like products at the surface of the electrodes and at the wall of

the glass tube. This undesirable deposit however had extremely important characteristics that are sought after in the modern technology of coating that is, i) excellent adhesion to substrate materials and ii) strong resistance to most chemicals.

To explain the reaction mechanism, many investigators discussed the effects of discharge conditions such as polymerization time monomer pressure, discharge current, and discharge power and substrate temperature on the polymerization rate.

In several cases, polymers formed by plasma polymerization show distinguished chemical composition and chemical and physical properties from those formed by conventional polymerization, if the same monomer is used for the two polymerization. To appreciate the uniqueness of plasma polymerization, it is useful to compare the steps necessary to obtain a good coating by a conventional coating process and by plasma polymerization. Coating a certain substrate with a conventional polymer, at least several steps are required (1) synthesis of a monomer, (2) polymerization of the monomer to form a polymer, (3) preparation of coating solution, (4) cleaning, (5) application of the coating, (6) drying of the coating and (7) curing of the coating. Polymers formed by plasma polymerization aimed at such a coating are in most cases branched and cross-linked. Such polymers also depend on (1) synthesis of a monomer, (2) Creation of plasma medium. (3) polymerization of the monomer to form a polymer, (4) cleaning, (5) application of the polymer film, and (6) curing of the film.

2.4 Different Types of Glow Discharge Reactors [23]

Glow discharge reactor is the important part of plasma polymerization system. Because reactor geometry influences the extent of charge particle bombardment on the growing films which affects the potential distribution in the system, Different kinds of reactors including capacitively coupled and inductively coupled RF reactors, microwave, dual-mode (MV/RF), etc, can be used for plasma polymerization processes. The presence of insulating layers on the electrodes deflects plasma current into any surrounding conducting areas and thus leads to gross plasma non-uniformity or plasma extinction. Therefore, when insulating materials are involved, AC power is usually employed so that power may pass through the insulator by capacitive coupling. Figure 2.7 shows the most widely used reactor configurations for plasma polymerization can be broadly divided in to three classes.

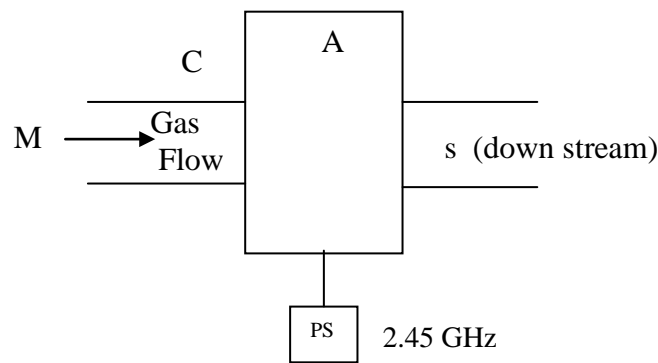
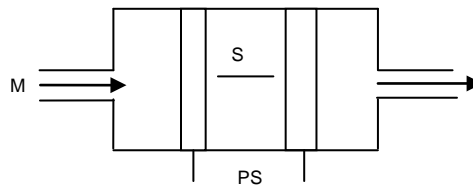
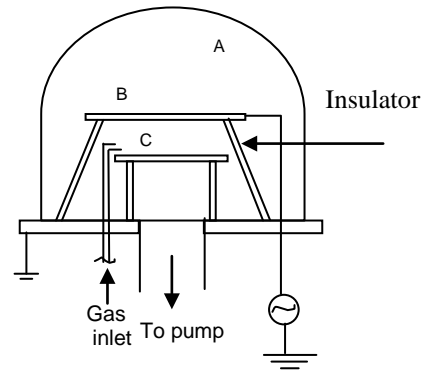
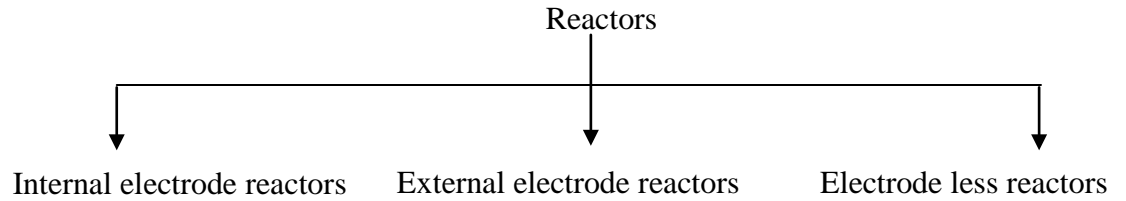


Fig.2.7: Different types of reactor configuration used for plasma polymerization (a) schematic of a bell jar reactor, (b) parallel plate internal electrode reactor, (c) electrode less microwave reactor.

Reactors with internal electrodes have different names, e.g. flat bed parallel plates, planar, diode etc. Their main features are power supply, coupling system, vacuum chamber, radio frequency (rf) driver electrode, grounded electrode, and eventually one or

most substrate holders. Among the internal electrode arrangements a bell-jar-type reactor with parallel plate metal electrodes is most frequently used by using ac (1-50 kHz) and rf fields for plasma excitation.

The vacuum chambers can be made either of glass or of conductive materials, such as metal. In the case of bell-jar reactors, no particular care is taken for the grounded electrode apart from its area. On the contrary, the design and arrangement of the cathode require special attention: a metallic shield surrounding the electrode highly improves the glow confinement inside interelectrode space; electrode material and area greatly affect the extent of sputtering on the target.

In the current research, capacitively coupled reactor (glow discharge plasma) system was used for the formation of thin films.

2.4.1 Capacitively coupled radio-frequency discharge

If an ac voltage (up to kHz) is used, the discharge is still basically of a dc type and each electrode really acts as a cathode and anode alternatively. The frequencies generally used for the alternating voltages are typically in the rf range.

Capacitively coupled (cc) discharge can also be generated by alternating voltages in another frequency range. Therefore, the term 'alternating current (ac) discharges' as opposed to dc discharges might be more appropriate. The term 'capacitively coupled' refers to the way of coupling the input power into the discharges i.e. by means of two electrodes and their sheaths forming a kind of capacitor. The cc rf discharges which also results from the differences in mass between electrons and ions, is the phenomenon of self bias. The self-bias or dc-bias is formed i) when both electrodes differ in size and ii) when a coupling capacitor is present between the rf power supply and the electrode or when the electrode is non conductive (because it then acts as a capacitor). When a certain voltage is applied over the capacitor formed by the electrodes, the voltage over the plasma will initially have the same value as the applied voltage.

2.4.2 Inductively coupled (IC) glow discharge

Basically, two different coil configurations can be distinguished in inductive discharges for processing applications, i.e. cylindrical and planar. In the first configuration,

a coil is wound around the discharge chamber, as a helix. In the second configuration, which is more commonly used for materials processing, a flat helix or spiral is wound from near the axis to near the outer radius of the discharge chamber, separated from the discharge region by a dielectric. Advantages of the latter are reduced plasma loss and better ion generation efficiency; disadvantage is the higher sputter-contamination, UV-damage and heating of neutrals at the substrate. Multipole permanent magnets can be used around the process chamber circumference to increase radial plasma uniformity. The planar coil can also be moved close to the wafer surface, resulting in near-planar source geometry, having good uniformity properties even in the absence of multipole confinement.

It should be mentioned that the coupling in IC plasma is generally not purely inductive, but has a capacitive component as well, through the wall of the reactor. Indeed, when an inductive coupling is used, deposition on the wall is often observed to follow a pattern matching the shape of the coil. This is an indication of localized stronger electric fields on the walls, showing that the coupling is at least partly capacitive through the walls of the reactor. It is mentioned that inductively coupled plasma are not only used as materials processing discharges, but they are also applied in other fields, albeit in totally different operating regimes. So IC plasmas are the most popular plasma sources in plasma spectrochemistry.

2.5 Overall reactions and growth mechanism in plasma polymerization

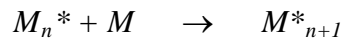
The mechanism of reaction by which plasma polymerization occurs is quite complex and cannot be specifically described for the general case. Operational parameters such as monomer flow rate, pressure frequency, and power affect the deposition rate and structure of the plasma film. The electrons or atoms generated by partial ionization of the molecules are the principle sources for transferring energy from the electric field to the gas in all glow discharges [24,25].

In plasma polymerization, free electrons gain energy from an imposed electrical field and then transfer the energy to neutral gas molecules, which lead to the formation of many chemically reactive species. By applying greater power to the rf source, the energy per unit mass of the monomer is increased and may bring about changes in the

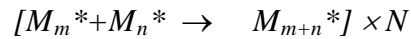
fragmentation process. As a result, free radicals may become entrapped in the plasma-polymerized film and increase in concentration with increasing rf power. The deposition of polymer films in low-pressure plasma is a complex phenomenon involving reactions, which occur both in the plasma phase and at the surfaces bounding the plasma.

The study of plasma polymerization kinetics is commonly employed to explain polymerization mechanisms. With this background a comparison of the polymer formation rates of various monomers by plasma polymerization would provide an overview of the kind of reaction mechanism responsible for plasma polymerization.

The probable chain growth polymerization is represented by

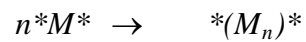


Where M_n^* is the reactive chain carrying species and M is the monomer molecules. But Yasuda and Lamaze [17] on the basis of their observation on plasma polymerization ruled out the chain growth polymerization. The rapid step-growth mechanism is very likely to be the reaction in plasma polymerization and this reaction is expressed as:

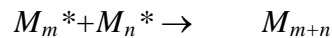


Where N represents the number of repetitions of similar reactions. In this case, the reaction occurs between molecules.

In case of parylene polymerization, $*M^*$ is a difunctional reactive species and the overall polymerization can be represented by



If the reactive species are monofunctional (M^*), such as free radical R^* , the reaction is given by



Which is essentially a termination process that occurs in free radical polymerization and does not contribute without additional elementary steps. Yasuda H and Lamaze C E [25] pointed out that the reactivation of the product of an elementary reaction was bound to occur in plasma.

The overall polymerization mechanism based on the rapid step-growth principle shown in Fig. 2.8. The figure shows the overall reaction, which contains two major routes

of rapid step-growth. Cycle (C-1) is via the repeated activation of the reaction products from monofunctional activated species, C-2 is via difunctional or multifunctional activated species.

Here, M_x refers to neutral species that can be original monomer molecule or any of the dissociation products including some atoms, such as hydrogen, chlorine, fluorine and others; M^* activated species; $*M^*$ difunctional activated species and the subscripts i, j, k indicate the difference in the size of the species involved ($i=j$ is possible, thus $i=j=1$ for initial monomer.)

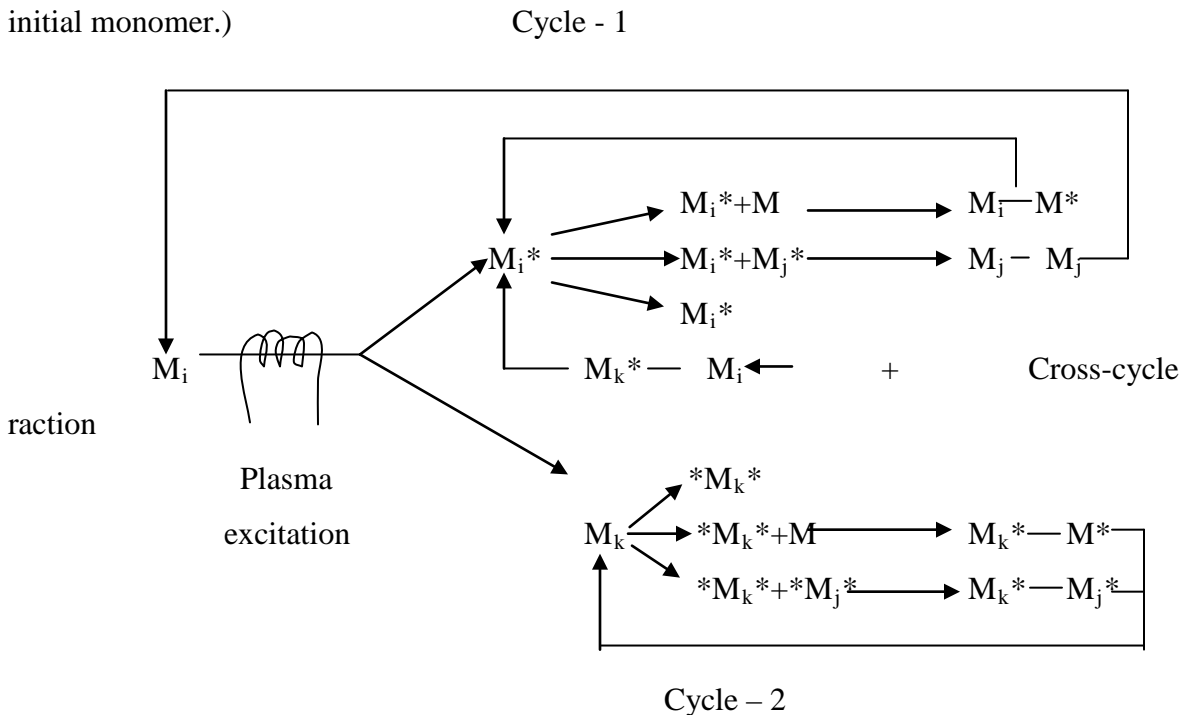


Fig.2.8: Schematic representation of bicyclic step growth mechanism of plasma polymerization.

One of the most important features of plasma polymers is that a large quantity of free radicals is often trapped in the polymer. Although, the amount varies with the type of monomer and the conditions of the plasma polymerization, it is safe to consider that plasma polymers contain a certain amount of trapped free radicals. Therefore, the free radicals play important role in plasma polymers.

In plasma polymerization, deposition rates and polymer film densities have been shown to vary with substrate temperature and discharge power. Some authors have observed that deposition rate decreases with increasing substrate temperature. Polymeric

films produced by plasma polymerization have branched and cross-linked structures and are difficult to dissolve in organic solvents. Their structure is irregular and amorphous and there may be no distinction between the main chain and branches.

2.6 Advantages and Disadvantages of Plasma Polymers [26,27]

The specific advantages of plasma-deposited films are summarized in here:

- Conformal: Because of the penetrating nature of low-pressure gaseous environment in which mass transport is governed in part by both molecular (line of sight) diffusion and convective diffusion, complex geometry shapes can be treated.
- Pinhole-free: Under common reaction conditions, the plasma film appears to coalesce during formation into a uniform over layer free of voids. Transport studies and electrical property studies suggest this continuous barrier structure.
- Barrier film: The pinhole-free and dense, cross-linked nature of these films suggests they have potential as barrier and protective films.
- Unique substrates: Plasma-deposited polymeric films can be placed upon almost any solid substrate including metals, ceramics, and semiconductors. Other surface grafting or surface modification technologies are highly dependent upon the chemical nature of the substrate.
- Good adhesion to the substrate: The energetic nature of the gas phase species in the plasma reaction environment can induce some mixing and implantation between the film and the substrate.
- Unique film chemistry: The chemical structure of the polymeric over layer films produced by rf plasma deposition cannot be synthesized by conventional organic chemical methods. Complex gas phase molecular rearrangements account for these unique surface chemical compositions.
- Easy preparation: Once the apparatus is set up and optimized for a specific deposition, treatment of additional substrates is rapid and simple. Through careful control of the polymerization parameters, it is possible to tailor the films with respect to specific chemical functionality, thickness, and other chemical and physical properties.

Disadvantages- The main disadvantages are:

- Costly to retrofit equipment.
- Polymerized coatings have low abrasion resistance.
- Low deposition rates. Only very thin films can be deposited economically on high production items.
- The process doesn't discriminate against what is coated. Everything in the coating range of the polymerization process is coated, or can become part of the coating.
- The process, used in mass production, is still in its infancy. More capabilities will likely be available as improvements to the process occur.

the chemistry produced on a surface is often not well defined, sometime a complex branched hydrocarbon polymer will be produced,

- Contamination can be a problem and care must be exercised to prevent extraneous gases, grease films, and pump oils from entering the reaction zone.

In spite of the drawbacks, plasma polymerization is far well developed process for many types of modification that simply cannot be done by any other technique.

2.7 Applications of Plasma-polymerized Organic Thin Films

The most important application of thin films are probably in the microelectronics industry and in materials technology, for surface treatment, etching of surfaces deposition of thin protective coatings, plasma polymerisation, plasma modification of polymers.

Plasma polymers are used as dielectric and optical coating to inhibit corrosion. A number of different plasma technologies are essential to different steps in the fabrication of ICs. Applications of plasma-polymerized films are associated with biomedical uses, the textile industry, electronics, optical applications, chemical processing and surface modification

References:

- [1] Sturrock Peter A., "Plasma Physics: An Introduction to the Theory of Astrophysical, Geophysical & Laboratory Plasmas" Cambridge University Press. ISBN 0521448107. (1994).

- [2] Cowie J. M. G., "Polymers: Chemistry and Physics of Modern Materials", Blackie Academic and Professionals, U K, 2nd Ed. (1991).
- [3] Ghosh P., "Polymer Science and Technology of Plastics and Rubbers" Tata McGraw-Hill Pub. Co. Ltd., New Delhi, 4th Ed. (1996).
- [7] Lieberman M. A., Lichtenberg A. J. , "Principles of Plasma Discharges and Materials Processing", John Wiley and Sons, New York (1994) .
- [5] Biederman H., Osada Y., "Plasma Chemistry of Polymers", Ad. in Polym. Sci., Berlin, Germany (1990).
- [6] Bogaerts A. and Neyts E., "Gas discharge plasma and their applications", Spectrochimica Acta Part B 57 (2002) 609.
- [8] Grill A., "Cold Plasma in Materials Fabrication: From Fundamentals to Applications", IEEE Press, New York (1994),
- [9] Bogaerts L., Wilken V., Hoffmann R, Gijbels K, Wetzig "Comparison of modeling calculations with experimental result for rf glow discharge optical emission spectroscopy", Spectrochim. Acta Part B 57 (2002) 109.
- [4] Chu, P. K.; Chen, J. Y.; Wang, L. P.; Huang, N. Plasma surface modification of biomaterials. Materials Science & Engineering, R: Reports 2002, R36 (5-6), 143
- [10] Yasuda H. Plasma Polymerisation; Academic Press, INC: NY, 1985.
- [11] Denes F., "Synthesis and surface modification by macromolecular plasma chemistry. Trends in Polymer Science (Cambridge, United Kingdom) 1997, 5 (1), 23.
- [12] Chan, C. M. Polymer Surface Modification and Characterization; Hanser/Gardner Publications, Inc.: Cincinnati, OH, 1994.
- [13] Chan C. M.; Ko T. M.; Hiraoka, H. Polymer surface modification by plasmas and photons. Surface Science Reports 1996, 24 (1/2), 1.
- [15] Stark R. H., Schoenbach K H , "Direct current high pressure glow discharges", J. Appl Phys. 85 (1999) 2075,
- [16] Stark R. H. , Schoenbach K H, "Direct current glow discharges in atmospheric air", Appl. Phys. Lett. 74 (1999) 3770.

- [17] Eijkel J. C. T., Stori H, and Manz A “A dc microplasma on a chip employed as an optical emission detector for gas chromatograph”, *Anal. Chem* 72 (2000) 2547.
- [18] Ohl A., Schleinitz W., Meyer A., Sievers A., Becker D., Keller K. Schroder, J. Conrads, *Surf. Coatings Technol.*, 116–119, 1999, 1006.
- [19] Sioshansi P., Tobin E.J., *Surf. Coatings Technol.* 83, 1996, 175.
- [20] Szycher M., Sioshansi P., Frisch E.E., *Biomaterials* for the 1990s: Polyurethanes. Silicones and Ion Beam Modification Techniques (Part 11), Spire Corporation, Patriots Park, Bedford, 1990.
- [21] Ohl A., Schroder K., *Surf. Coatings Technol.*, 116–119, 1999, 820.
- [22] Vargo T.G., Bekos E.J., Kim Y.S., Ranieri J.P., Bellamkonda R., Aebischer P., Margevich D.E., Thompson P.M., Gardella J.A., Jr., *J. Biomed. Mater. Res.*, 29, 1995, 767.
- [23] Yasuda H., Vossen J. L., and Kern W., “Thin Film Processes”, Academic Press, New York (1978).
- [24] Yasuda H. and Hirotsu T., *J. Polym. Sci., Polym. Chem. Ed.*, 16 (1978) 313.
- [25] Yasuda H. and Lamaze C. E., *J. Appl. Polym. Sci.* 17 1533 (1973)
- [26] Vurzel F. B., Acad. Sci., Moscow, USSR, “Plasma Chemistry Technology, Application”, Inst. Plasma Chem. and Technol., Carlsbad, CA(1983).
- [27] Mathai C. J., Saravanan S., Jayalekshmi S., Venkitachalam S., Anantharaman M. R., “Conduction mechanism in plasma polymerized aniline thin films”, *Mater Lett.* 57 (2003) 2253.

CHAPTER 3

EXPERIMENTAL DETAILS

- 3.1. Introduction
- 3.2. The Monomer
- 3.3. Substrate Material and its Cleaning Process
- 3.4. Capacitively Coupled Plasma Polymerization Set-up
- 3.5. Generation of Glow Discharge Plasma in the Laboratory
- 3.6. Deposition of Plasma Polymerized Thin Film
- 3.7. Contact Electrodes for Electrical Measurements
- 3.8. Measurement of Thickness of the Thin Films

References

3.1. Introduction

Plasma polymerization of CWO including the details of monomer and substrate, capacitively coupled glow discharge plasma polymerization set up for polymer formation, thickness measurement method and contact electrode deposition technique for electrical measurement on PPCWO thin films are discussed in this chapter.

3.2. The Monomer

Cedar wood essential oil is known for its tranquilizing and soothing effects. The botanical name for Cedar wood is *Cedrus Atlantica*. It is perhaps the first oil to have been extracted from plant. In the bygone times, CWO has been brought to extensive use by the Egyptians for varied purposes such as preserving mummies. It is a fabulous antiseptic and expectorant.

Cedar wood aids in restoring and revitalizing the energy that is lost after having had a hectic work schedule. It is sure to sooth each and every nerve of our body, thereby invigorating us completely. It stabilizes the functioning of the body; therefore there is a sense of well being associated with it. CWO not just provides relaxation to the body, but also to the mind. It takes the charge of alleviating stress that has caused energy loss. Talking about the health benefits of Cedar wood essential oil, it has proved to be of great use in treating many diseases such as arthritis, cystitis, cellulite, bronchitis, dandruff, acne, eczema etc.

The monomer CWO is manufactured by BDH Chemicals Ltd., Poole, England and is collected from local market. The chemical structure of the monomer is shown in Fig 3.1 and its typical properties are stated below.

Details of Atlas CWO:

Cedrus Aatlantica

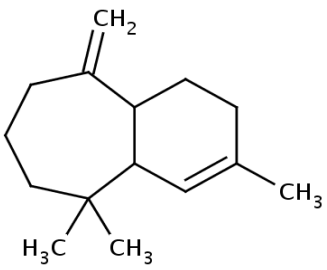
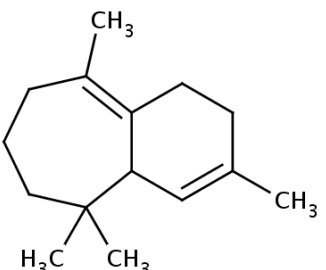
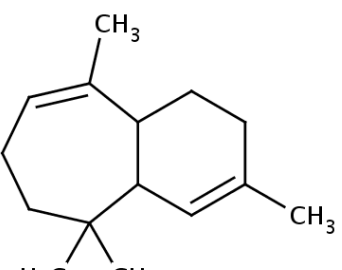
Odour: It is a yellow-brown to brown oil with dirty-woody, resinous, urinous odour. The dry-down on a perfumers strip is still woody-dirty, and takes on an almost Plasticine impression. It is very persistent.

Chemistry: Essential oil is mainly composed of sesquiterpene hydrocarbons α -himalchene, β -himalchene, and γ -himalchene which together can make up almost 70% of the composition. The oil also contains a number of α - and γ -atlantone isomers, especially (*E*)-(+)- α -atlantone, which can constitute 10-15% in total of the oil.

Table 3.1 General properties of Cedar Wood Oil

Commercial Name	Cedar Wood Oil
Botanical Name	<i>Cedrus atlantica</i>
Source	Steam distillation of wood.
Form	Clear liquid
Color	Yellowish-brown
Odor	Rich sweet woody almost balsamic odour
Properties	Aromatic and Healing
Specific Gravity	0.9720 - 0.9830 @ 250C
Density	²⁵ D 0.939-0.958 (0.947)
Melting point	81%(Celsius)min
Boiling point	279 °C
Flash point	135 °F
Refractive Index	1.456

The oil is widely used for insect repellent activities; Turkish carpet shops are walled with cedarwood boards to deter moths. Cedarwood oil Atlas is used in local ethnobotanical medicine for a wide variety of purposes.

		
•-himachalene (17.22%)	β-himachalene (54.00%)	γ-himachalene (10.87%)
IUPAC Name :2,9,9-trimethyl-5-methylidene-4,4a,6,7,8,9a-hexahydro-3H-benzo annulene	IUPAC Name:2,5,9,9-tetramethyl-3,4,6,7,8,9a-hexahydrobenzo annulene	IUPAC Name : 2,5,9,9-tetramethyl-3,4,4a,7,8,9a-hexahydrobenzo annulene
Compound Formula: C ₁₅ H ₂₄	Compound Formula: C ₁₅ H ₂₄	Compound Formula: C ₁₅ H ₂₄
Fig.3.1 Chemical Structure of Cedar Wood Oil		

3.3. Substrate Materials and its Cleaning Process

The substrates used were pre-cleaned glass slides (25.4 mm X 76.2 mm X 1.2 mm) of Sail Brand, China, purchased from local market. The samples were prepared by depositing the PPCWO thin film and electrodes onto them.

To get a homogeneous, smooth and flawless thin polymer film, which is a common property of plasma polymers, it is essential to make the substrate as clean as possible. The substrates were chemically cleaned by acetone and thoroughly rinsed with distilled water then dried in hot air.

3.4. Capacitively Coupled Plasma Polymerization Set-up

A capacitively coupled reactor was used for deposition of plasma polymerized CWO(PPCWO). The reactor consists of three parts, namely, vacuum system, gas inlet system and discharge system. The glow discharge system has two stainless steel parallel circular plates with a diameter of 0.09 m and thickness of 0.01 m placed 0.04 m apart. The frequency of electric supply is 50 Hz for plasma generation by utilizing the ac mains. The substrates were positioned at the center on the lower electrode. A round bottom flask was used as the monomer container. Prior to the polymerization process the glow discharge chamber was evacuated by a rotary pump down to a base pressure of about 1.33 Pa. Plasma was generated in the chamber with a step-up transformer by applying a potential of about 850 Volt between the electrodes at the line frequency 50 Hz. During the reaction, a vacuum gauge was used to measure the pressure inside the plasma chamber. A heating element of nichrome wire was used to heat the monomer container. Monomer vapor was produced and introduced into the reactor through a flow meter at a flow rate of about 20 sccm per minute. During polymerization the power of the glow discharge was kept at 40 watt and deposition was made for 45 minutes. After the plasma was extinguished, the chamber was evacuated for 15 minutes and the films were taken out for characterization. The thickness of the plasma polymerized films deposited on glass substrates was measured by using a multiple-beam interferometric method [1]. The glow discharge plasma polymerization setup which was used to deposit the PPCWO thin films consists of the following components is shown in Fig.3.2.

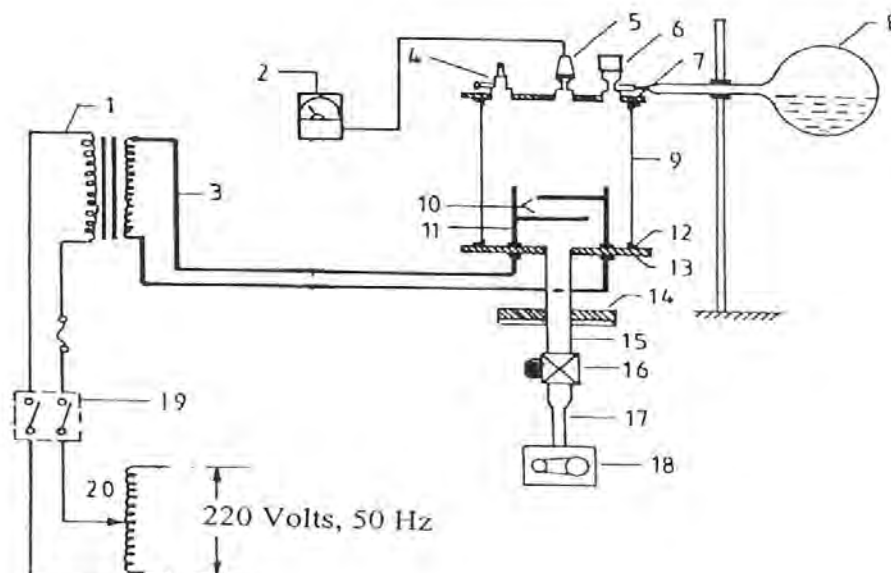


Fig.3.2 Schematic diagram of the plasma polymerization set-up:

1 high voltage power supply, 2 pirani gage, 3 high tension leads, 4 gas inlet valve, 5 gauge head, 6 monomer injection valve, 7 flowmeter, 8 monomer container, 9 Pyrex glass dome, 10 metal electrodes, 11 electrode stands, 12 gasket, 13, lower flange, 14 bottom flange, 15 brass tube, 16 valve, 17 liquid nitrogen trap, 18 rotary pump, 19 switch and 20 variac.

i. Plasma reaction chamber

The glow discharge reactor is made up of a cylindrical Pyrex glass bell-jar having 0.15 m in inner diameter and 0.18 m in length. The top and bottom edges of the glass bell-jar are covered with two rubber L-shaped (height and base 0.015m, thickness, 0.001 m) gaskets. The cylindrical glass bell jar was placed on the lower flange. The lower flange is well fitted with the diffusion pump by an I joint. The upper flange is placed on the top edge of the bell-jar. The flange is made up of brass having 0.01 m in thickness and 0.25 m in diameter. On the upper flange a laybold pressure gauge head, Edwards high vacuum gas inlet valve and a monomer injection valve are fitted. In the lower flange two highly insulated high voltage feed-through are attached housing screwed copper connectors of 0.01m high and 0.004 m in diameter via TeflonTM insulation.

ii. Electrode system

A capacitively coupled electrode system is used in the system. Two circular stainless steel plates of diameter 0.09 m and thickness of 0.001m are connected to the high voltage copper connectors. The inter-electrode separation can be changed by moving the electrodes through the electrode stands. After adjusting the distance between the electrodes they are fixed with the stands by means of screws. The substrates were kept on the lower electrode for plasma deposition.

iii. Pumping unit

For creating laboratory plasma, first step is pumping out the air/gas from the plasma chamber. In this system a rotary pump of vacubrand (Vacubrand GMBH & Co: Germany) is used.

iv. Vacuum pressure gauge

A vacuum pressure gauge head (Laybold AG, Germany) and a gauge meter (Thermotron™ 120) are used to measure inside pressure of the plasma deposition chamber.

v. Input power for plasma generation

The input power supply for plasma excitation comprises of a step-up high-tension transformer and a variac. The voltage ratio at the output of the high-tension transformer is about 16 times that of the output of the variac. The maximum output of the variac is 220V and that of the transformer is about 3.5 kV with a maximum current of 100 mA. The deposition rate increases with power at first and then becomes independent of power at high power values at constant pressure and flow rate.

vi. Monomer injecting system

The monomer injecting system consists of a conical flask of 25 ml capacity and a Pyrex glass tube with capillarity at the end portion. The capillary portion is well fitted with metallic tube of the nozzle of the high vacuum needle valve. The conical flask with its components is fixed by stand-clamp arrangement.

vii. Supporting frame

A metal frame of dimension 1.15mX0.76mX0.09m is fabricated with iron angle rods, which can hold the components described above. The upper and lower bases of the frame are made with polished wooden sheets. The wooden parts of the frame are varnished and the metallic parts are painted to keep it rust free. The pumping unit is placed on the lower base of the frame. On the upper base a suitable hole is made in the wooden sheet so that the bottom flange can be fitted with nut and bolts.

viii. Flowmeter

The system pressure of a gas flow is determined by the feed in rate of a gas and the pumping out rate of a vacuum system. The monomer flow rate is determined by a flowmeter. In the plasma polymerization set up a flowmeter (Glass Precision Engineering LTD, Meterate, England) is attached between the needle valve and the monomer bottle.

ix. Liquid nitrogen trap

Cold trap, particularly a liquid N₂ trap, acts as a trap pump for different type gas. The liquid N₂ trap system is placed in the fore line of the reactor chamber before the pumping unit in the plasma deposition system. It consists of a cylindrical shape chamber having 6.4 cm diameter and 11.5 cm in length using brass material.

3.5 Deposition of Plasma Polymerized Thin Film

The important feature of glow discharge plasma is the non-equilibrium state of the overall system. In the plasmas considered for the purpose of plasma polymerization, most of the negative charges are electrons and most of the positive charges are ions. Due to large mass difference between electrons and ions, the electrons are very mobile as compared to the nearly stationary positive ions and carry most of the current. Energetic electrons as well as ions, free radicals, and vacuum ultraviolet light can possess energies well in excess of the energy sufficient to break the bonds of typical organic monomer molecules which range from approximately 3 to 10 eV. Some typical energy of plasma species available in glow discharge as well as bond energies encountered at pressure of approximately 0 .01 mbar.



Fig.3.3 Glow discharge plasma during deposition

After finding the desired plasma glow in the reactor the monomer vapor is injected downstream to the primary air glow plasma for some time. Incorporation of monomer vapor changed the usual color of plasma into a light bluish color. Fig3.5 is the photograph of glow discharge plasma across the electrodes in the capacitively coupled parallel plate discharge chamber. The optimized conditions of thin film formation for the present study are:

Separation between two electrodes	4 cm
Position of the substrate	Lower electrode

Deposition voltage	15 W
Pressure in the reactor	10^{-2} Torr
Maximum deposition time	1 hr 15 min

3.6 Contact Electrodes for Electrical Measurements

i. Electrode material

Aluminium (Al) (purity of 4N British Chemical Standard) was used for electrode deposition. Al has been reported to have good adhesion with glass slides. Al film has advantage of easy self-healing burn out of flaws in sandwich structure. Schematic diagram of sandwich A/PPCWO/Al film is shown in figure 3.4.

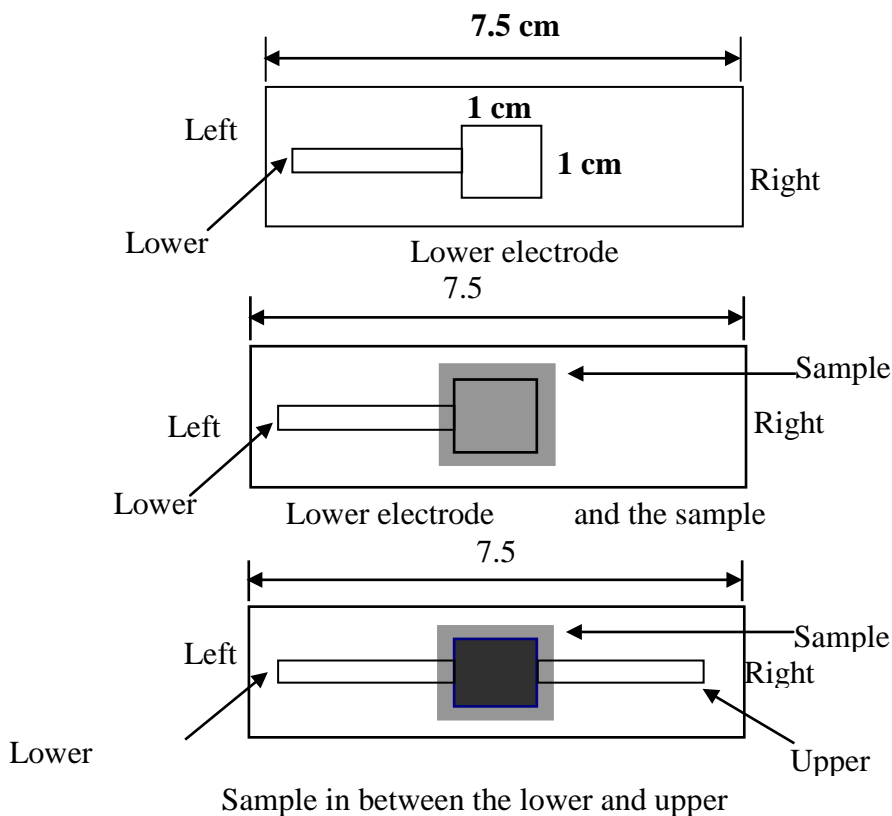


Fig 3.4 Schematic diagram of sandwich Al/PPCWO/Al film

ii. Electrode deposition

Electrodes were deposited using an Edward coating unit E-306A(Edward, UK). The system was evacuated by an oil diffusion pump backed by an oil rotary pump. The chamber could be evacuated to a pressure less than 10^{-5} Torr. The glass substrates with mask were supported by a metal rod 0.1 m above the tungsten filament. For the electrode deposition Al was kept on the tungsten filament.

The filament was heated by low-tension power supply of the coating unit. The low-tension power supply was able to produce 100 A current at a potential drop of 10 V. During evacuation of the chamber by diffusion pump, the diffusion unit was cooled by



Fig.3.5 The Edward vacuum coating unit E306A.

the flow of chilled water and its outlet temperature was not allowed to rise above 305 K. When the penning gauge reads about 10^{-5} Torr, the Al on tungsten filament was heated by low-tension power supply until it was melted.

The Al was evaporated, thus lower electrode onto the glass slide was deposited. Al coated glass substrates were taken out from the vacuum coating unit and were placed on the middle of the lower electrode of the plasma deposition chamber for CWO thin film deposition under optimum condition. The top Al electrode was also prepared on the PPCWO film as described above.

3.7 Measurement of Thickness of the Thin Films

Thickness is the single most significant film parameter. Any physical quantity related to film thickness can in principle be used to measure the film thickness. It may be measured either by several methods with varying degrees of accuracy. The methods are chosen on the basis of their convenience, simplicity and reliability. Since the film thicknesses are generally of the order of a wavelength of light, various types of optical interference phenomena have been found to be most useful for measurement of film thicknesses. Several of the common methods are i) During Evaporation, ii) Multiple-Beam Interferometry, (Tolansky Fezeau fringes method, Fringes of equal chromatic order, Donaldson method etc.) iii) Michelson interferometer iv) Using a Hysteresis

graph etc. Multiple Beam Interferometric set-up in the laboratory are shown in figure 3.6 and this technique is described below:



Fig.3.6 Multiple Beam Interferometric set-up in laboratory

This method utilizes the resulting interference effects when two silvered surfaces are brought close together and are subjected to optical radiation. This interference technique may be applied simply and directly to film-thickness determination. When a wedge of small angle is formed between unsilvered glass plates, which are illuminated by monochromatic light, broad fringes are seen arising from interference between the light beams reflected from the glass on the two sides of the air wedge. At points along the wedge where the path difference is an integral and odd number of wavelengths, bright and dark fringes occur respectively. If the glass surfaces of the plates are coated with highly reflecting layers, one of which is partially transparent, then the reflected fringe system consists of very fine dark lines against a bright background. A schematic diagram of the multiple-beam interferometer along with a typical pattern of Fizeau fringes from a film step is shown in Fig.3.7. As shown in this figure, the film whose thickness is to be measured is over coated with a silver layer to give a good reflecting surface and a half-silvered microscope slide is laid on top of the film whose thickness is to be determined. The thickness of the film d can then be determined by the relation,

$$d = \frac{\lambda b}{2 a}$$

where, λ is the wavelength and b/a is the fractional discontinuity identified in the figure. In general, the sodium light is used, for which $\lambda = 5893 \text{ \AA}$. In conclusion, it might be mentioned that the Tolansky method of film-thickness measurement is the most widely used and in many respects also the most accurate and satisfactory one [1].

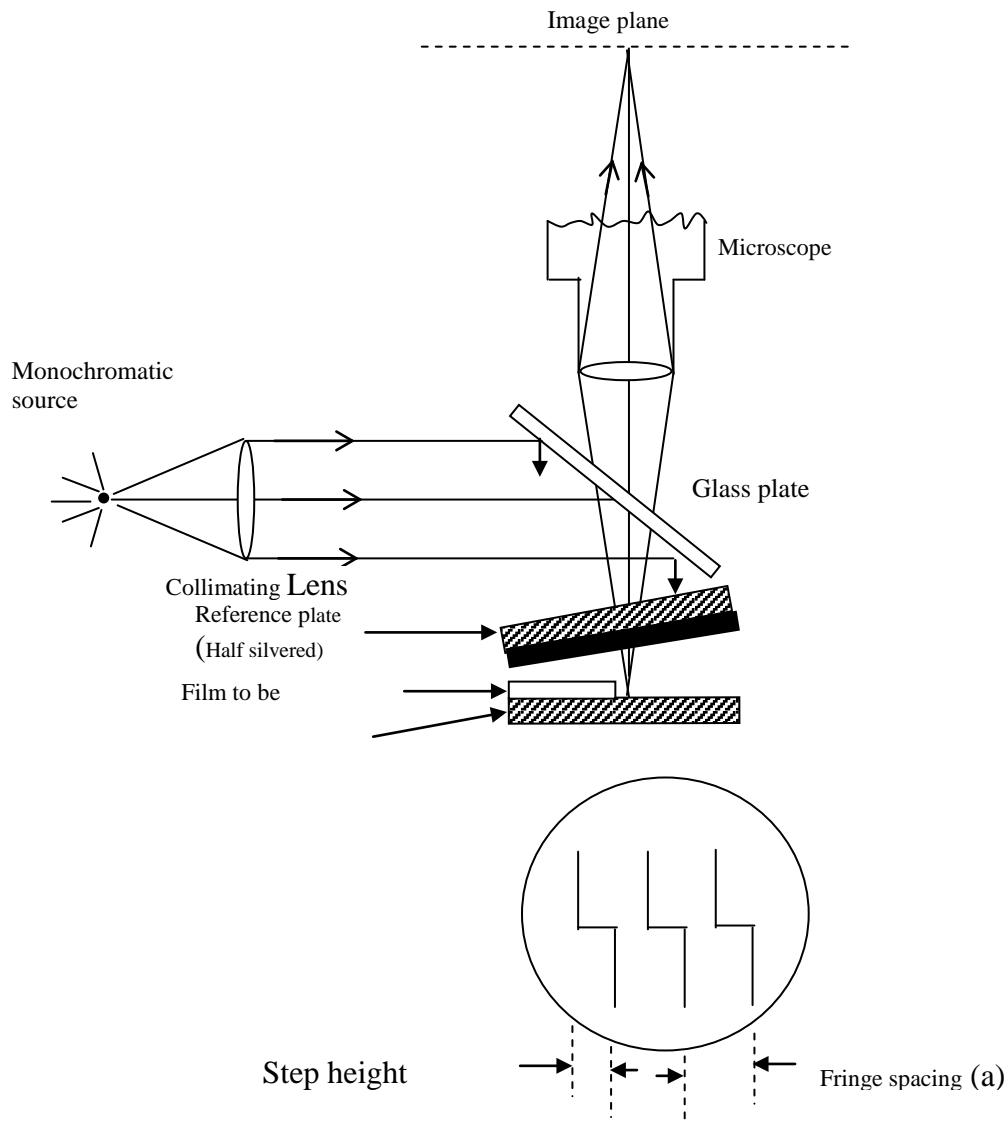


Fig. 3.7 Interferometer arrangement for producing reflection Fizeau fringes of equal thickness.

References

- [1] Tolansky S., "Multiple Beam Interferometry of Surfaces and Films", Clarendon Press, Oxford (1948).

CHAPTER 4

STRUCTURAL AND THERMAL ANALYSES OF PPCWO

4.1. Introduction

4.2 Thermal Analyses

4.2.1 Differential thermal analysis

4.2.2 Thermogravimetric analysis

4.2.3 Applications of DTA/TGA

4.2.4. Experimental procedure

4.2.5 Results and discussion

4.3 Theory of Infrared spectroscopy

4.3.1 Introduction

4.3.2 Importance of FTIR

4.3.3 Infrared frequency range and spectrum presentation

4.3.4 Infrared absorption

4.3.5 Molecular Vibrations

4.3.6 Infrared Activity

4.3.7 The Fingerprint Region

4.3.8 Sample Preparation

4.3.9 Results and Discussion

References

4.1. Introduction

Structural characterization of plasma polymerized thin films may be possible by several methods, such as FTIR, analysis, and DTA/TGA. The experimental findings are analyzed by DTA/TGA, and FTIR. The DTA is applied to study structural and phase change that occurs during heating a polymeric sample. The TGA is to measure the mass loss of the sample as a function of temperature. The FTIR analysis is a digital technique that may be used for the investigation of molecular structure, bonding and identification of chemical functional groups in organic compounds. The experimental results are discussed in this chapter.

4.2 Thermal analyses

4.2.1 Differential thermal analysis

DTA may be defined formally as a technique for recording the difference in temperature between a substance and a reference material against either time or temperature as the two specimens are subjected to identical temperature regimes in an environment heated or cooled at a controlled rate.

So in a word, we can say that DTA is a thermo analytic technique in recording the temperature and heat flow associated with thermal transitions in a material. This enables to determine the phase transitions characteristics (e.g. melting point, glass transition temperature, crystallization etc.). In DTA the material under study and an inert reference are made to undergo identical thermal cycles, while recording any temperature difference between sample and reference. This differential temperature is then plotted against time, or against temperature (DTA curve or thermo gram). Changes in the sample, either exothermic or endothermic, can be detected relative to the inert reference. Thus, a DTA curve provides data on the transformations that have occurred, such as glass transitions, crystallization, melting and sublimation. The area under a DTA peak is the enthalpy change and is not affected by the heat capacity of the sample. The principle of DTA consists of measuring heat changes associated with the physical or chemical changes occurring when any substance is gradually heated. The thermocouple (platinum-platinum rhodium 13%) for DTA is incorporated at the end of each of the balance beam ceramic tubes, and the temperature difference between the holder on the sample side and the holder on the references side is detected. This signal is amplified and becomes the temperature difference signal used to measure the thermal change of the sample. Fig. 4.1 shows a schematic illustration of a DTA cell.

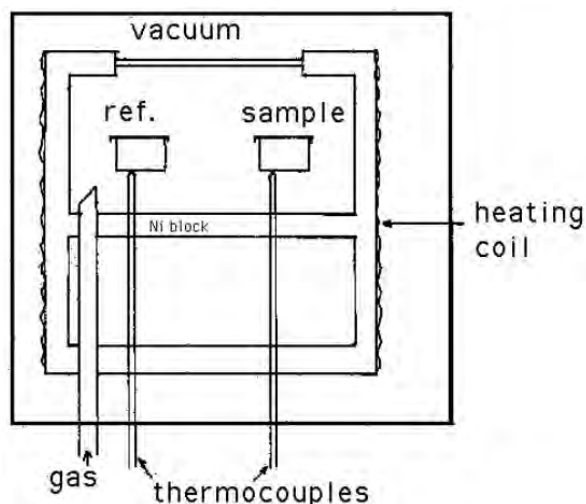


Fig.4.1: Schematic illustration of a DTA cell.

It contains two holders attached with thermocouples. Sample is inserted in one holder and a reference sample is placed in the other. The difference in temperature is measured from the difference in e.m.f between the thermocouples. These differences of temperatures appear because of the phase transitions or chemical reactions in the sample involving the evolution of heat and are known as exothermic reaction or absorption of heat known as endothermic reaction. The exothermic and endothermic reactions are generally shown in the DTA traces as positive and negative deviations respectively from a base line. So DTA offers a continuous thermal record of reactions in a sample. The areas under the bands or peaks of DTA spectra are proportional to the amount of heat absorbs or evolved from the sample under investigation, where temperature and sample dependent thermal resistance are the proportionality factors. Thus DTA is needed primarily for the measurement of transition temperature. It can be used to study thermal properties and phase changes which do not lead to a change in enthalpy. The baseline of the DTA curve exhibits discontinuities at the transition temperatures and the slope of the curve at any point will depend on the micro structural constitution at that temperature.

4.2.2 Thermogravimetric analysis

Thermo gravimetric analysis is a technique in which the mass of a substance is measured as a function of temperature while the substance is subjected to a controlled temperature programme. The record is the thermogravimetric or TG curve; the mass is plotted on the ordinate decreasing downwards and temperature (T) or time (t) on the abscissa increasing from left to right.

TGA measures the weight change in a material as a function of temperature and time, in a controlled environment. This can be very useful to investigate the thermal stability of a material, or to investigate its behavior in different atmospheres (e.g. inert or oxidizing). It is suitable for use with all types of solid materials, including organic or inorganic materials. Such analysis relies on a high degree of precision in three measurements: weight, temperature, and temperature change. As many weight loss curves look similar, the weight loss curve may require transformation before results may be interpreted. A derivative weight loss curve can be used to tell the point at which weight loss is most apparent. TGA is commonly employed in research and testing to determine characteristics of materials such as polymers, to determine degradation temperatures, absorbed moisture content of materials, the level of inorganic and organic components in materials, decomposition points of explosives, and solvent residues. The technique can analyze materials that exhibit either mass loss or gain due to decomposition, oxidation or loss of volatiles (such as moisture). It is especially useful for the study of polymeric materials, including thermoplastics, thermosets, elastomers, composites, films, fibers, coatings and paints.

4.2.3 Applications of DTA/TGA

Simultaneous TGA-DTA/DSC measures both heat flow and weight changes (TGA) in a material as a function of temperature or time in a controlled atmosphere. Simultaneous measurement of these two material properties not only improves productivity but also simplifies interpretation of the results. The complementary information obtained allows differentiation between endothermic and exothermic events which have no associated weight loss (e.g., melting and crystallization) and those which involve a weight loss (e.g., degradation). Thus the ideal uses for TGA/DTA are :

- Thermal stability/degradation investigation of organic or inorganic materials, e.g. polymers, composites, glasses, metals, minerals etc.
- Thermal stability/degradation investigations in inert or oxidative atmospheres, or in vacuum.
- Curing kinetics (e.g. adhesives, polymers)
- Chemical composition measurements (using appropriate reference standards, accurate quantification of sample composition can be determined)
- Phase transition measurement (e.g. glass transition, clustering, crystallinity, melting point)
- Quantum - size effect investigation for nanomaterials

- Reaction kinetics with reactive gases (e.g., oxidation, hydrogenation, chlorination, adsorption/desorption)
- Pyrolysis kinetics (e.g., carbonization, sintering)

4.2.4 Experimental procedure

The TGA is a special branch of thermal analysis, which examines the mass change of a sample as a function of temperature in the scanning mode or as a function of time in the isothermal mode. Not all thermal events bring about a change in the mass of the sample (for example melting, crystallization or glass transition), but there are some very important exceptions, which include absorption, sublimation, vaporization, oxidation, reduction and decomposition. The TGA is used to characterize the decomposition and thermal stability of materials under a variety of conditions, and to examine the kinetics of the physico-chemical process occurring in the sample. Sample weight changes are measured as described in Fig. 4.2.

Fig. 4.2 shows the sample balance beam and reference balance beam are independently supported by a driving coil/pivot. When a weight change occurs at the beam end, the movement is conveyed to the opposite end of the beam via the driving coil/pivot, when optical position sensors detect changes in the position of a slit. The signal from the optical position sensor is sent to the balance circuit.

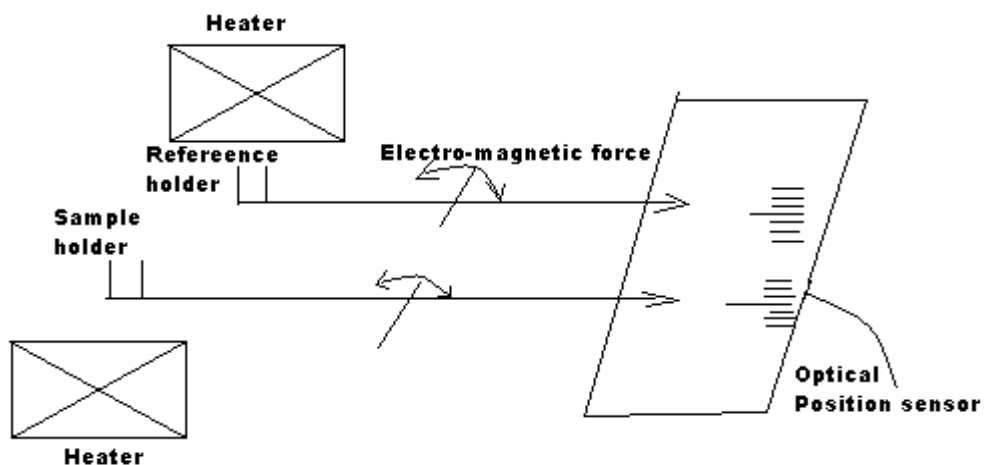


Fig. 4.2: A pictorial set-up for TGA measurements.

The balance circuit supplies sufficient feedback current to the driving coil so that the slit returns to the balance position. The current running to the driving coils to the sample side and the current running to the driving coil on the reference side is detected and converted into weight signals.

4.2.5 Results and discussion

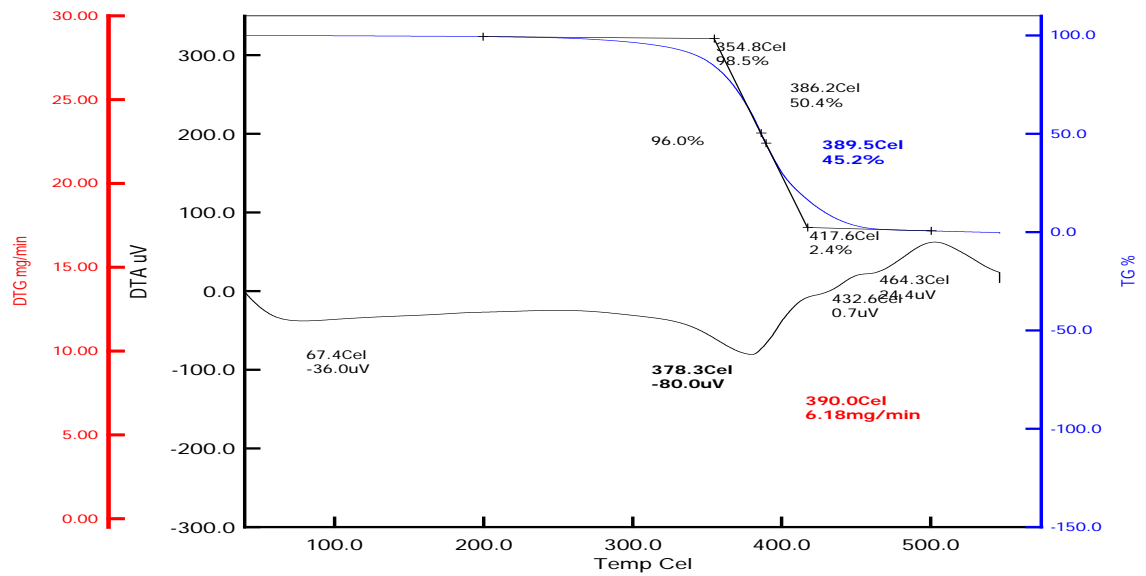


Figure 4.3 The DTA/TGA traces of Cedar Wood Oil Monomer

Figure.4.3 shows the DTA and TGA traces taken in the temperature range of (100°C to 500°C) 373 to 773 K at a scan rate of 20 K/min for CWO monomer in nitrogen atmosphere. It is observed in the DTA curve shows the endothermic trace around a temperature (378.3°C) 651.3 K a transition occurs and the corresponding TGA shows a small amount of loss. The DTA thermogram shows an exothermic broad band which has a maximum centered around (500°C) 773 K indicating a gradual change of its original properties. The DTG thermogram shows an endothermic broad band around a temperature (390°C) 663 K.

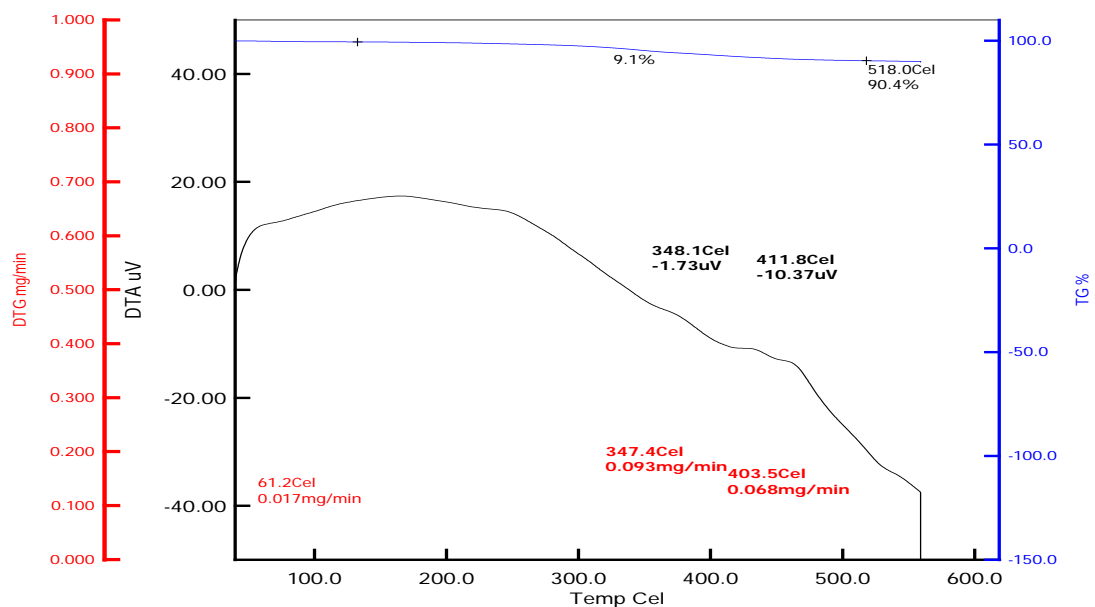


Figure 4.4 The DTA/TGA traces of as deposited PPCWO

Figure 4.4 shows the DTA/TGA traces of as deposited PPCWO. It is observed from the fig. 4.4 that in the DTA trace around a temperature 340 K a transition occurs and the corresponding TGA shows a peak that may be due to the removal of water content. The DTA thermogram shows an exothermic broad band which has a maximum around 473 K indicating a gradual change of its original properties. The corresponding TGA trace shows a uniform weight loss up to 673 K and above this temperature the weight loss is comparatively faster. The TGA trace may be divided into two regions. Both individual regions may be associated with weight loss due to different structural change. The weight loss in region A (upto 673 K) and B (over 873 K) are approximately 4% and 10 % respectively in reference to its original weight. In region A the weight loss may be due to structural change in PPCWO owing to hydrogen evolution. The weight loss in the B region may be due to the loss of low molecular mass hydrocarbon gases. The gradual fall of DTA may be a cause of thermal breakdown of PPCWO structure and expulsion of oxygen. From the DTG curve it is observed that no significant mass change occurs below (347°C) 620 K and a very little change occurs within (347°C to 500°C) 620 to 773 K indicating sample homogeneity and stability.

4.3 Theory of Infrared Spectroscopy

4.3.1 Introduction

There is an indispensable tool for the determination of structural information concerning organic substances which is known as Infrared (IR) spectroscopy. It is an important tool of the organic chemist that is used to gather information about compound's structure, assess its purity, and sometimes to identify it. Spectroscopy is the study of the interaction of electromagnetic radiation with matter.

It measures different IR frequencies by a sample positioned in the path of an IR beam and it reveals information about the vibrational states of a molecule. Some of the infrared radiation is absorbed by the sample and some of it is transmitted. The resulting spectrum represents the molecular absorption and transmission, creating a molecular fingerprint of the sample. Like a fingerprint, no two unique molecular structures produce the same infrared spectrum. This makes infrared spectroscopy useful for several types of analyses. Intensity and spectral position of IR absorptions allow the identification of structural elements of molecule. Different functional groups absorb characteristic frequencies of IR radiation and this absorption results due to the changes in vibrational and rotational status of the molecules. Actually, a molecule, when exposed to radiation produced by the thermal emission of a hot source (a source of IR

energy), absorbs only at frequencies corresponding to its molecular modes of vibration in the region of the electromagnetic spectrum between visible (red) and short waves (microwaves). These changes in vibrational motion give rise to bands in the vibrational spectrum; each spectral band is characterized by its frequency and amplitude. The absorption frequency depends on the vibrational frequency of the molecules, whereas the absorption intensity depends on how effectively the infrared photon energy can be transferred to the molecule, and this depends on the change in the dipole moment that occurs as a result of molecular vibration. As a consequence, a molecule will absorb infrared light only if the absorption causes a change in the dipole moment. Thus, all compounds except for elemental diatomic gases such as N₂, H₂ and O₂, have infrared spectra and most components present in a flue gas can be analyzed by their characteristic infrared absorption. Furthermore, using various sampling accessories, IR spectrometers can accept a wide range of sample types such as gases, liquids, and solids. Thus, IR spectroscopy is an important and popular tool for structural elucidation and compound identification [1].

When a spectrum is recorded using a conventional, dispersive IR spectrometer, each data point reveals the transmitted light at the respective frequency. The signal provided by the IR technique, however, contains information about the complete spectrum of the probe. This signal has to be transformed from the time-domain into the frequency-domain in order to reveal the spectrum. This transformation is called Fourier transformation and then the spectroscopic analysis then termed as Fourier Transform Infrared (FTIR) spectroscopy.

The researchers use infrared analysis qualitatively for determining the presence or absence of specific functional groups in polymers. Its application to organic systems has been in the areas of both quantitative and qualitative analysis. Its principal strengths are:

- (i) it is a quick and relatively cheap spectroscopic technique,
- (ii) it is useful for identifying certain functional groups in molecules and
- (iii) IR spectrum of a given compound is unique and can therefore serve as a fingerprint for this compound.

4.3.2 Importance of FTIR

Spectroscopy is the study of the interaction of electromagnetic radiation with matter. There are many forms of spectroscopy, each contributing useful information to identify substances and to determine various characteristics of their structure.

FTIR is a powerful tool identifying types of chemical bonds in a molecule by producing an infrared absorption spectrum that is like a molecular “fingerprint”. FTIR is most useful for identifying chemicals that are either organic or inorganic. It can be utilized to quantitate some components of an unknown mixture. It can be applied to the analysis of solids, liquids and gasses. The term FTIR refers to a fairly recent development in the manner in which the data is collected and converted from an interference pattern to a spectrum.

Therefore, infrared spectroscopy can result in a positive identification (qualitative analysis) of every different kind of material. In addition, the size of the peaks in the spectrum is a direct indication of the amount of material present. With modern software algorithms, infrared is an excellent tool for quantitative analysis. Today’s FTIR instruments are computerized which makes them faster and more sensitive than the older dispersive instruments.

Because the strength of the absorption is proportional to the concentration, FTIR can be used for some quantitative analyses. FTIR can also be used to identify chemicals from spills, paints, polymers, coating, drugs and contaminants. FTIR is perhaps the most powerful tool for identifying types of chemical bonds (functional groups). The wavelength of light absorbed is characteristic of the chemical bond as can be seen in this annotated spectrum.

By interpreting the infrared absorption spectrum, the chemical bonds in a molecule can be determined. FTIR spectra of pure compounds are generally so unique that they are like a molecular “fingerprint”. While organic compounds have rich, detailed spectra, inorganic compounds are usually much simpler. For most common materials, the spectrum of an unknown can be identified by comparison to a library of known compounds. To identify less common materials, IR will need to be combined with nuclear magnetic resonance, mass spectrometry, emission spectrometry, X-ray diffraction, and/or other techniques.

Fourier transform infrared spectroscopy is preferred over dispersive or filter methods of infrared spectral analysis for several reasons:

- ❖ It is a non-destructive technique
- ❖ It provides a precise measurement method which requires no external calibration
- ❖ It can increase speed, collecting a scan every second
- ❖ It can increase sensitivity – one second scans can be co-added together to ratio out random noise
- ❖ It has greater optical throughput
- ❖ It is mechanically simple with only one moving part

4.3.3 Different frequency range and spectrum of Infrared

IR absorption positions are generally presented as either wave-numbers ($\bar{\nu}$) or wavelengths (λ). Wave-number defines the number of waves per unit length. Thus, wave-numbers are directly proportional to frequency, as well as the energy of the IR absorption. The wave-number unit (cm^{-1}) is more commonly used in modern IR instruments that are linear in the cm^{-1} scale. In the contrast, wavelengths are inversely proportional to frequencies and their associated energy. At present, the recommended unit of wavelength is μm (micrometers). Wave-numbers and wavelengths can be interconverted using the following equation:

$$\bar{\nu}(\text{cm}^{-1}) = \frac{1}{\lambda(\mu\text{m})} \times 10^4 \quad (1)$$

IR absorption information is generally presented in the form of a spectrum with wavelength or wavenumber as the x-axis and absorption intensity or percent transmittance as the y-axis.

Transmittance, T , is the ratio of radiant power transmitted by the sample (I) to the radiant power incident on the sample (I_0). Absorbance (A) is the logarithm to the base 10 of the reciprocal of the transmittance (T).

$$A = \log_{10}(1/T) = \log_{10}(I_0/I) \quad (2)$$

The transmittance spectra provide better contrast between intensities of strong and weak bands because transmittance ranges from 0 to 100% T whereas absorbance ranges from infinity to zero. The analyst should be aware that the same sample will give quite different profiles for the IR spectrum, which is linear in wave-number, and the IR plot,

which is linear in wavelength. It will appear as if some IR bands have been contracted or expanded.

The IR region is commonly divided into three smaller areas: near IR, mid IR, and far IR.

Table-4.1: Common subdivisions of the Infrared regions

Region	Frequency Range (cm^{-1})	Wavelength Range (μm)
Near-infrared(overtone)	13300-4000	0.75-2.5
Fundamental rotation-vibration	4000-400	2.5-25
Far-infrared (skeletal vibration)	400-20	25-500

The region of most interest for chemical analysis is the mid-infrared region ($4,000 \text{ cm}^{-1}$ to 400 cm^{-1}) which corresponds to changes in vibrational energies within molecules. The far infrared region (400 cm^{-1} to 10 cm^{-1}) is useful for molecules containing heavy atoms such as inorganic compounds but requires rather specialized experimental techniques. The far- and near IR are not frequently employed because only skeletal and secondary vibrations (overtones) occur in these regions producing spectra that are difficult to interpret.

In particular, the energy of most molecular vibrational modes corresponds to that of the IR part of the electromagnetic spectrum, that is, between around 650 cm^{-1} and 4000 cm^{-1} . However, in practice, the analysis and assignment of spectral features is difficult, and correspondingly, attention is focused instead upon characteristic functional groups and the associated familiar bands. This though, neglects a great deal of the information contained within the IR spectrum.

4.3.4 Infrared absorption

At temperatures above absolute zero, all the atoms in molecules are in continuous vibration with respect to each other. When the frequency of a specific vibration is equal to the frequency of the IR radiation directed on the molecule, the molecule absorbs the radiation.

The total number of observed absorption bands is generally different from the total number of fundamental vibrations. It is reduced because some modes are not IR active and a single frequency can cause more than one mode of motion to occur. Conversely, additional bands are generated by the appearance of overtones (integral multiples of the fundamental absorption frequencies), combinations of fundamental frequencies, differences of fundamental frequencies, coupling interactions of two fundamental

absorption frequencies, and coupling interactions between fundamental vibrations and overtones or combination bands (Fermi resonance). The intensities of overtone, combination, and difference bands are less than those of the fundamental bands. The combination and blending of all the factors thus create a unique IR spectrum for each compound.

IR radiation does not have enough energy to induce electronic transitions as seen with UV. Absorption of IR is restricted to compounds with small energy differences in the possible vibrational and rotational states.

For a molecule to absorb IR, the vibrations or rotations within a molecule must cause a net change in the dipole moment of the molecule. The alternating electrical field of the radiation (remember that electromagnetic radiation consists of an oscillating electrical field and an oscillating magnetic field, perpendicular to each other) interacts with fluctuations in the dipole moment of the molecule. If the frequency of the radiation matches the vibrational frequency of the molecule then radiation will be absorbed, causing a change in the amplitude of molecular vibration.

The simplest treatment of IR absorption in molecular systems is a semi-classical treatment. Essentially, classical electromagnetism requires that, if a system is to absorb radiation, that it does so by virtue of periodic changes in its electric dipole moment. The frequency of the dipole oscillations must be equal to the frequency of the incident radiation for absorption to occur.

The dipole moment is a vector quantity, thus, absorption may occur provided that at least one component of the dipole moment can oscillate at the incident frequency. Of course, as a molecule vibrates, the dipole moment will oscillate at the frequency of the molecular oscillations, as the dipole moment is a function of the nuclear coordinates. In the harmonic approximation used throughout this work, any molecular vibration may be expressed as a sum over normal modes; thus, the dipole moment may only oscillate at these normal mode frequencies, and radiation may only be absorbed at these normal mode frequencies. However, selection rules may ensure that certain normal modes are so-called "silent" modes, *i.e.* they do not absorb radiation.

4.3.5 Molecular Vibrations

The energy of a molecule consists of translational, rotational, vibrational and electronic energy

$$E = E_{\text{electronic}} + E_{\text{vibrational}} + E_{\text{rotational}} + E_{\text{translational}} \quad (3)$$

Translation energy of a molecule is associated with the movement of the molecule as a whole, for example in a gas. Rotational energy is related to the rotation of the molecule, whereas vibrational energy is associated with the vibration of atoms within the molecule. Finally, electronic energy is related to the energy of the molecule's electrons.

Like radiant energy, the energy of a molecule is quantized too and a molecule can exist only in certain discrete energy levels. Within an electronic energy level a molecule has many possible vibrational energy levels. To raise the electronic energy state of a molecule from the ground state to the excited state will cost more energy than to raise the vibrational energy state.

The vibrational energy of a molecule is not determined by the orbit of an electron but by the shape of the molecule, the masses of the atoms and, eventually by the associated vibronic coupling. For example, simple diatomic molecules have only one bond allowing only stretching vibrations. More complex molecules may have many bonds, and vibrations can be conjugated. The atoms in a CH_2 group, commonly found in organic compounds, can vibrate in six different ways: symmetrical and antisymmetrical stretching, scissoring, rocking, wagging and twisting.

The major types of molecular vibrations are stretching and bending. The various types of vibrations are illustrated in Fig. 4.5 and Fig. 4.6. Infrared radiation is absorbed and the associated energy is converted into these types of motions. The absorption involves discrete, quantized energy levels. However, the individual vibrational motion is usually accompanied by other rotational motions. These combinations lead to the absorption bands, not the discrete lines, commonly observed in the mid IR region.

Stretching: Change in inter-atomic distance along bond axis

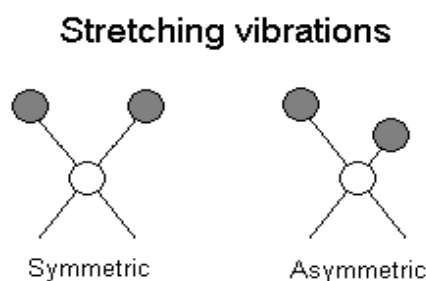


Fig. 4.5 Stretching vibrations

Bending: Change in angle between two bonds. There are four types of bend:

- Rocking
- Scissoring
- Wagging
- Twisting

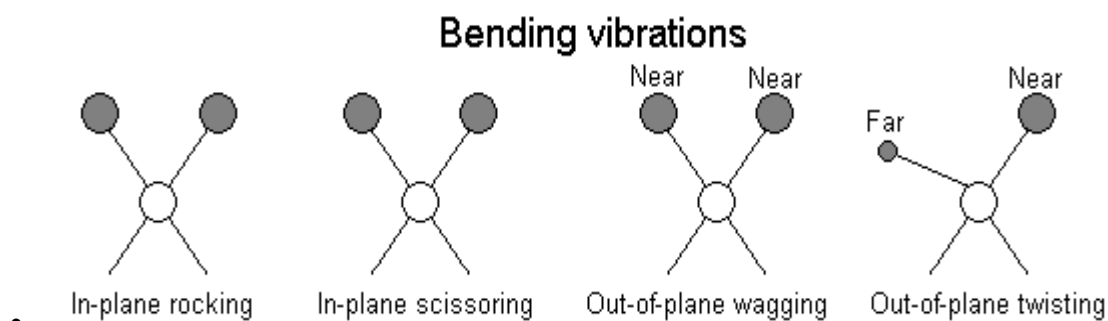


Fig. 4.6 Bending vibrations

Vibrational coupling

In addition to the vibrations mentioned above, interaction between vibrations can occur (*coupling*) if the vibrating bonds are joined to a single, central atom. Vibrational coupling is influenced by a number of factors;

- Strong coupling of stretching vibrations occurs when there is a common atom between the two vibrating bonds
- Coupling of bending vibrations occurs when there is a common bond between vibrating groups
- Coupling between a stretching vibration and a bending vibration occurs if the stretching bond is one side of an angle varied by bending vibration
- Coupling is greatest when the coupled groups have approximately equal energies
- No coupling is seen between groups separated by two or more bonds

Some General Trends

- ◆ Stretching frequencies are higher than corresponding bending frequencies. (It is easier to bend a bond than to stretch or compress it.)
- ◆ Bonds to hydrogen have higher stretching frequencies than those to heavier atoms.
- ◆ Triple bonds have higher stretching frequencies than corresponding double bonds, which in turn have higher frequencies than single bonds (Except for bonds to hydrogen).

4.3.6 Infrared Activity

Not all possible vibrations within a molecule will result in an absorption band in the infrared region. To be infrared active the vibration must result in a change of dipole moment during the vibration. This means that for homonuclear diatomic molecules such as Hydrogen (H_2), Nitrogen (N_2) and Oxygen (O_2) no infrared absorption is observed, as these molecules have zero dipole moment and stretching of the bonds will

not produce one. For heteronuclear diatomic molecules such Carbon monoxide (CO) and Hydrogen chloride (HCl), which do possess a permanent dipole moment, infrared activity occurs because stretching of this bond leads to a change in dipole moment (since Dipole moment = Charge \times distance). It is important to remember that it is not necessary for a compound to have a permanent dipole moment to be infrared active. In the case of Carbon dioxide (CO₂) the molecule is linear and centrosymmetric and therefore does not have a permanent dipole moment. This means that the symmetric stretch will not be infrared active. However in the case of the asymmetric stretch a dipole moment will be periodically produced and destroyed resulting in a changing dipole moment and therefore infrared activity.

4.3.7 Interpretation of FTIR Spectra

To obtain a more detailed interpretation of an IR spectrum it is necessary to refer to correlation charts and tables of infrared data. There are many different tables available for reference and a brief summary is given below for some of the main groups. When assigning peaks to specific groups in the infrared region it is usually the stretching vibrations which are most useful. Broadly speaking, these can be divided into four regions:

- 3700 – 2500 cm⁻¹ → Single bonds to hydrogen
- 2300 – 2000 cm⁻¹ → Triple bonds
- 1900 – 1500 cm⁻¹ → Double bonds
- 1400 – 650 cm⁻¹ → Single bonds (other than hydrogen)

It should also be noted that the region 1650 – 650 cm⁻¹ contains peaks due to bending vibrations but it is rarely possible to assign a specific peak to a specific group

4.3.8 The Fingerprint Region

The fact that there are many different vibrations even within relatively simple molecules means that the infrared spectrum of a compound usually contains a large number of peaks, many of which will be impossible to confidently assign to vibration of a particular group. Particularly notable is the complex pattern of peaks below 1500 cm⁻¹ which are very difficult to assign. However, this complexity has an important advantage in that it can serve as a *fingerprint* for a given compound. Consequently, by referring to known spectra, the region can be used to identify a compound.

4.3.9 Sample Preparation

The FTIR spectra of PPCWO were recorded at room temperature by using a double beam IR spectrophotometer (SHIMADZU, FTIR-8900 spectrophotometer, JAPAN) in the wavenumber range of 400-4000 cm^{-1} . The FTIR spectrum of the monomer CWO was obtained by putting the liquid monomer in a potassium bromide (KBr) measuring cell. PPCWO powder was collected from the PPCWO deposited substrates and then pellets of PPCWO powder mixed with KBr were prepared for recording the FTIR spectra of PPCWO sample. The FTIR spectra of the CWO and the PPCWO were recorded in transmittance (%) mode.

4.3.10 Results and Discussion

The FTIR spectra of CWO, PPCWO as-deposited and PPCWO heat treated in air at 473 and 673 K are shown in Fig. 4.7 as curves a, b, c and d respectively.

Table 4.2 describes the different assigned functional groups corresponding to the different wavenumbers of absorption bands in the monomer and that in the PPCWO.

These spectra reveal the structural changes due to plasma polymerization of the monomer and heat treatment of the PPCWO. In Fig. 4.7 spectrum a shows a well matching with the standard IR spectrum of the monomer similar to the khanturgaev, et al [2] except for a few extra bands (3417.6 cm^{-1}), which may be due to absorbed water and hydrogen bonded OH stretching. The characteristic absorption band at 3006.8 cm^{-1} may be assigned to aromatic C-H stretching vibration.

The bands observed at 2925.8 and 2852.5 cm^{-1} in the monomer spectrum may be attributed to CH_2 and CH_3 asymmetric and symmetric stretching vibrations respectively. There are some overtones or a combination of bands in the 2000-1800 cm^{-1} region.

The strong absorption bands between 1652.9 -1508.2 and 1463.9-1417.6 cm^{-1} are due to C=C and C=N stretching vibrations in the aromatic ring.

The absorption bands between 1242.1 and 968.2 cm^{-1} indicate C-H in plane (symmetrical) bending vibration in CWO. The sharp absorption peaks at 725.2 cm^{-1} are due to C-H out-of-plane bending vibrations.

The absorptions at 592.1 cm^{-1} indicate C=C out of plane bending. The FTIR spectrum of the PPCWO (spectrum b) is not well resolved compared to that of CWO. The characteristic absorption bands at 3006.8 cm^{-1} present in the monomer spectrum due to

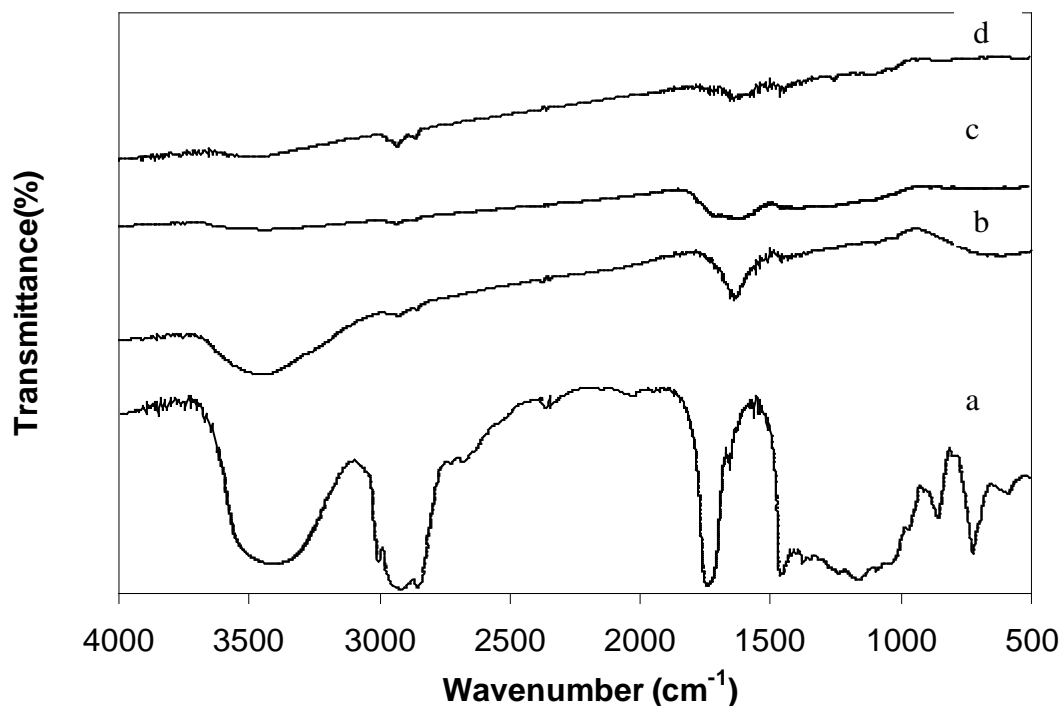


Fig. 4.7 The FTIR spectra of different samples: CWO, spectrum a; as deposited PPCWO, spectrum b; PPCWO heat treated at 473 K, spectrum c; PPCWO, heat treated at 673 K, spectrum d. (Curves are linearly shifted for convenience)

C-H stretching vibration is not present in this spectrum. The absorption bands assigned to CH_2 and CH_3 stretching vibrations are shifted to 2922 and 2852.5 cm^{-1} compared to that of the monomer. It is observed that a new prominent band at 3421.5 cm^{-1} corresponding to O-H stretching has arisen due to absorbed water.

The absorption band due to C=C stretching vibrations within 1683-1577 cm^{-1} is shifted slightly to higher frequency in PPCWO spectrum.

The strong absorption band for C-H in-plane bending at 1242.1 cm^{-1} in the monomer spectrum is shifted to 1261.4 cm^{-1} and become very weak in the as-deposited PPCWO. The absorption band present at 1020.3 cm^{-1} due to C-H in-plane bending becomes very weak compared to 1035.7 cm^{-1} in the monomer. The bands corresponding to C-H out of plane bending are absent in this spectrum.

The IR spectra of PPCWO heat treated at 473, and 673 K are represented as curves c and d respectively. In spectra c and d absorption bands observed at 3384.8, and 3384.8 cm^{-1} respectively may be due to O-H stretching. The absorption bands present around 2923.2 and 2922 cm^{-1} represent C-H stretching. The absorption bands between 1610 and 1652.9 cm^{-1} present in spectra b, c and d is due to C=C aromatic stretching vibrations.

Table-4.2: Assignments of IR absorption bands for CWO and PPCWO

Assignments	Wavenumber (cm ⁻¹)			
	CWO Monomer a	PPCWO		
		As-deposited b	Heat treated in air for one hour	
			473 K c	673 K d
O-H stretching	3417.5	3421.5	3384.8	3384.8
C-H aromatic stretching	3006.8			
CH ₂ asymmetric stretching	2925.8	2922	2923.9	2922
CH ₃ symmetric stretching	2852.5	2852.5	2854.5	2852.5
C=C stretching vibration	1652.9,1577.7, 1508.2	1683, 1577.7, 1521.7	1610.5, 1550.7	1652.9,1577.7, 1521.7
C=N stretching vibration	1463.9, 1417.6	1490.9,1436.9		1458.1, 1419.5
C-H in-plane bending vibrations	1242.1,1164.9, 1097.4,1035.7	1261.4, 101.3, 1020.3	1269.1,1116.7, 1020.3	1253.6,1114.8, 1033.8,999.1
C-H out-of-plane bending vibrations	725.2			
C=C out-of-plane bending	592.1, 464.8	605.6, 474.5, 407	451.3	

Therefore it is observed from the above discussion that the structure of the PPCWO thin films deposited by plasma polymerization process deviates to some extent from that of the CWO structure (spectrum a). However, these observations indicate that the aromatic ring structure is retained to a large extent in the PPCWO thin films. It is seen from the FTIR spectra of the PPCWO thin films that the intensity of the absorption bands decreased significantly compared to that of the monomer spectrum. This is an indication of monomer fragmentation during plasma polymerization. It is also observed in table 4.2 that in PPCWO films the absorption bands are shifted to lower or higher wavenumbers due to heat treatment at higher temperatures which is an indication of structural modification due to conjugation and cross-linking.

The formation of carbonyl group is usually due to the oxidation after exposure to air owing to oxygen reactions with a radical species trapped in the structure of the plasma polymer. The cross-link amorphous nature of the plasma polymer originates due to the random addition of fragments that produces a molecular structure quite different from that of the conventional polymer. Cross linking may also occur between carbon atoms due to abstraction or loss of hydrogen atoms, because of the impact of energetic particles within the plasma during deposition. Therefore it can be noted from the above discussion that the structure of the PPCWO thin films deposited by plasma polymerization process deviates to some extent from that of the CWO structure. It is seen from FTIR spectrum of PPCWO that the intensity of some of the absorption bands decreases significantly compared to those of the monomer spectrum. This is an indication of monomer fragmentation during plasma polymerization.

References

- [1] Conley R. T., *Infrared spectroscopy* (Allyn and Bacon Inc., Boston), (1975)
- [2] Khanturgaevi A. G., Shiretorovai V. G., Radnaeva L. D., Khanturgaeva G. I., Averina, E. S. and Bodoev N. V., ‘ Investigation of the composition of Lipids of Siberian Pine Seeds’, *Chemistry for Sustainable Development* 11 (2003) 589.

CHAPTER 5

UV-VIS SPECTROSCOPY OF PPCWO

5.1 Introduction

5.2 Theory of UV-Vis Spectroscopy

5.2.1 Different types of Electronic transitions

5.2.2 Absorbing species containing π , σ , and n electrons

5.2.3 Direct and Indirect optical transitions

5.2.4 Beer –Lambert Law: The law of Absorption

5.3 Experimental Procedure

5.4 Results and Discussion

5.4.1 Ultraviolet-visible Spectroscopic Analysis

References

5.1 Introduction

Plasma polymers have received much attention for their potential applications as light guide material, optical fibers, as photovoltaic energy converters, photodiodes, optical coatings to inhibit corrosion, etc. [1-3]. For these kinds of applications, plasma polymerized thin films need optical investigations. The optical energy gaps, the allowed direct transition and allowed indirect transitions have been determined from the UV-Vis spectroscopic studies and are discussed in this chapter.

UV-Vis spectroscopy is the measurement of the wavelength and intensity of absorption of near-ultraviolet and visible light by a sample. Ultraviolet and visible light are energetic enough to promote outer electrons to higher energy levels. UV-Vis spectroscopy is usually applied to molecules and inorganic ions or complexes in solution. The UV-Vis spectra have broad features that are of limited use for sample identification but are very useful for quantitative measurements. UV-Vis spectroscopy probes the electronic transitions of molecules as they absorb light in the UV and visible regions of the electromagnetic spectrum. Any species with an extended system of alternating double and single bonds will absorb UV light, and anything with color absorbs visible light, making UV-Vis spectroscopy applicable to a wide range of samples. The objective of the present research work is to go into insight of the optical properties of organic thin films prepared under glow discharge. The optical properties of PPCWO thin films have been investigated by UV-Vis spectroscopy. These studies have been performed on the PPCWO thin film of different thicknesses. The effect of heat treatment on the optical properties was investigated and was analyzed in the light of structural modification. The investigation of the optical properties may help to propose possible applications of these thin films in different fast growing industrial fields.

5.2 Theory of UV-Vis Spectroscopy

UV-Vis light can cause electronic transitions. When a molecule absorbs UV-Vis radiation, the absorbed energy excites an electron into an empty, higher energy orbital. The absorbance of energy can be plotted against the wavelength to yield a UV-Vis spectrum shown in figure 5.1.

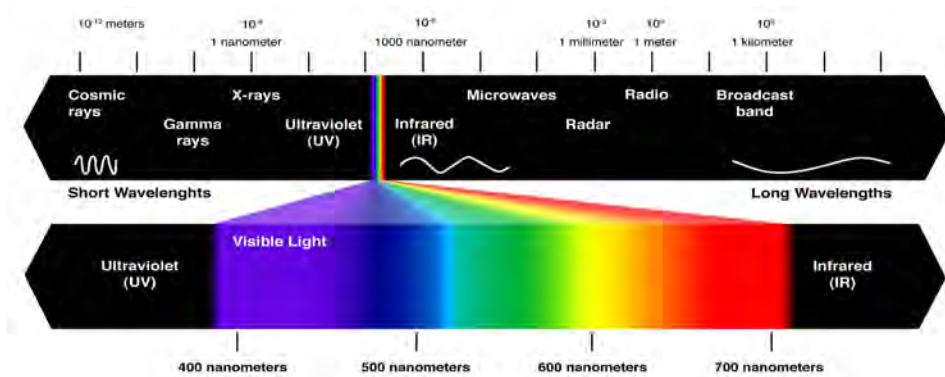


Fig 5.1: Light Spectrum

5.2.1 Different types of Electronic transitions

The absorption of UV or visible radiation corresponds to the excitation of outer electrons. There are three types of electronic transition which can be considered;

1. Transitions involving π , σ , and n electrons
2. Transitions involving charge-transfer electrons
3. Transitions involving d and f electrons.

When an atom or molecule absorbs energy, electrons are promoted from their ground state to an excited state. In a molecule, the atoms can rotate and vibrate with respect to each other. These vibrations and rotations also have discrete energy levels, which can be considered as being packed on top of each electronic level. Absorption of energy is quantized, resulting in the elevation of electrons from orbitals in the ground state to higher energy orbitals in an excited state.

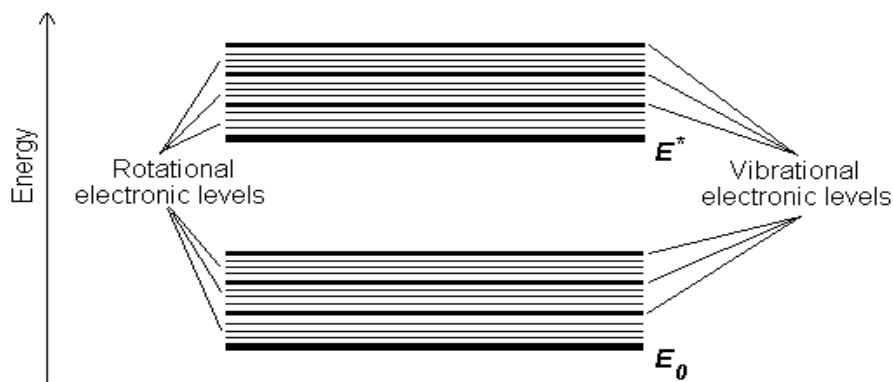


Fig. 5.2 Vibrational and rotational energy levels of absorbing materials

When an atom or molecule absorbs energy, electrons are promoted from their ground state to an excited state. In a molecule, the atoms can rotate and vibrate with respect to each other. These vibrations and rotations also have discrete energy levels, which can be considered as being packed on top of each electronic level. During

promotion, the electron moves from a given vibrational and rotational levels within one electronic mode to some other vibrational and rotational levels within the next electronic mode. Thus, there will be a large number of possible transitions responsible for change in electronic, rotational and vibrational levels and a large number of close bands are formed. The total energy of the molecule is the sum of its electronic energy, vibrational energy and rotational energy. The magnitude of these energies decreases in the following order: $E_{\text{elec}} > E_{\text{vib}} > E_{\text{rot}}$. Fig. 5.2 shows the vibrational and rotational energy levels of absorbing materials.

5.2.2 Absorbing species containing π , σ , and n electrons

Absorption of ultraviolet and visible radiation in organic molecules is restricted to certain functional groups (*chromophores*) that contain valence electrons of low excitation energy. The spectrum of a molecule containing these chromophores is complex. This is because the superposition of rotational and vibrational transitions on the electronic transitions gives a combination of overlapping lines. This appears as a continuous absorption band. Electronic energy levels are shown in figure 5.3.

Possible *electronic* transitions of π , σ , and n electrons are:

An electron in a bonding σ orbital is excited to the corresponding antibonding orbital. The energy required is large. For example, methane (which has only C-H bonds, and can only undergo $\sigma \rightarrow \sigma^*$ transitions) shows an absorbance maximum at 125 nm. Absorption maxima due to $\sigma \rightarrow \sigma^*$ transitions are not seen in typical UV-Vis. spectra (200 - 700 nm)

$n \rightarrow \sigma^*$ Transitions

Saturated compounds containing atoms with lone pairs (non-bonding electrons) are capable of $n \rightarrow \sigma^*$ transitions. These transitions usually need less energy than $\sigma \rightarrow \sigma^*$ transitions. They can be initiated by light whose wavelength is in the range 150 - 250 nm. The number of organic functional groups with $n \rightarrow \sigma^*$ peaks in the UV region is small.

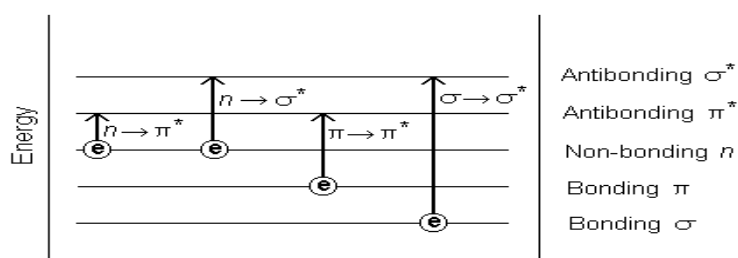


Fig. 5.3: Summary of electronic energy levels

$n \rightarrow \pi^*$ and $\pi \rightarrow \pi^*$ Transitions

Most absorption spectroscopy of organic compounds is based on transitions of n or π electrons to the π^* excited state. This is because the absorption peaks for these transitions fall in an experimentally convenient region of the spectrum (200 - 700 nm). These transitions need an unsaturated group in the molecule to provide the π electrons. Molar absorptivities from $n \rightarrow \pi^*$ transitions are relatively low, and range from 10 to 100 L mol⁻¹ cm⁻¹. $\pi \rightarrow \pi^*$ transitions normally give molar absorptivities between 1000 and 10,000 L mol⁻¹ cm⁻¹.

The solvent in which the absorbing species is dissolved also has an effect on the spectrum of the species. Peaks resulting from $n \rightarrow \pi^*$ transitions are shifted to shorter wavelengths (*blue shift*) with increasing solvent polarity. This arises from increased solvation of the lone pair, which lowers the energy of the n orbital. Often (but *not* always), the reverse (i.e. *red shift*) is seen for $\pi \rightarrow \pi^*$ transitions. This is caused by attractive polarisation forces between the solvent and the absorber, which lower the energy levels of both the excited and unexcited states. This effect is greater for the excited state, and so the energy difference between the excited and unexcited states is slightly reduced - resulting in a small red shift. This effect also influences $n \rightarrow \pi^*$ transitions but is overshadowed by the blue shift resulting from solvation of lone pairs.

5.2.3 Direct and Indirect optical transitions

Materials are capable of emitting visible luminescence when subjected to some form of excitation such as UV light (photoluminescence). The mechanism of photoluminescence in semiconducting materials is schematically illustrated in Fig. 5.4, which plots the E - k diagrams for a direct band gap material (*left*) and an indirect gap material (*right*), where E and k are respectively the kinetic energy and wave vector (or "momentum vector") of the electron or hole ($E = k^2 \hbar^2 / 2m_*$, where $\hbar \equiv h / 2\pi$ is the Planck constant h divided by 2π , and m_* is the electron or hole effective mass).

The shaded states at the bottom of the conduction band and the empty states at the top of the valence band respectively represent the electrons and holes created by the absorption of an UV or visible photon with an energy $\hbar\omega_{\text{exc}}$ exceeding the band gap E_g (the gap in energy between the valence band and the conduction band) of the material, an electron-hole pair is created and the electron (hole) is excited to states high up in the conduction (valence) band.

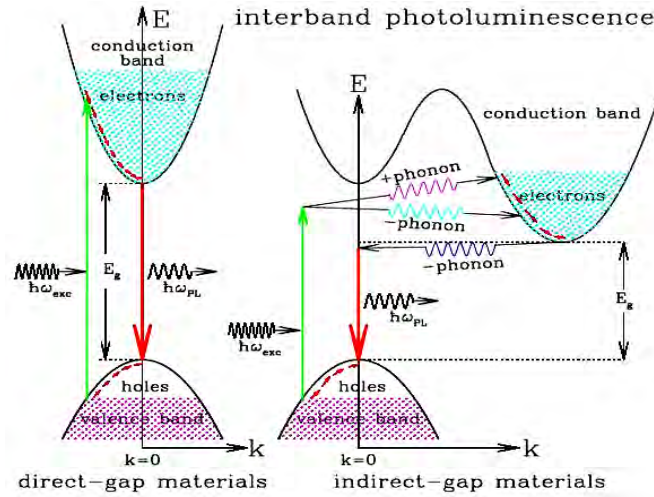


Fig.5.4: Schematic band diagrams for the photoluminescence processes in a direct gap material (*left*) and an indirect gap material (*right*).

In a direct gap material (*left*), the conduction band minimum and the valence band maximum occur at the same k values (i.e., $\hbar\vec{k}_i = \hbar\vec{k}_f$, where \vec{k}_i and \vec{k}_f are respectively the wave vectors of the initial and final electron states; this implies that the electron wave vector should not change significantly during a photon absorption process). The conservation of momentum is guaranteed for the photoexcitation of the electron which only involves a UV or visible photon: $\hbar\vec{k}_i + \hbar\vec{k}_{\text{phot}} \approx \hbar\vec{k}_i = \hbar\vec{k}_f$, since \vec{k}_{phot} , the wave vector of the absorbed photon (which is in the order of $2\pi/\lambda \sim 10^5 \text{ cm}^{-1}$), is negligible compared to the electron wave vector (which is related to the size of the Brillouin zone $\pi/a \sim 10^8 \text{ cm}^{-1}$, where the unit cell dimension a is in the order of a few angstroms). This implies that in a direct band gap material, the electron wave vector does not change significantly during a photon absorption process. This is represented by photon absorption and emission processes by vertical arrows on E - k diagrams.

In contrast, for an indirect band gap material (*right*), of which the conduction band minimum and the valence band maximum have different k values, conservation of momentum implies that the photon absorption process must be assisted by either absorbing (indicated by a "+" sign) or emitting (indicated by a "-" sign) a phonon (a quantum of lattice vibration), because the electron wave vector must change significantly in jumping from the valence band in state (E_i, \vec{k}_i) to a state (E_f, \vec{k}_f) in the conduction band, and the absorption of a photon alone can not provide the required momentum change since $|\vec{k}_{\text{phot}}| \ll |\vec{k}_i - \vec{k}_f|$.

5.2.4 Beer –Lambert Law: The law of Absorption

Electromagnetic radiation of suitable frequency can be passed through a sample so that the photons are absorbed by the samples so that the samples and changes in the

electronic energies of the molecules can be brought about. So it is possible to affect the changes in a particular type of molecular energy using appropriate frequency of the incident radiation. Two empirical laws have been formulated about the absorption intensity. Lambert's law states that the fraction of the incident light absorbed are independent of the intensity of the source. Beer's law states that the absorption is proportional to the number of absorbing molecules [2]. For most spectra the solution obeys Beer's Law. This is only true for dilute solutions. Combining these two laws gives the Beer-Lambert law:

$$I = I_0 e^{-\alpha d} \dots\dots\dots(5.1)$$

$$\log_e \left(\frac{I_0}{I} \right) = \alpha d \dots\dots\dots(5.2)$$

where I_0 is the intensity of the incident radiation, I is the intensity of the transmitted radiation, d is the path length of the absorbing species and α is the absorption coefficient. The absorption spectrum can be analyzed by Beer-Lambert law, which governs the absorption of light by the molecules. It states that, "When a beam of monochromatic radiation passes through a homogeneous absorbing medium the rate of decrease in intensity of electromagnetic radiation in UV-Vis region with thickness of the absorbing medium is proportional to the intensity coincident radiation".

The intensity of transmittance I , is expressed as the inverse of intensity of absorbance.

The absorption coefficient α , can be calculated from the absorption data using the relation (5.3)

$$\alpha = \frac{2.303A}{d} \dots\dots\dots(5.3)$$

where $A = \log_{10} \left(\frac{I_0}{I} \right)$ is the Absorbance.

The relation of extinction coefficient k with α is

$$\alpha = \frac{4\pi k}{\lambda} \dots\dots\dots(5.4)$$

where λ is the wavelength.

To estimate the nature of absorption a random phase model is used where the momentum selection rule is completely relaxed. The integrated density of states $N(E)$ has been used and defined by

$$N(E) = \int_{-\infty}^{+\infty} g(E) dE \dots\dots\dots(5.5)$$

The density of states per unit energy interval may be represented by $g(E) = \frac{1}{V} \sum \delta(E - E_n)$, where V is the volume, E is energy at which $g(E)$ is to be evaluated and E_n is the energy of the n th state.

If $g_v \propto E^p$ and $g_c(E) \propto (E - E_{opt})^q$, where energies are measured from the valance band mobility edge in the conduction band (mobility gap), and substituting these values into an expression for the random phase approximation, the relationship obtained $v^2 I_2(v) \propto (hv - E_0)^{p+q+1}$, where $I_2(v)$ is the imaginary part of the complex permittivity. If the density of states of both band edges is parabolic, then the photon energy dependence of the absorption becomes $\alpha \propto v^2 I_2(v) \propto (hv - E_{opt})^2$. So for higher photon energies the simplified general equation is

$$\alpha hv = B(hv - E_{opt})^n \dots\dots\dots(5.6)$$

where hv is the energy of absorbed light, n is the parameter connected with distribution of the density of states and B is the proportionality factor. The index n equals 1/2 and 2 for allowed direct transition and indirect transition energy gaps respectively.

Thus, from the straight-line plots of $(\alpha hv)^2$ versus hv the direct and indirect energy gaps of insulators and/or dielectrics can be determined.

5.3 Experimental Procedure

The PPCWO thin films were deposited on to glass substrates (Sail brand, China) having a dimension of 18mm×18mm×1mm. The polymer thin films were treated at three temperatures: 373, 473 and 573 K. The UV-Vis spectrum of the monomer (CWO) and the as-deposited and heat-treated PPCWO thin films were recorded in absorption mode using a dual beam UV-vis spectrophotometer (SHIMADZU UV-1601, JAPAN) in the wavelength range of 190-800 nm at room temperature.

PPCWO thin films were heat-treated for one hour using a furnace, (Muffle Furnace, India). For measuring the optical absorption of the monomer, it was kept in a quart cell and for the PPCWO films a similar glass slide was used as the reference.

5.4 Results and Discussion

5.4.1 Ultraviolet-visible spectroscopic analyses

In the present study UV-visible absorption spectra was used to investigate the optical induced transition and to provide information about the band structure of PPCWO thin films. Fig. 5.5 shows the UV-vis spectral behavior of absorbance of PPCWO thin films for various thicknesses. The UV-vis spectra were recorded both for as-deposited and

heat-treated samples at 300, 373 and 473 K for 1 hour. From the Fig. 5.5 it is seen that the absorbance increases with the increase of thickness of the PPCWO thin films. From the absorbance spectra it is observed that the absorbance rises very rapidly before 300 nm, attains its maximum value and then decreases rapidly up to 800 nm. It is also observed that the peak wavelength (λ_m) corresponding to maximum absorbance decreases with the increase of thickness.

The absorption coefficient, α , is calculated from the measured absorbance data for different wavelengths corresponding to different photon energies at room temperature using equation (1).

$$\alpha = 2.303 \frac{A}{d} \quad (1)$$

where $A = \log_{10} \left(\frac{I_0}{I} \right)$ is the absorbance and d is the thickness of the film.

The spectral dependence of α , on the photon energy, $h\nu$, for all the as-deposited samples are presented in fig. 5.6 The dependence of optical absorption coefficient on the photon energy helps to study the band structure and the type of electron transition involved in absorption process. It is noticed that the curves have sharp fall in the higher experimental photon energy range. This may indicate the presence of direct optical transitions in the PPCWO thin films.

In crystalline and amorphous materials the photon absorption is observed to obey the Tauc relation [4] equation (2).

$$\alpha h\nu = B (h\nu - E_{opt})^n \quad (2)$$

where $h\nu$ is the incident photon energy, h is Planck constant, ν is the frequency of

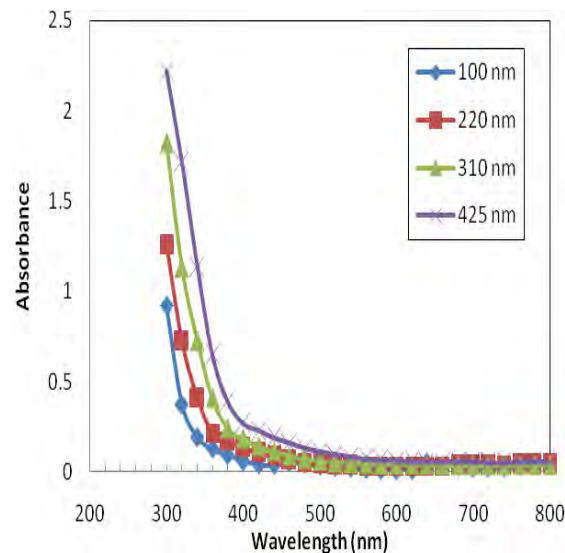


Fig.5.5 Wavelength versus absorbance plot for different PPCWO thin films.

incident radiation, B is an energy independent constant, E_{opt} is the optical band gap and n is an index depending on the type of optical transition caused by photon absorption. The index n equals $\frac{1}{2}$ and 2 for allowed direct and indirect transitions respectively.

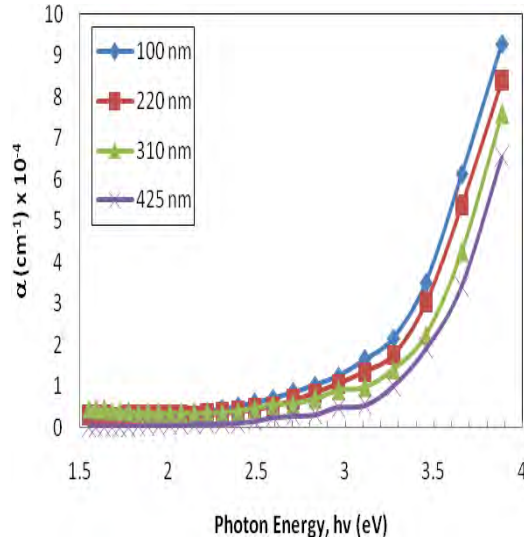


Fig.5.6 Photon energy versus absorption coefficient (α) plot for PPCWO of different thicknesses

The direct transition energy gap (E_{qd}) was obtained by plotting $(\alpha \cdot hv)^2$ versus $h\nu$ curve and then extrapolating the linear portion of the curve to $(\alpha \cdot hv)^2 = 0$. Plots of $(\alpha \cdot hv)^2$ versus $h\nu$ for as-deposited PPCWO films are shown in fig.5.7 and direct transition energy gaps were determined from the intercept of the linear part of the curve extrapolated to zero α in the photon energy axis [5]. The values of direct transition energy gaps lie between 3.5 and 3.55 and 3.6 and 3.65 eV respectively. From table 5.1 it is found that the values of direct transition energy gap increases slightly with increasing thickness of the films.

Table 5.1: Values of direct band gap energy

Thickness d (nm)	Direct Band Gap E_d (eV)
100	3.50
220	3.55
310	3.6
425	3.65

It is observed that the values of E_d for as deposited PPCWO thin films have an increasing trend with the increase of film thickness. As the thickness of the films increases, some crosslinking may develop within the bulk of the material as a

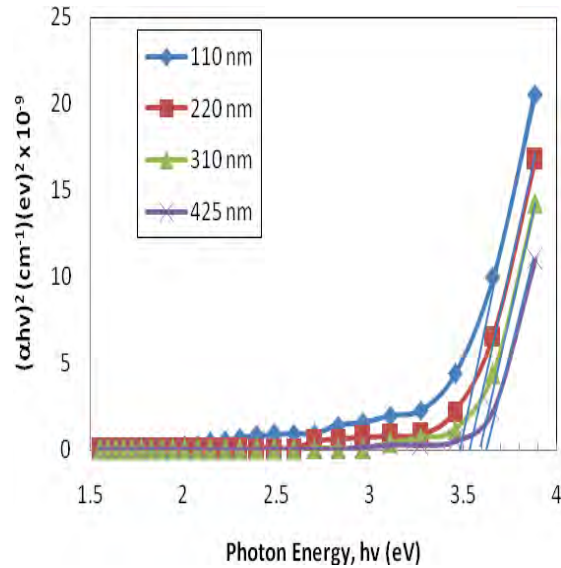


Fig. 5.7 $(\alpha \cdot h\nu)^2$ vs. $h\nu$ curves for as deposited PPCWO thin films of different thicknesses.

result of the impact of plasma on the surface during deposition process and as a consequence higher energy gaps are observed.

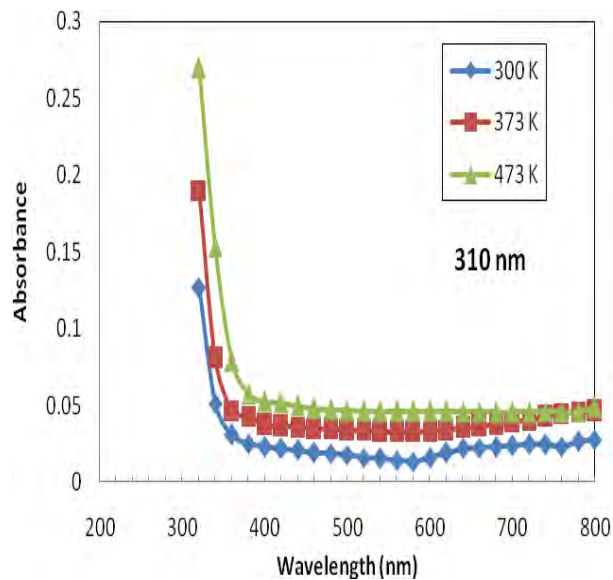


Fig.5.8 Absorbance versus wavelength plot at different temperature of PPCWO films with thickness 310nm.

For direct transitions the change in the optical band gap with thickness was assumed to appear due to the variation of localized gap states in thin films. The changes in direct energy gap for the PPCWO films are calculated for 220 nm and 310 nm. The values obtained for E_d of as deposited and heat treated PPCWO thin films are summarized in Table 5.2.

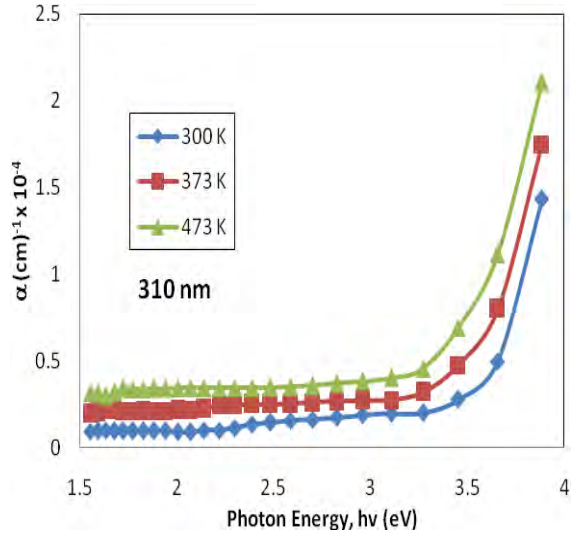


Fig. 5.9 Variation of absorbance with wavelength for PPCWO thin film heat treated at different temperatures (Thickness: 310 nm)

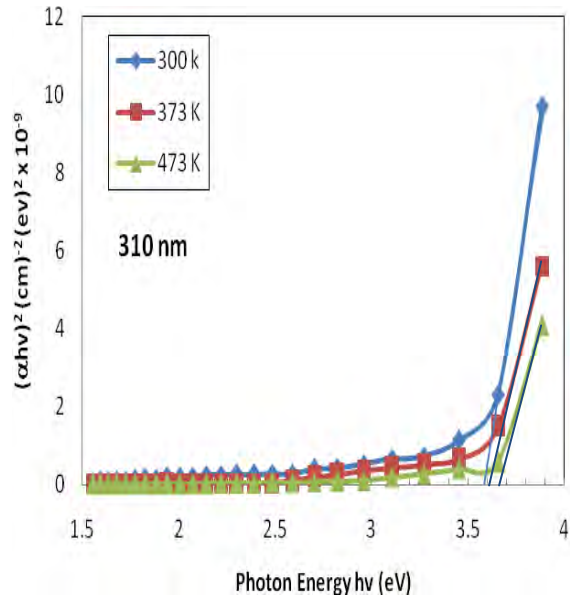


Fig.5.10 $(\alpha \cdot h \cdot c)^2$ vs. $h \cdot c$ curves for PPCWO thin film heat treated at different temperatures (Thickness: 310 nm)

Table 5.2: Comparison of Direct band gap of PPCWO thin film and PPCWO heat treated at different temperatures

Thickness, nm	Direct band gap, eV (As deposited)	Direct band gap, eV 373 K	Direct band gap, eV 473 K
220	3.55	3.60	3.70
310	3.6	3.65	3.69

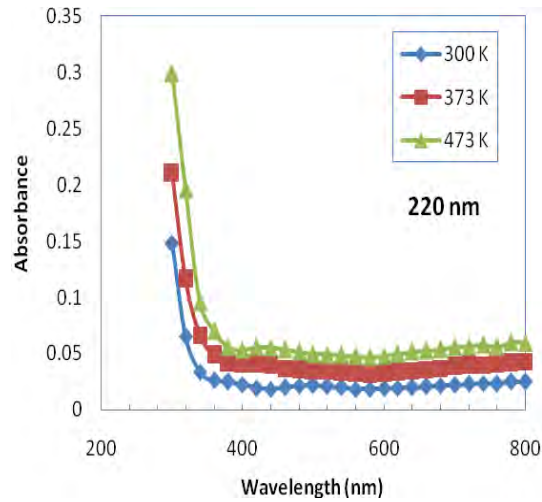


Fig.5.11 Absorbance versus wavelength plot at different temperature of PPCWO films with thickness 220nm.

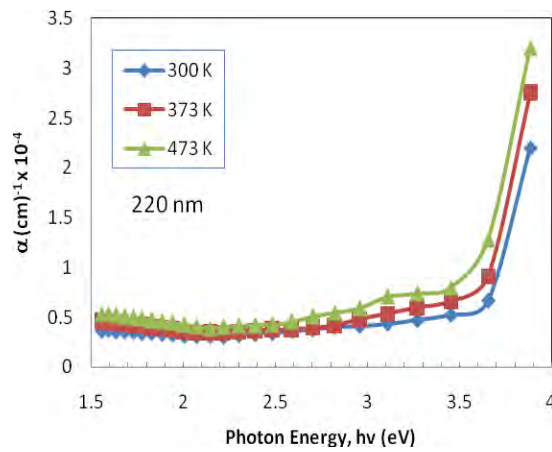


Fig. 5.12 Variation of absorbance with wavelength for PPCWO thin film heat treated at different temperatures (Thickness: 220 nm)

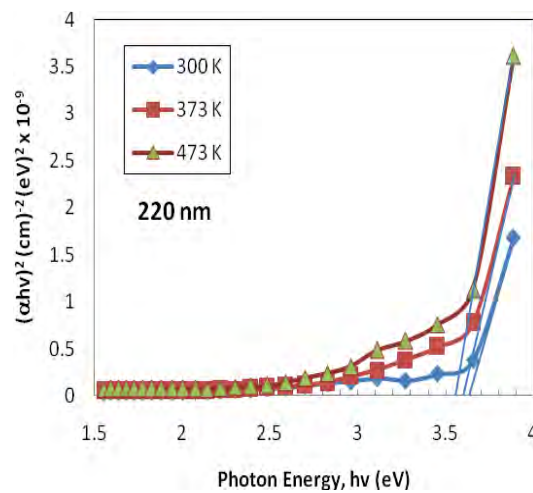


Fig.5.13 $(\alpha \cdot h \cdot \nu)^2$ vs. $h \cdot \nu$ curves for PPCWO thin film heat treated at different temperatures (Thickness: 220 nm)

It is observed that E_d increases when the PPCWO thin films are heat treated, more conjugation may form within the samples. The structural rearrangement due to heat treatment causes the band gaps to increase. When the PPCWO thin films are heat treated conjugation increases owing to structural rearrangement and as a consequence the band gap of PPCWO films reduces on heat treatment at higher temperatures.

References:

- [1] Morosoff N., Crist B., Bumgarner M., Hsu T. and Yasuda H., 'Free radicals resulting from plasma polymerization treatment', *J. Macromol. Sci. A* 10 (1976) 451.
- [2] Yasuda H., Marsh H. C., Bumgarner M. O. and Morosoff N., 'Polymerization of organic compounds in an electrodeless glow discharge', *J. Appl. Polym. Sci.* 19 (1975) 2845.
- [3] Chakraborti K., Basu M., Chaudhuri S., Pal A. K. and Hanzawa H., 'Mechanical, electrical and optical properties a-C-H-N films deposited by plasma CVD technique', *Vacuum* 53 (1999) 405.
- [4] Tauc J., Menth A. and Wood D., 'Optical and magnetic investigations of the localized states in semiconducting glasses', *Phys. Rev. Lett.* 25 (1970) 749
- [5] Davis E. A. and Mott N. F., "Conduction in non-crystalline system, Optical absorption and photoconductivity in amorphous semiconductors", *Philos. Mag.* 22 (1970) 903.

CHAPTER 6**AC ELECTRICAL PROPERTIES OF PPCWO**

- 6.1 Introduction
- 6.2 Brief Description of dielectrics
 - 6.2.1 Plasma Polymers as Dielectrics
 - 6.2.1.1 Polarization and its classification
 - 6.2.1.2 Dielectric constant
 - 6.2.1.3 Dielectric Losses
 - 6.2.2 The Debye theory of dielectrics
 - 6.2.2.1 The Cole-Cole function
- 6.3 Experimental Details
- 6.4 Results and Discussion
 - 6.4.1 Frequency and temperature dependence of ac electrical conductivity
 - 6.4.2 Frequency and temperature dependence of the dielectric constant
 - 6.4.3 Frequency and temperature dependence of dielectric loss tangent
 - 6.4.4 Cole- Cole plot
- References

6.1 Introduction

Plasma polymerization is a versatile and important technique for depositing uniform, pinhole-free and flawless thin films of organic materials. By this process it is possible to prepare uniform, pinhole free, insoluble, highly resistive, chemically inert, highly cross linked, adherent, thermally stable and amorphous thin films of few angstroms order, on different substrates. These films have potential applications in the field of ultra large-scale integration and very large-scale integration, capacitors, light emitting diodes, sensors, rechargeable batteries, as intermetallic dielectrics in integrated circuits and other electronic circuits as insulators and dielectric materials. [1-6]

The electrical properties of polymers cover a vastly various range of molecular phenomena. In contrast to metals, polymers respond in a more varied manner, such as resulting from distortion and alignment of molecules under the influence of an applied field become apparent. Polarization gives valuable insight into the nature of the electrical response and it also provides an effective way to probe molecular dynamics. Therefore electrical studies correspond to mechanical properties of polymers on a molecular level. Not only this but also a correspondence is initiated for fundamental understanding of the thermal and optical properties of polymers. Obviously insulating polymers have low level conduction may be contributed by impurities that provide a small concentration of charge carriers in the form of electrons or ions.

The ac electrical properties of as-deposited and heat-treated PPCWO thin films are discussed in this chapter. The ac conductivity and dielectric relaxation processes of PPCWO thin films have been discussed in the subsequent sections. This provides information regarding the conduction mechanism and relaxation processes in PPCWO.

Because of good dielectric properties, plasma-polymerized thin films have been found to be useful as thin film insulators and capacitors in electrical and electronic devices like, thin film dielectrics, separation membrane for batteries, etc. As the materials have good dielectric properties, plasma-polymerized thin films have been found to be useful as dielectrics in integrated microelectronics and insulating layers for semiconductors [7-9]. Thin films produced through glow discharge are known to have free radicals or polar groups independent of the nature of monomers. Owing to this reason, these polymers are good candidates for the investigation of dielectric properties. A dielectric study throws light on the molecular structure and relaxation behaviors of the polymers.

The detail investigation of the ac conductivity and dielectric properties of plasma-polymerized thin films provide information about the conduction process, dielectric constant, relaxation process, etc. which are dependent on frequency and temperature .

6.2 Brief Description of dielectrics

6.2.1 Plasma Polymers as Dielectrics

A capacitor essentially consists of two conducting surface separated by a layer of an insulating medium called dielectric. The conducting surfaces may be in the form of either circular or rectangular plates or be of spherical or cylindrical shape. The purpose of a capacitor is to store electrical energy by electrostatic stress in the dielectric.

In industrial applications electrical and thermal stability is a concern regardless of polar and nonpolar molecules. No matter how idealized in electrical and electronic purposes, materials with unvarying dielectric constant within the wide working temperature and frequency range is highly recommended. Instability of the properties and high dielectric loss of plasma polymers made it less satisfying than conventional polymers. Plasma polymers contain a certain number of polar groups independent of whether the monomer was polar or non-polar. And this presence of polar groups has significant role for the relatively high dielectric losses in plasma polymers. Most conventional polymers are non-polar and their dielectric losses are extremely low. Polar polymer has dielectric losses significantly higher. The dielectric constants of plasma polymerized films are slightly higher than those of the conventional polymers .The losses of plasma polymers are at least an order of magnitude higher. Very simply speaking dielectrics are insulators. In capacitor dielectric materials serve following three purposes:

- (a) Keeps the conducting plates at a small separation and therefore higher capacitances;
- (b) It increases the effective capacitance by reducing the electric field strength, which means it is possible to get the same charge at a lower voltage; and
- (c) Dielectric material reduces the possibility of shorting out by sparking (more formally known as dielectric breakdown) during operation at high voltage.

6.2.1.1 Polarization and its classification

A dielectric subjected to a homogeneous field carries a dipole moment per unit volume. Dipole moment per unit volume is called the polarization of the dielectric. When a

polymer is subjected to the influence of an applied electric field, different processes of polarization take place due to the distortion and alignment of the molecules. With changing the field, both the distortion of the molecules and their average orientations change. Different types of polarization occur at different range of frequencies.

The total polarization is consists by the following four types of polarizations:

i) Electronic polarization: If the atom is in the absence of the field then the system is neutral one and has no dipole moment. In the absence of the field the system is still neutral, but has a non-zero dipole moment because the nucleus and the centre of charge cloud are separated by a certain distance. In this case the atom carries a dipole moment and this dipole moment is proportional to the field strength and the proportionality factor is called the electronic poarizability of the atom. The term “electronic” used here as this dipole moment results from a shift of the electron cloud relative to nucleus.

ii) Orientational polarization: If two different atoms A and B form a chemical bond, one of the two is more apart with one or more of its valence electrons than the other. As a result, the bond between A and B is at least partly ionic. If the bond between A and B has ionic character, it is obvious that the molecule AB carries an electric dipole moment even in the absence of an applied field, such a dipole moment is called permanent. The magnitude of the dipole moment is given by the product of the average charge transferred from A to B and the internuclear distance. For a molecule consisting of more than two atoms, several bonds may carry a permanent dipole moment of the molecule as a whole is obtained by vector addition of the moments associated with the various bonds. When an external field is applied to a molecule carrying a permanent dipole moment, the permanent dipole moment aligns along the direction of the field. The contribution of this process of orientation of the permanent dipoles to the polarization is called orientational polarization.

iii) Ionic polarization: When in a molecule some of the atoms have an excess positive or negative charge (resulting from the ionic character of the bonds), an electric field will tend to shift positive ions relative to negative ones. This leads to an induced moment of different origin from the moment induced by electron clouds shifting relative to nuclei. The ionic polarization occurs due to shift of the ions relative to each other.

iv) Interfacial polarization: In a real crystal there inevitably exists a large number of defects such as lattice vacancies, impurity centers, dislocations etc. Free

charge carriers, migrating through the crystal, under the influence of an applied field, may be trapped by, or pile up against a defect. The effect of this will be the creation of a localized accumulation of charge which will induce its image charge on an electrode and give rise to a dipole moment. This constitutes a separate mechanism of polarization in the crystal, and is given the name interfacial polarization.

The molar polarization of a material is found to depend on the frequency of the applied alternating electric field Fig 6.1

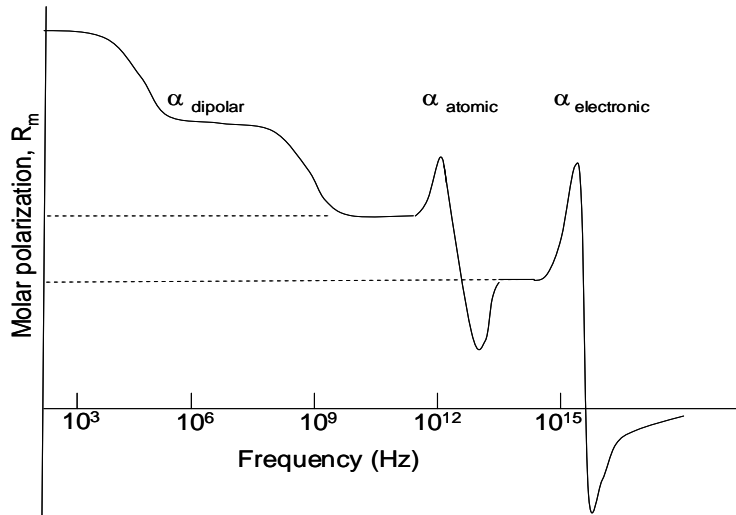


Fig. 6.1 Dispersion of molar polarization in a dielectric (schematic)

In general the polarizability can be written as the sum of four terms i.e.

$$\alpha = \alpha_e + \alpha_a + \alpha_d + \alpha_i$$

where , e = electronic contribution

a = atomic contribution

d = the dipolar contribution

i = the interfacial contribution.

6.2.1.2 Dielectric constant

It is known that the capacitance of a condenser in a vacuum is C_v and if C is the capacitance with a different dielectric medium, then,

$$C = \epsilon' C_v$$

Where ϵ' is the dielectric constant of the substituting material. In other words dielectric constant represents the ratio of the electrical energy of the field set up in a dielectric material to that set up in vacuum

Dielectric materials are electrical insulators i.e have direct current resistivities greater than about 10^8 ohm-cm. Insulators have the very useful ability to store electrical

charge. A common device used for this purpose is a capacitor. The capacitance of such a device measures the extent to which it is able to store charge.

6.2.1.3 Dielectric Losses

When an electric field acts on any matter the latter dissipates a certain quantity of electric energy that transforms into heat energy. This phenomenon is commonly known as ‘the expense’ or ‘loss’ of power, meaning an average electric power dissipated in matter during a certain interval of time. As a rule the loss of power in a specimen of material, all other conditions being equal, is directly proportional to the square of the electric voltage applied to the specimen.

$$P = U^2/R$$

Most of the dielectrics display a characteristic feature: under a given voltage the dissipation of power in these dielectrics depends on the voltage frequency; the expense of power frequency, voltage and capacitance and also depends on the material of dielectric.

The amount of power losses in a dielectric under the action of the voltage applied to it is commonly known as ‘dielectric losses’. This is the general term determining the loss of power in an electrical insulation both at a direct and an alternating voltage.

If an alternating electric field \mathbf{E} is applied, which has amplitude \mathbf{E}_0 and angular frequency ω , across a dielectric material then

$$\mathbf{E} = \mathbf{E}_0 \cos \omega t$$

This will produce polarization which alternates in direction, and if the frequency is high enough, the orientation of any dipoles which are present will inevitably lag behind the applied field. Mathematically, this is expressed as a phase lag δ in the electric displacement. This parameter is usually described by loss tangent $\tan \delta$. The loss tangent is a parameter of a dielectric material that quantifies its inherent dissipation of electromagnetic energy. The term refers to the angle in a complex plane between the resistive (lossy) component of an electromagnetic field and its reactive (lossless) component.

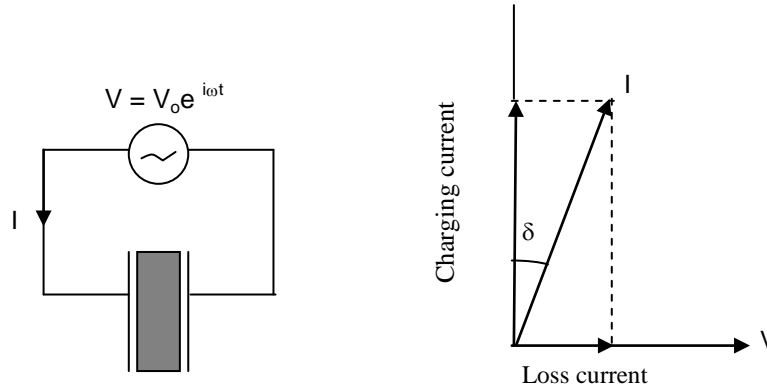


Fig.6.2 AC losses in a dielectric : (a) circuit diagram, (b) simplified diagram of current-voltage relationship.

6.2.2 The Debye theory of dielectrics

The capacitance of a parallel plate capacitor having a dielectric medium is expressed as

$$C = \frac{\epsilon_0 \epsilon' A}{d} \dots\dots\dots (6.1)$$

where ϵ_0 is the permittivity of free space, ϵ' is the dielectric constant of the medium, A is the surface area of each of the plates/electrodes and d is the thickness of the dielectric.

A real capacitor can be represented with a capacitor and a resistor. The parameters such as angular frequency (ω) of The applied field, the parallel resistance R_p , parallel capacitance C_p and the series resistance R_s and series capacitance C_s are related to the dielectric constant , dielectric dissipation factor ϵ'' and loss tangent as:

$$\epsilon' = \frac{C_p}{C_0} \dots\dots\dots (6.2)$$

$$\epsilon'' = \frac{1}{R_p C_0 \omega} \dots\dots\dots (6.3)$$

and
$$\tan \delta = \frac{\epsilon''}{\epsilon'} = \frac{1}{R_p C_p \omega} = G_p / 2\pi f C_p \dots\dots\dots(6.4)$$

The ac conductivity, σ_{ac} , was calculated using eqn.

$$\sigma_{ac} = G_p d/A \dots\dots\dots (6.5)$$

The dependence of ac conductivity, σ_{ac} , on frequency may be described by the power law represents by equation (6.6)

$$\sigma_{ac}(\omega) = A \omega^n \dots\dots\dots (6.6)$$

where A is a proportionality constant and ω ($=2\pi f$, f is the linear frequency) is the angular frequency and n is the exponent, which generally takes the value less than unity

for Debye type mechanism and is used to understand the conduction/relaxation mechanism in amorphous materials.

The dielectric behavior of a material is usually described by Debye dispersion equation 6.7

$$\epsilon^*(\omega, T) = \epsilon' - i\epsilon'' \dots\dots\dots (6.7)$$

Where ϵ^* is the complex dielectric permittivity, ϵ' (energy dissipated per cycle) is the real part of complex dielectric permittivity and ϵ'' (energy stored per cycle) is the imaginary part of the complex dielectric permittivity.

$$\epsilon' = \epsilon_\infty + \frac{\epsilon_s - \epsilon_\infty}{1 + \omega^2 \tau^2} \dots\dots\dots (6.8)$$

$$\epsilon'' = \frac{(\epsilon_s - \epsilon_\infty)\omega\tau}{1 + \omega^2 \tau^2} \dots\dots\dots (6.9)$$

where ϵ_s is the static dielectric constant, ϵ_∞ is the high frequency dielectric constant and the quantity τ is a characteristic time constant, usually called the dielectric relaxation time, it refers to a gradual change in the polarization following an abrupt change in applied field.

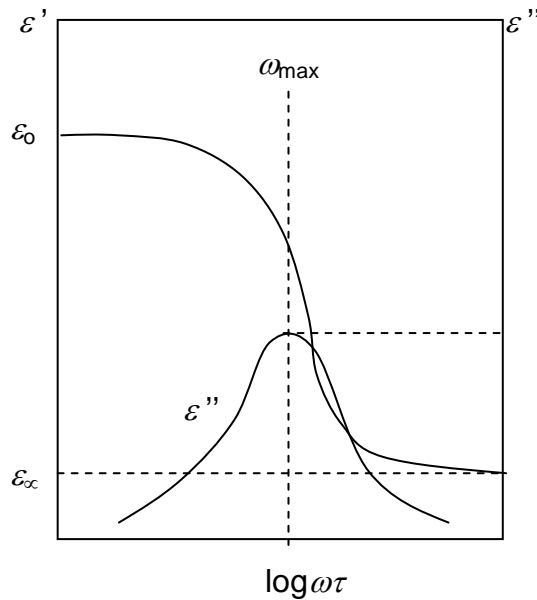


Fig.6.3 Debye dielectric dispersion curves.

The dielectric loss tangent is expressed by

$$\tan \delta = \frac{\epsilon''}{\epsilon'} \dots\dots\dots (6.10)$$

The graphs of ϵ' and ϵ'' against frequency of the applied field (logarithmic scale) through the dispersion regions show that the maximum loss value occurs when $\omega\tau = 1$,

corresponding to a critical frequency $\omega_{\max} = 1/\tau$, and location of this peak provides the easiest way of obtaining the relaxation time from the experimental results.

The activation energy (ΔE) of the relaxation process is related to the relaxation time by the Arrhenius equation:

$$\tau = \frac{1}{2\pi f_{\max}} = \tau_0 \exp\left(\frac{\Delta E}{k_B T}\right) \dots\dots\dots (6.11)$$

Where f_{\max} , is the frequency of maximum loss for a given temperature, τ_0 is a constant and T is the absolute temperature and k_B is the Boltzman constant. ΔE was evaluated in the present work from the slope of the plot $\ln f_{\max}$, versus $1/T$.

6.2.2.1 The Cole-Cole function

The difference in dielectric constant measured at low and high frequencies is called the strength of the relaxation. By eliminating the parameter $\omega\tau$ between equations. (6.8) and (6.9), it can be obtained

$$\left(\epsilon' - \frac{\epsilon_s + \epsilon_\infty}{2}\right)^2 + \epsilon''^2 = \left(\frac{\epsilon_s - \epsilon_\infty}{2}\right)^2 \dots\dots\dots (6.12)$$

This is the equation of a circle, centre $[(\epsilon_s + \epsilon_\infty)/2, 0]$, radius $(\epsilon_s - \epsilon_\infty)/2$, so that a plot of ϵ' against ϵ'' should give a semicircle.

Relaxation in polymers shows broader dispersion curves and lower loss maxima than those predicted by the Debye model and $\epsilon' - \epsilon''$ curve fails under the semicircle. This led Cole and Cole [10] to suggest the following semi-empirical equation for the dielectric relaxation of polymers

$$\epsilon^* = \epsilon_\infty + \frac{\epsilon_s - \epsilon_\infty}{1 + (i\omega\tau)^\alpha} \dots\dots\dots (6.13)$$

where $0 < \alpha \leq 1$. Davison and Cole has improved the above Equation. as

$$\epsilon^* = \epsilon_\infty + \frac{\epsilon_s - \epsilon_\infty}{1 + (i\omega\tau)^\beta} \dots\dots\dots (6.14)$$

where $0 < \beta \leq 1$. The parameter β is representative of relaxation time distribution. If ϵ'' is plotted against ϵ' , this equation represents a circle with the centre at $(\epsilon_s + \epsilon_\infty)/2, 1/[2(\epsilon_s + \epsilon_\infty) \cot \beta\pi/2]$ and radius $1/[2(\epsilon_s + \epsilon_\infty) \csc \beta\pi/2]$

From the fig.6.4,

$$\sin\theta = \left[\frac{1}{2}(\epsilon_s - \epsilon_\infty)\right] / \left[\frac{1}{2}(\epsilon_s - \epsilon_\infty) \csc \beta\pi/2\right]$$

or $\theta = \beta\pi / 2$ (6.15)

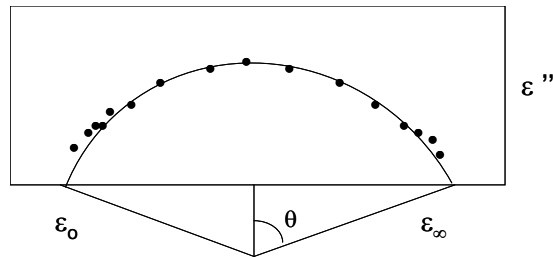


Fig. 6.4 A Cole-Cole circular arc plot constructed from the ϵ' and ϵ'' data.

6.3 Measurement of dielectric properties by an Impedance Analyzer

The ac measurement was performed in the frequency range from 10^1 to 10^6 Hz and temperature range 298-423 K, by a low frequency (LF) Impedance analyzer, Agilent 4192A, 5Hz-13MHz, Agilent Technologies Japan, Ltd. made in Japan. Electrical Specification and Characteristics of dielectric measuring system:

- (i) Measuring Frequency (f) : 50-500 kHz
- (ii) Capacitance (C_x): (a) Measurement range 270-2.2 nm
(b) Minimum 2.2nm.
- (iii) Conductance (G_x): (a) Maximum range 10.2ms
(b) Minimum ranges 1.2 μ s.



Fig. 6.5 Photographs of the the ac electrical measurement set-up.

The temperature was recorded by a Chromel- Alumel thermocouple placed very close to the sample which was connected to a Keithley 197A digital microvoltmeter (DMM). To avoid oxidation, all measurements were performed in a vacuum of about 10^{-2} Torr. Photographs of the Impedance analyzer and ac measurement set-up are shown in Figs. 6.5

6.4 Results and Discussion

6.4.1 Frequency and temperature dependence of ac electrical conductivity

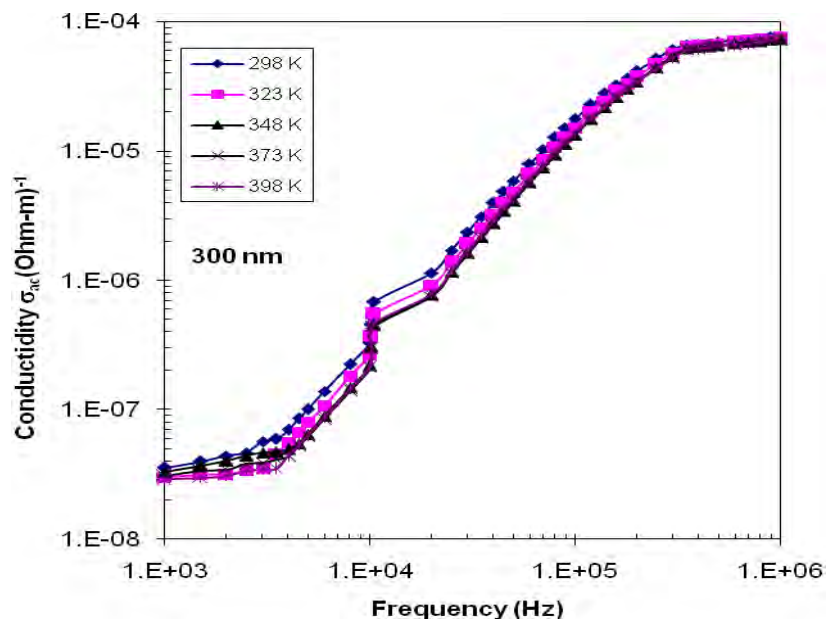


Fig.6.6 Dependence of ac conductivity, σ_{ac} , on frequency at different temperatures for PPCWO thin films of thicknesses 300 nm

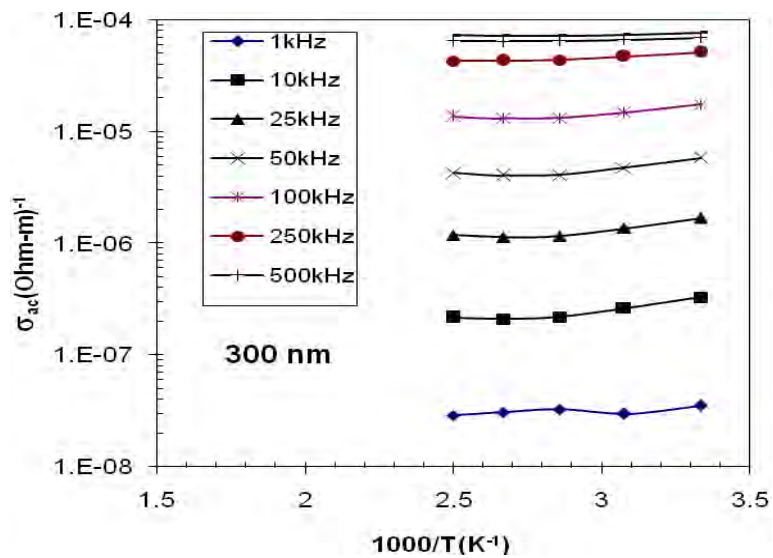


Fig. 6.7 Dependence of ac conductivity, σ_{ac} , on temperature at different frequencies for PPCWO thin films of thicknesses 300 nm.

The measured value of the conductance $G_p(\omega)$ was used to calculate the ac conductivity, σ_{ac} at different frequencies using the following expression (1):

$$\sigma(\omega) = \frac{G_p d}{A} \quad (1)$$

where d is the thickness of the sample and A is the effective cross-sectional area of the electrode.

The ac electrical conductivity, σ_{ac} as a function of frequency in the frequency range 10^3 to 10^6 Hz for PPCWO thin films of thickness 300 nm at temperatures 298, 323, 348, 373 and 398 K is shown in Fig. 6.6.

It is found that σ_{ac} increases linearly with the frequency of the applied signal with higher slope in the lower frequency region and lower slope in the high frequency region ($f > 100$ kHz) for all the measurement temperatures. It is also clear that the variation in the logarithmic ac conductivity is almost linear with the variation in logarithmic frequency and that $\sigma_{ac}(\cdot)$, increases with increasing frequency. The observed frequency dependence of σ_{ac} reveals that the mechanism responsible for ac conduction could be due to hopping.

It is also observed that σ_{ac} decreases slightly with the increase in temperature. The variation of σ_{ac} with frequency can be expressed by the relation (2)

$$\sigma_{ac}(\omega) = A\omega^n \quad (2)$$

where $\omega = 2\pi f$ is the angular frequency and n is an index which is used to determine the possible conduction or relaxation mechanism operative in amorphous materials. The values of the exponent 'n' for as deposited PPCWO thin films were calculated to be 2.5-3.25 in the low frequency (10Hz-50 kHz) region and 0.27-0.52 in the high frequency region (above 100 kHz). The value of the index n in the low frequency region is high enough that required for Debye-type relaxation process. The ac conductivity curve shows that the conductivity is very sensitive to the frequency both in the low and intermediate frequencies except for the dispersion process in the high frequencies. The observed frequency dependence of ac conductivity indicates that the mechanism of carrier conduction in PPCWO films at low frequencies is due to hopping of carriers between the localized states. Fig. 6.8 shows the variation of ac conductivity as a function of reciprocal temperature at different frequencies for PPCWO thin film of thickness 300 nm.

From the plots shown in Fig. 6.7 the activation energies, $\bullet E$ for carrier conduction were calculated and it is found that the values of the activation energies increases with increasing frequency and have a very small value (~ 0.030 eV). The low value of the ac activation energy and the increase of $\bullet_{ac}(\bullet)$, with the increase of frequency confirm that hopping conduction is the dominant current transport mechanisms in PPCWO films.

6.4.2 Frequency and temperature dependence of the dielectric constant

The dielectric constants of liquids and solids depend mainly on the frequency of measurement. This dependence can be expressed by the well known Debye dispersion formula which expresses the complex permittivity related to the free dipoles oscillating in an alternating electric field

$$\varepsilon^*(\omega) = \varepsilon' - j\varepsilon'' = \varepsilon_\infty + \frac{\varepsilon_s - \varepsilon_\infty}{1 + j\omega\tau} \quad (1)$$

where \bullet' and \bullet'' are the real and imaginary part of $\varepsilon^*(\omega)$ respectively, τ is the characteristic relaxation time of the process, \bullet_s and \bullet_∞ are the permittivity in low and high frequency limit. The dielectric constant (real part of \bullet) can be expressed as

$$\varepsilon'(\omega) = \varepsilon_\infty + \frac{\varepsilon_s - \varepsilon_\infty}{1 + (\omega\tau)^2} \quad (2)$$

At very low frequencies ($\omega \ll 1/\tau$), dipoles follow the field and we get $\bullet' = \bullet_s$. As the frequency increases dipoles begin to “lag” behind the field and \bullet' slightly decreases. This nature of the dielectric constant is observed in PPCWO thin films. When frequency reaches the characteristic frequency ($\omega = 1/\tau$) the dielectric constant drops abruptly. At very high frequencies ($\omega \gg 1/\tau$) the dipoles can no longer follow the field and we get $\bullet' \approx \bullet_\infty$.

The capacitance of PPCWO thin films as a function of frequency, f , is measured at different temperatures using a LF impedance analyzer. The dielectric constant of the deposited PPCWO thin film is then calculated using the following equation from the measured capacitance data

$$\varepsilon' = \frac{cd}{\varepsilon_0 A} \quad (3)$$

Where C is the capacitance, d is the thickness of the film, A is the effective film area and \bullet_0 is the electric permittivity of free space. The capacitance measurement was performed in the frequency range 100 Hz to 1 MHz at temperatures 300, 325, 350, 375 and 400 K.

Fig. 6.8 shows the dependence of ϵ' on frequency at different temperatures for a PPCWO thin film of thickness 300 nm. It can be seen from this figure that the dielectric constant decreases slowly with the increase of frequency in the low frequency region and after a particular frequency (near 50 kHz) it drops sharply and approaches a constant value at higher frequencies. The value of the dielectric constant of the PPCWO thin film is found to vary between 9 and 11 in the low frequency region (<10 kHz).

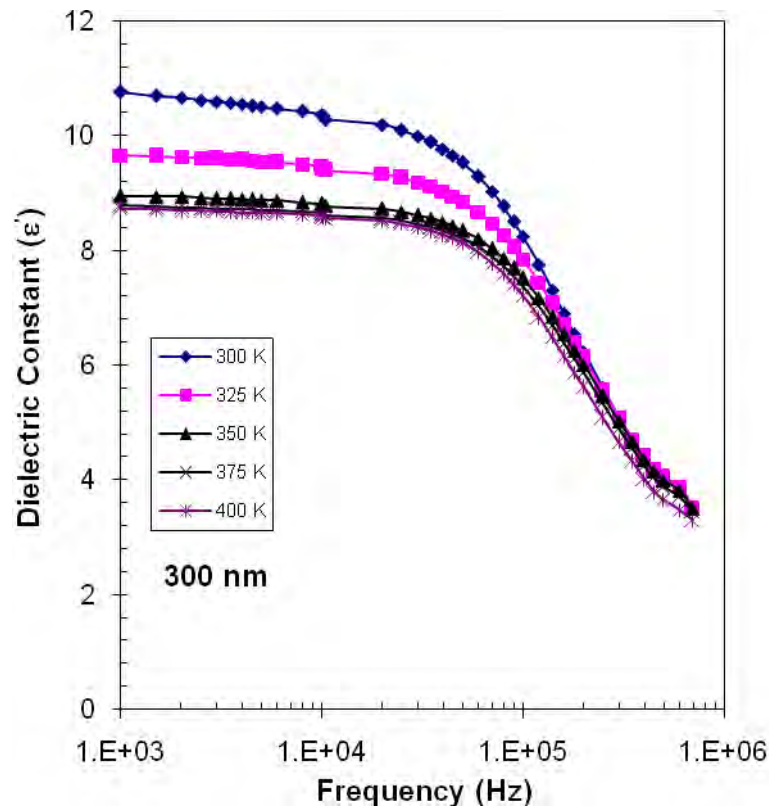


Fig. 6.8 Variation of dielectric constant with frequency at different temperatures for PPCWO thin films of thicknesses 300 nm

It is also observed that for a particular frequency the dielectric constant is decreased from its initial value with the increase in sample temperature. This kind of frequency dependence of the dielectric constant is due to the interfacial polarization which is very common in sandwiched type configurations.

6.4.3 Frequency and temperature dependence of dielectric loss tangent

The variation of loss tangent with frequency at different temperatures is depicted in Fig. 6.9. It is noticed that $\tan\delta$ increases with the increase in frequency having a peak around 100 kHz and then decreases with the further increase in frequency. It is also observed that similar peaks are present at the higher temperatures with a slight shift in the peak position.

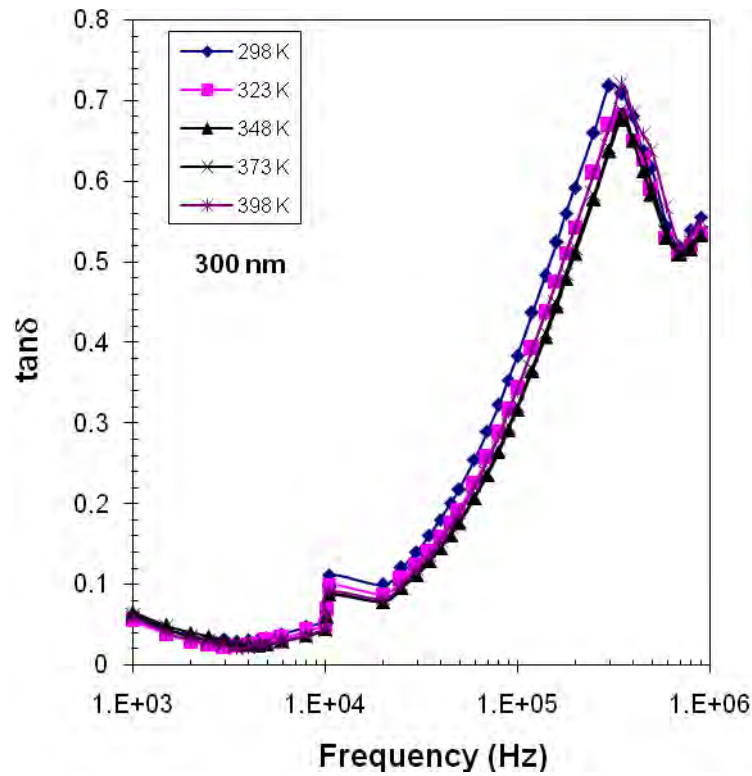


Fig. 6.9 Dependence of loss tangent, $\tan \delta$, on frequency at different temperatures for PPCWO thin films of thicknesses 300 nm

The Conductivity, Dielectric Constant and $\tan \delta$ for thickness 215 nm are given below:

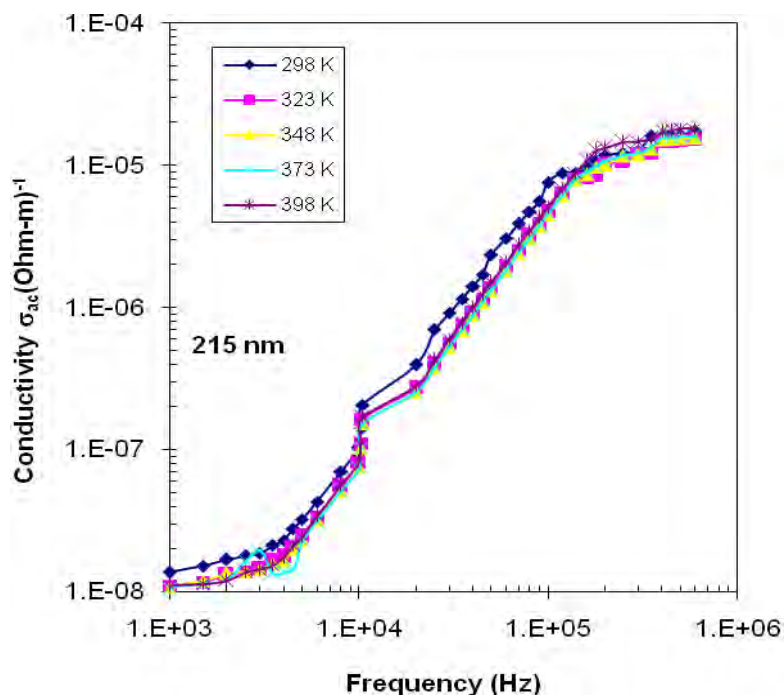


Fig. 6.10 Dependence of ac conductivity, σ_{ac} , on frequency at different temperatures for PPCWO thin films of thicknesses 215 nm

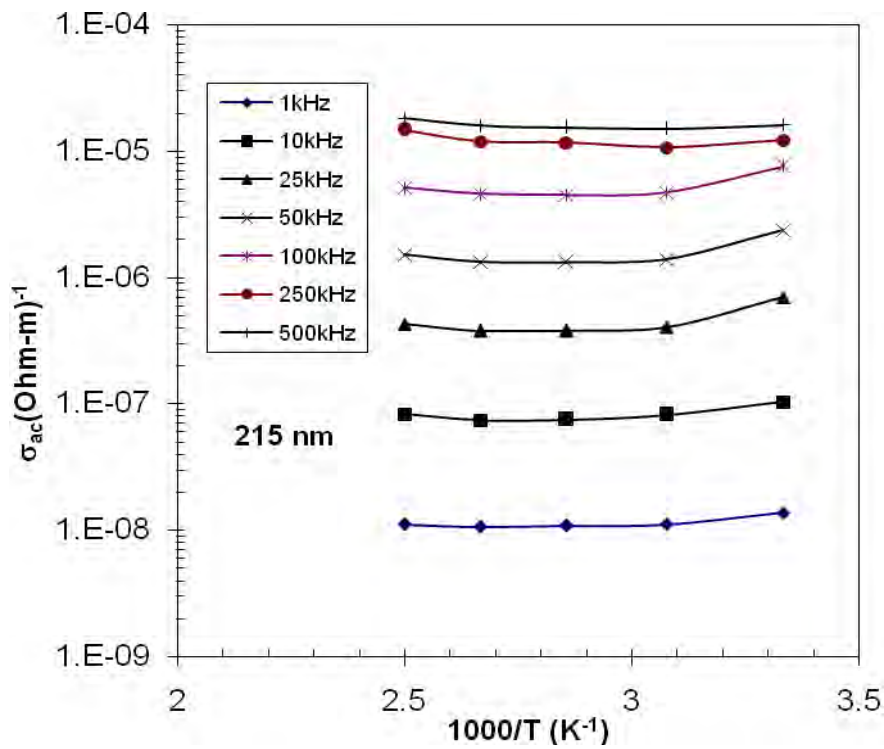


Fig. 6.11 Dependence of ac conductivity, σ_{ac} , on temperature at different frequencies for PPCWO thin films of thicknesses 215 nm.

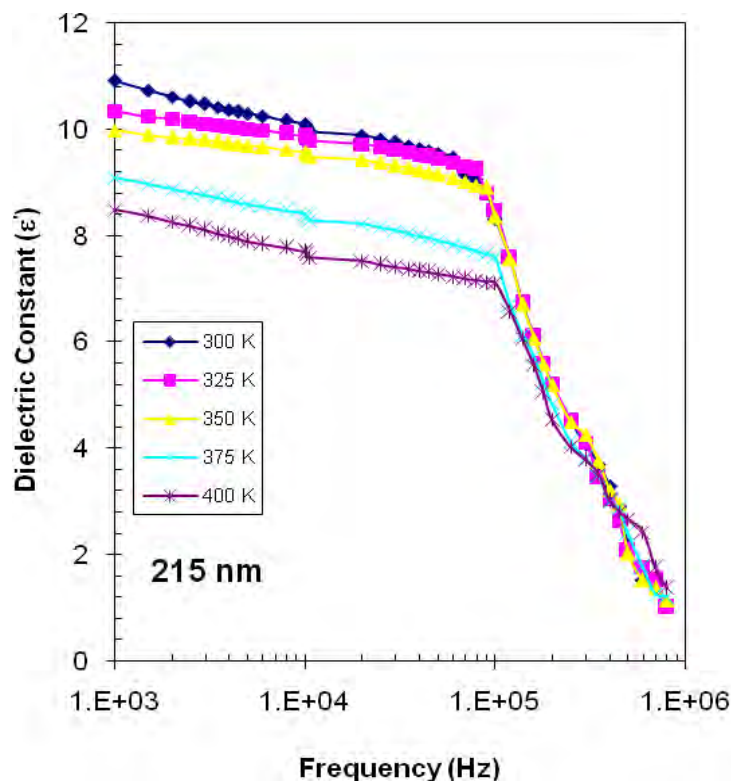


Fig. 6.12 Variation of dielectric constant with frequency at different temperatures for PPCWO thin films of thicknesses 215 nm

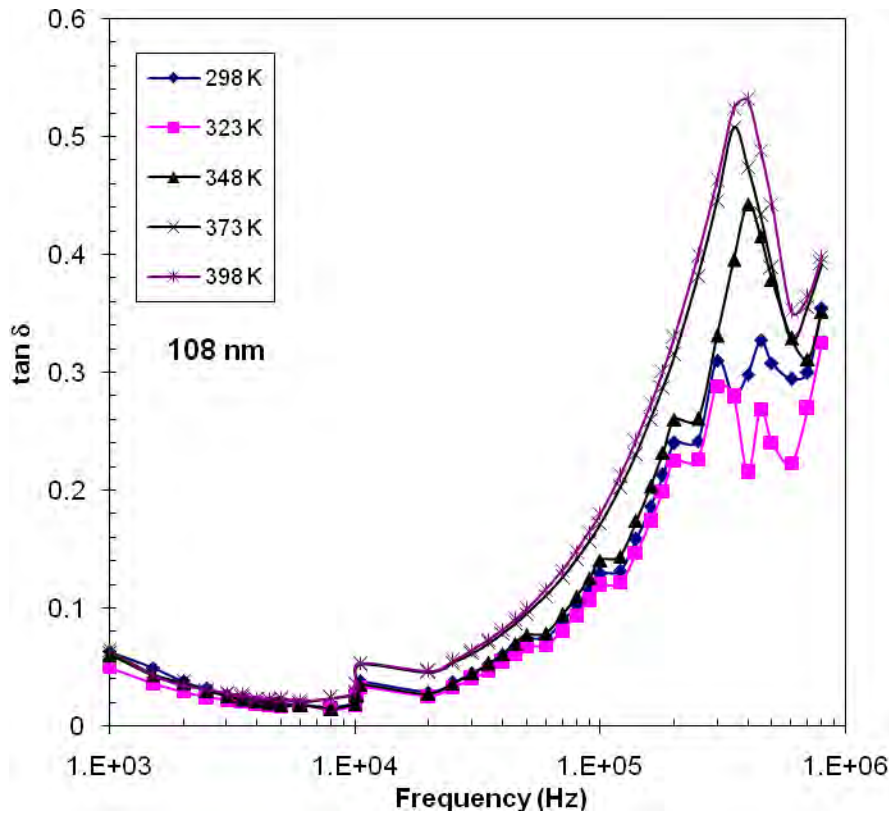


Fig. 6.13 Dependence of loss tangent, $\tan \delta$, on frequency at different temperatures for PPCWO thin films of thicknesses 215 nm

6.6.4 Cole- Cole plot

The ideal or Debye relaxation mechanism is very rarely observed in the real situation. The dependence of ϵ'' on ϵ' may be used to test how well the Debye model fits a real case. Any deviation from the ideal Debye response is accommodated by fitting the experimental data to different empirical relations. However, relaxation observed in polymers shows broader dispersion curves and lower loss maxima than those predicted by Debye model [11]. The ideal Debye nature can be expressed as

$$\epsilon^*(\omega) = \epsilon_{\infty} + \frac{\epsilon_s - \epsilon_{\infty}}{1 + j\omega\tau_0}$$

The non-ideal response is termed as non-Debye response which is expressed by the following empirical equation known as Cole and Cole :

$$\epsilon^*(\omega) = \epsilon_{\infty} + \frac{\epsilon_s - \epsilon_{\infty}}{1 + (j\omega\tau_0)^{\alpha}}$$

Where α is a parameter, $0 < \alpha < 1$. This equation better describes a broad dispersion and gives a ϵ'' - ϵ' plot where the center of the semicircle is depressed below the abscissa.

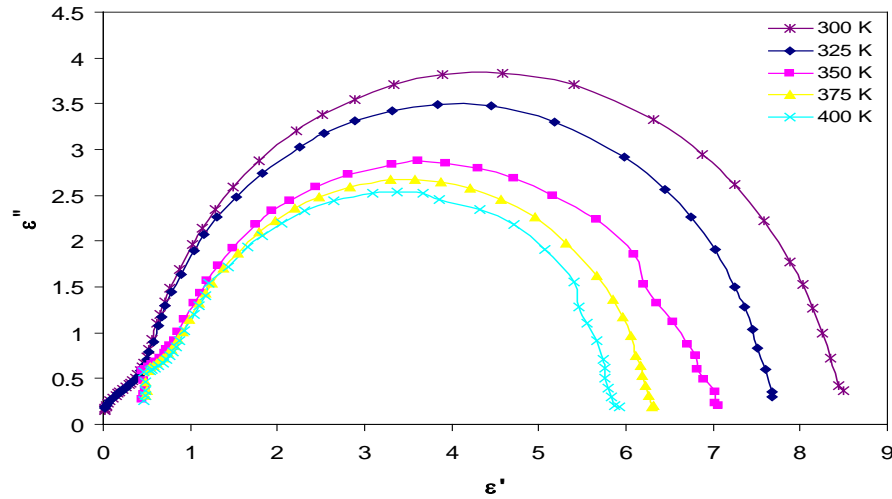


Fig. 6.14: Cole-Cole plot between ϵ' and ϵ'' for a PPCWO thin film of thickness 300.

Davidson and Cole improved the fit with experiment by using the slightly different semi-empirical equation:

$$\epsilon^*(\omega) = \epsilon_{\infty} + \frac{\epsilon_s - \epsilon_{\infty}}{(1 + j\omega\tau_0)^{\beta}}$$

where β is a parameter, $0 < \beta < 1$. This equation corresponds to a skewed distribution of relaxation times about τ_0 .

Fig. 6.14 shows the Cole-Cole plot between ϵ' and ϵ'' for a PPCWO thin film of thickness 300 nm at different temperatures. The trend of the real and imaginary parts of dielectric constant obtained exhibits almost perfect semicircle indicating a single conduction or relaxation mechanism in PPCWO thin films. The almost perfect semicircle obtained also shows evidence that the PPCWO thin film obeys Debye type relaxation processes and indicates unavailability of electrode effect during measurement. It is also seen that the radius of the semicircle decreases gradually with the increase of temperature indicating that the sample become more conductive at the elevated temperatures.

References

- [1] Yasuda H., Plasma Polymerization, academic Press, New York, 1985.
- [2] Polka L.S., Yu a Labedev, Eds. Plasma Chemistry, Cambridge International Science Publishing, UK 1998.
- [3] Saravanan S., Joseph M. C., Venkatachalam S. and Ananharaman M.R., 'Low k thin films based on rf plasma- polymerized aniline' New J. Phys. 3004; 6(64): 1.

- [4] Dey S. K., Yoshida Y., ' Dielectric Properties of plasma polymerized pyrrole thin film capacitors." Surf. Coat. Technol. 3003; 169-170: 600.
- [5] Xiong-Yan Zhao, Ming – Zhu Wang, Zhi Wang. Deposition of plasma polymerized 1- cyanoisoquinoline thin films and their dielectric properties. Plasma Process. Polym. 3007; 4: 840.
- [6] Sajeev U. S., Joseph M. C., Saravanan S., Ashokabn R. R., Venkatachalam S. and Anantharaman M. R., "On the optical and electrical properties of rf and a.c. plasma polymerized aniline thin films". Bull. Mater. Sci. 3006; 29(2): 159.
- [7] Inagaki N., "Plasma Surface Modification and Plasma Polymerization", Tehnomic Publishing Co. Inc. UA, (1996) p.144.
- [8] Morosoff N. in: R. d'Agostino (Ed), "Plasma Deposition, Treatment, and Etching of Polymers", Academic Press, San Diego, CA, (1990) p.1.
- [9] Chowdhury F-U-Z., PhD Thesis " Preparation and Characterization of Plasma – Polymerized Diphenyl Thin Films", (3000), Bangladesh University of Engineering and Technology, (BUET), Dhaka.
- [10] Cole K. H. and Cole R. H., J. Chem. Phys., 9 (1941) 341.
- [11] Blythe A. R., "Electrical Properties of Polymers" Cambridge University Press, Cambridge (1979) 69.

Chapter-7

7.1 Conclusions

7.2 Suggestions for further Study

7.1 Conclusions

The DTA and TGA traces taken in the temperature range of 303 to 1073 K at a scan rate of 20 K/min for PPCWO in nitrogen atmosphere. It is observed in the DTA trace around a temperature 373 K a transition occurs and the corresponding TGA shows a peak that may be due to the removal of water content. The DTA thermogram shows an exothermic broad band which has a maximum centered around 560 K indicating a gradual change of its original properties. The weight loss up to 763 K and above 763 K are approximately 4% and 6 % respectively in reference to its original weight may be due to structural change in PPCWO owing to hydrogen evolution and due to the loss of low molecular mass hydrocarbon gases. The gradual fall of DTA trace may be a cause of thermal breakdown of PPCWO structure and expulsion of oxygen containing compounds such as CO, CO₂, etc.

The FTIR analyses of monomer and as deposited PPCWO impressed from the absence and shifting of some absorption bands that plasma polymerization technique yields PPCWO thin films with slightly different chemical structure due to some structural rearrangement during glow discharge and further modification occurs in the PPCWO structure after heat treatment at higher temperatures due to higher degree of cross linking and abstraction of hydrogen/fragmentation.

From the UV-Vis spectroscopic study it is observed that the maximum absorbance increases with increasing thickness of the as deposited PPCWO thin films. An increasing trend is observed in the values of band gap. Thus it can be attributed that the band gap of the PPCWO thin films is dependent of thickness. This may be due to homogeneous nature of the PPCWO thin films of different thicknesses. The PPCWO thin films are homogeneous with in these thicknesses and have consistent optical properties. The analysis of the optical absorption data for PPCWO thin films of thickness 310 nm revealed that the absorption increases and band gap increases due to heat treatment.

AC conductivity, σ_{ac} , increases as the frequency increases with a lower slope in the high frequency (above 1×10^5 Hz) region at all temperature. The values of “n” in the higher frequency region are in accordance with the theory of Debye type loss mechanism and other mechanisms (Havriliak- Negami, Cole-Davidson) may be operative in the low frequency region indicating asymmetry and broadness of the

dielectric dispersion. The dielectric constant (ϵ') decreases slowly with increasing frequency up to 100 kHz and the values lie between 12.90 to 1.0 and then decreases very sharply in the high frequency region. The Cole –Cole plot is deviated from a semicircle clearly indicating a single conduction or relaxation mechanism.

7.2 Suggestions for further Study

Physical sputtering and chemical etching are two important processes of ablation of materials by plasma during the deposition of thin films from organic monomer. Deposition rate is highly dependent on ionization and molecular fragmentation. Due to different parameters the surface properties are affected by the bulk properties. Consequently it became a tough job to comment on thickness dependence. The main focus of this thesis was to investigate the thermal, structural, optical and the electrical properties of PPCWO thin films. We tried to analyze the experimental data with the help of the previous published literature and our results were explained by using present existing theories.

The FTIR spectra could be taken for the films of different thickness separately and analyzed to study the thickness dependence. The optical study revealed that band gap is independent of thickness but depends on temperature. It was observed that the electrical properties are thickness and temperature dependent. A very few literature was found that emphasizes on the properties with thickness variation.

In electrical measurement heat treated sample may be taken into consideration. The aging effect of a large number of samples may be studied. All the results of the above analyses might then be correlated with the thickness dependent optical and electrical properties of the thin films.